

# **Preparation and Characterization of Poly (4-Vinyl Pyridine) Grafted Chitin Beads**

**Hasan Oylum**

Submitted to the  
Institute of Graduate Studies and Research  
in partial fulfillment of the requirements for the Degree of

Doctor of Philosophy  
in  
Chemistry

Eastern Mediterranean University  
February 2013  
Gazimağusa, North Cyprus

Approval of the Institute of Graduate Studies and Research

---

Prof. Dr. Elvan Yılmaz  
Director

I certify that this thesis satisfies all the requirements as a thesis for the degree of Doctor of Philosophy in Chemistry.

---

Prof. Dr. Mustafa Halilsoy  
Chair, Department of Chemistry

We certify that we have read this thesis and that in our opinion it is fully adequate in scope and quality as a thesis for the degree of Doctor of Philosophy in Chemistry.

---

Prof. Dr. Elvan Yılmaz  
Supervisor

---

Examining Committee

Prof. Dr. Ayfer Saraç

---

Prof. Dr. Filiz B. Şenkal

---

Prof. Dr. Elvan Yılmaz

---

Assoc. Prof. Dr. Mustafa Gazi

---

Assist. Prof.Dr. Mehmet Garip

---

## ABSTRACT

The subject of this thesis is the preparation and characterization of chitin gel beads by thermoreversible gelation, which followed by nonsolvent addition, and via chemical modification followed by non-solvent addition. Physical properties of the chitin gels obtained by nonsolvent addition and by heating to the gelation point followed by nonsolvent addition were investigated. The effects of the type and composition of the solvent system on the gelation time, gelation temperature, swelling ratio and the Young's modulus were studied. Another aspect of this study was to exploit the gel formation capability of chitin to form modified gel beads based on the polymer. To fulfill this aim, a new combined approach was taken to carry out redox initiated grafting under homogeneous conditions followed by nonsolvent addition to prepare poly(4-vinyl pyridine) (P4VP) grafted chitin gel beads. Grafting percentages up to 226% were obtained.

The grafted and nongrafted products were characterized by FTIR spectrophotometry, XRD and SEM analyses and by TGA. The swelling behaviour of the beads was studied in aqueous solution in neutral, acid and phosphate buffers. XRD analysis showed that the characterized product had a lower crystallinity when compared to the pure chitin. Thermal analysis carried out by TGA revealed that the products were less stable against thermal treatment than chitin. While chitin had a weight loss of 75 % at 500°C the grafted product showed 90 % weight loss. The maximum decomposition temperature for chitin was 380°C, but for the grafted products this value was as low as 305°C. The DSC analysis of the chitin and the grafted chitin confirmed less heat stability of chitin-*g*-P4VP.

The potential of the gel beads for wastewater treatment applications was tested by studying their heavy metal and fat binding properties. The P4VP grafted and nongrafted gel beads were tested for their cholesterol and  $\text{Fe}^{3+}$  adsorption capacities. The beads derived from chitin-g-P4VP were found to have higher adsorption capacities than chitin beads due to a microporous bead surface and chemical modification. The quaternized chitin-g-P4VP gel bead proved to be a potential  $\text{Hg}^{2+}$  adsorbent.

**Keywords:** Bioadsorbent, biopolymer, chitin, chitosan, poly(4-vinyl pyridine), grafting, cholesterol, heavy metals, iron, mercury, chitin beads, thermoreversible gelation, quaternized chitin.

## ÖZ

Bu tezin konusu; kitin jel boncukların ısıt tersinir jelleşme, ısıt tersinir jelleşme işlemi sonrasında çöktürücü eklenmesi ve kimyasal modifikasyon sonrasında çöktürücü eklenmesi yöntemleri ile hazırlanması ve karakterizasyonudur. Çöktürücü eklenerek ve jelleşme noktasına kadar ısıtıldıktan sonra çöktürücü eklenerek hazırlanan jellerin fiziksel özellikleri incelendi. Çöktürücü sistem türünün ve bileşiminin jelleşme zamanı, jelleşme sıcaklığı, şişme oranı ve esneklik katsayısı üzerinde etkileri incelendi. Bu çalışmanın diğer bir boyutu ise, kitinin jelleşme özelliklerinin, modifikasyon sonrası da kullanılarak modifiye kitin jel küreler hazırlanmasıdır. Bu amaçla, yeni bir yaklaşımla kimyasal modifikasyon ve jelleşme bir arada kullanılarak poly(4-vinil piridin) aşılansmış kitin jel küreler hazırlanmıştır. En fazla 226% aşılansma yüzdesine ulaşılmıştır.

Aşılansmış ve aşılansmamış ürünler FTIR spektrofotometresi, XRD, SEM ve TGA yöntemleri ile karakterize edildi. Kürelerin şişme davranışları sulu ortamda çalışılmıştır. XRD analizi, ürünlerin kitine göre daha düşük kristallik oranına sahip olduğunu göstermiştir. Kitin-g-(poli(4-vinil piridin)) kürelerin termal özellikleri ise TGA ile belirlenmiştir. Aşılansmış ürünlerin kitine göre ısıt kararlılıklarının daha düşük olduğu gözlemlenmiştir. 500°C civarında kitin, %75 ağırlık kaybına uğrarken, aşılansmış kitinde bu oran %90 civarındadır. Normal kitinin maksimum bozunma sıcaklığı 380°C iken, aşılansmış kitin için bu sıcaklık 305°C'dir. Kitin ve aşılansmış kitinin DSC analizi, aşılansmış kitinin ısıt kararlılığının daha düşük olduğunu desteklemektedir.

Potansiyel olarak jel kürelerin atıksu arıtım sistemlerinde kullanılabilirliğini test etme amaçlı olarak; metal ve yağ tutuculuk özellikleri üzerinde çalışılmıştır. Bu amaçla kitin-g-P4VP boncukların Fe<sup>3+</sup> ve kolesterol tutuculuk kapasiteleri de incelenmiş ve aşılansmış

boncukların aşılammamış boncuklara göre daha fazla tutuculuk kapasitelerine sahip olduđu gözlemlenmiştir. Bunun sebebi ise aşılammış kitin boncukların mikrogözenekli bir yapıya sahip olması ve kimyasal modifikasyona uğratılmış olmasıdır. Deneysel çalışmalar, kloroasetamid fonksiyonlu kuaterner kitin-g-P4VP kürelerin, Hg<sup>2+</sup> iyonu yüzey tutuculuk uygulamaları için potansiyel olduğunu göstermiştir.

**Anahtar Kelimeler:** Biyoadsorban, biyopolimer, kitin, kitosan, poly(4-vinil piridin), aşılama, kolesterol, ağır metal, demir, cıva, kitin küre, ısıl tersinir jelleşme, kuaterner kitin.

## ACKNOWLEDGMENT

The presented thesis has been carried out at Eastern Mediterranean University, in Polymer Chemistry Laboratory Department of Chemistry, under the supervision of Prof. Dr. Elvan Yılmaz.

I would like to express my deepest gratitude to my supervisor Prof. Dr. Elvan Yılmaz for her help, comments and suggestions throughout the thesis. I would also like to thank Prof Dr. Osman Yılmaz for his support and to behave in a friendly manner, thanks to Prof. Dr. Nesrin Hasırcı for the mechanical tests of the gels in METU, thanks to Prof. Dr. Murat Bengisu, thanks to Assoc. Prof. Dr. Mustafa Gazi and my friends Mustafa Toprakoğlu (the deceased, 2010), Ersan Güven, Hamit Caner, Terin Adalı, Zülal Yalınca, Alev Elçi, and cousin Halil Oylum for their psychological and logistic at different stages of my thesis.

Finally, special thanks go to my family, my wife Akgül, daughters Gülşen & Sare, father Halil and mother Hafize for their support by heard, during my Ph. D.'s degree.

# TABLE OF CONTENTS

ABSTRACT.....	iii
ÖZ.....	v
ACKNOWLEDGMENT.....	vii
LIST OF TABLES.....	xi
LIST OF FIGURES.....	xiii
1 INTRODUCTION.....	1
1.1 Chitin and Chitosan.....	1
1.2 Solution Properties of Chitin .....	4
1.2.1 Dissolution of Chitin .....	4
1.2.2 Characterization of Chitin Solution.....	6
1.2.2.1 Dilute Solution Viscometry.....	6
1.2.2.2 Dilute Solution Properties of Chitin/Chitosan.....	11
1.3 Gel Formation in Polymeric Systems.....	12
1.3.1 Gelation of Chitin Solutions.....	14
1.4 Heavy Metal Adsorption by Chitin/Chitosan Gels .....	16
1.5 Present Work.....	17
2 EXPERIMENTAL.....	19
2.1 Chitin, Solvent System, Chitin Solution, Thermoreversible Gelation, Dilute Solution Viscometry.....	19
2.1.1 Materials.....	19
2.1.2 Purification of Chitin Powder.....	19
2.1.3 Preparation of Solvent Systems.....	20
2.1.4 Preparation of Chitin Solutions.....	20



2.1.5 Thermoreversible Gelation.....	21
2.1.6 Dilute Solution Viscometry.....	21
2.2 Preparation and Characterizations of Chitin-Organic Acid Gels.....	22
2.2.1 Preparation of Chitin-Organic Acid Solutions.....	22
2.2.2 Preparation of Chitin-Organic Acids Gels.....	22
2.2.3 FTIR Spectrum of Chitin-Organic Acids Gels.....	23
2.2.4 Mechanical Tests of Chitin-Organic Acids Gels.....	23
2.2.5 Swelling Tests for Chitin-Organic Acids Gels.....	23
2.3 Preparation and Characterization of P4VP Grafted Chitin Beads.....	23
2.3.1 Materials.....	24
2.3.2 Purification of Chitin.....	24
2.3.3 Preparations of Solvent Systems.....	24
2.3.4 Preparations of Chitin Solution.....	24
2.3.5 Purification of 4VP.....	25
2.3.6 Preparation of Chitin-Grafted P4VP Solution.....	25
2.3.7 Preparations of P4VP Grafted Chitin Beads.....	26
2.3.8 Purification of P4VP Grafted Chitin Beads.....	26
2.3.9 Percent Grafting of P4VP onto Chitin Solution.....	26
2.3.10 FTIR Spectroscopy Analysis.....	27
2.3.11 X-Ray Diffraction XRD.....	27
2.3.12 Thermal Analysis (DSC and TGA) .....	27
2.3.13 Swelling Behaviour.....	28
2.3.14 SEM Analysis.....	28
2.3.15 Fe <sup>3+</sup> Adsorption onto the Beads.....	28
2.3.16 Determination of Fe <sup>3+</sup> in Solution.....	29

2.3.17 Cholesterol Adsorption onto the Beads.....	29
2.4 Quaternization of P4VP Grafted Chitin Beads.....	29
2.4.1 Quaternization of Crosslinked P4VP Beads.....	30
2.4.2 Chloride Analysis.....	30
2.4.3 Mercury Adsorption.....	30
2.4.4 Kinetics of the Mercury Adsorption .....	31
3 RESULTS AND DISCUSSION.....	32
3.1 Solution Properties of Chitin.....	32
3.1.1 Dilute Solution Viscometry.....	32
3.1.2 Thermoreversible Gelation of Chitin.....	35
3.2 Preparation and Characterizations of Chitin-Organic Acid Gels.....	39
3.2.1 Gel Formation.....	39
3.2.2 FTIR Spectroscopy.....	41
3.2.3 Mechanical Analysis.....	42
3.2.4 Swelling Properties.....	43
3.3 The Formation and Characterization of P4VP Grafted Chitin Beads.....	44
3.3.1 The Formation of P4VP Grafted Chitin Beads.....	44
3.3.2 Grafting Yield.....	48
3.3.3 FTIR Analysis.....	50
3.3.4 XRD Analysis.....	52
3.3.5 Thermal Analysis.....	53
3.3.6 Swelling Behavior.....	56
3.3.7 Beads Morphology (SEM) .....	58
3.3.8 Fe <sup>3+</sup> Adsorption Behavior.....	61
3.3.9 Cholesterol Adsorption Behavior.....	65

3.4 Quaternization of Chitin-g-P4VP Beads.....	67
3.4.1 Extraction of Trace Mercury.....	70
3.4.2 Pseudo-First Order Kinetic Model.....	71
3.4.3 Pseudo-Second-Order Model.....	72
3.4.4 Regeneration.....	74
4 CONCLUSION.....	75
REFERENCES.....	80
APPENDIX.....	88

## LIST OF TABLES

Table 1: Dilute Solution Viscometry -Definitions.....	7
Table 2: MHS constants for chitin in DMAc/LiCl5%.....	12
Table 3: Flow times of the solvents and the chitin solutions.....	32
Table 4: Reduced viscosity and inherent viscosity of chitin solutions studied.....	34
Table 5: Gelation temperatures of DMAc and NMP solutions.....	35
Table 6: Colors of DMAc and NMP solutions.....	36
Table 7: Gel forming and melting temperatures of Chitin/DMAc/LiCl system in the presence of Ascorbic Acid and Maleic Acid.....	37
Table 8: pH values of the used solvent systems for Chitin.....	38
Table 9: pH Values, gelation times of solutions and melting times of gels.....	38
Table 10: Young's Modulus (E) Values and Swelling Indices (Q) and Gelation Temperatures ( $T_{gel}$ ) of chitin gels formed by heating to gelation temperature followed by ethanol addition.....	43
Table 11: Percent grafting values for different initial amounts of 4VP.....	49
Table 12: XRD data .....	52
Table 13: Crystallinity index calculated by using equation (2) .....	52
Table 14: Cholesterol adsorption onto, chitin-g-P4VP and chitin beads in 1mg/mL cholesterol solution.....	63
Table 15: $Fe^{3+}$ adsorption onto, chitin-g-P4VP and processed blank chitin beads in 1mM $Fe^{3+}$ solution.....	66

Table 16: Comparison of pseudo-first order and pseudo-second order rate constants, correlation coefficients and equilibrium adsorptions ( $q_e$ ).....	74
---	----

## LIST OF FIGURES

Figure 1: Cellulose, Chitin and Chitosan.....	2
Figure 2: Conversion of Chitin to Chitosan.....	3
Figure 3: Conversion of Chitosan to Chitin.....	4
Figure 4. Proposed structures of Chitin DMAc-LiCl complexes (Cell:cellulose or chitin).....	5
Figure 5: Solvation of chitin by [DMAc-Li] <sup>+</sup> complex .....	6
Figure 6: Multigradient Ubbelohde viscometer.....	21
Figure 7: $\eta_{inh}$ and $\eta_{red}$ values for Chitin DMAc/LiCl5% solutions.....	33
Figure 8: $\eta_{inh}$ and $\eta_{red}$ for Chitin NMP/LiCl5% solution as a function of concentration..	34
Figure 9: Optical picture of the chitin gel formed from ((a) 0.5, (b) 1.0, (c) 1.5) % w/w solution of DMAc/LiCl5% by heating to gelation temperature followed by ethanol addition, (d) chitin gel formed from 0.5 % w/w solution of DMAc/LiCl5% by nonsolvent gelation.....	40
Figure 10: FTIR spectra of the chitin gel formed from 0.5%w/w solution of (a) Chi/NMP/LiCl5% (b) Chi/DMAc/LiCl5% and (c) original chitin sample..	41
Figure 11: Chemical modification followed by non-solvent gelation on chitin solution to form beads.....	45
Figure 12: Chemical Modification, chitin-g-P4VP formation.....	46
Figure 13: Optical picture of P4VP grafted chitin beads formed by non-solvent addition.....	47

Figure 14: Purification (Et-OH (left), H <sub>2</sub> O (right)), P4VP grafted chitin beads.....	47
Figure 15: Purified beads, (a) Et-OH, H <sub>2</sub> O purified-grafted, (b) Et-OH purified-grafted, (c) Et-OH, H <sub>2</sub> O purified-blank processed, (d) H <sub>2</sub> O purified-blank processed.....	48
Figure 16: Percent grafting of P4VP grafted chitin with respect to amount of 4VP (KPS 1.2 g).....	49
Figure 17: FTIR spectrum of (a) chitin (b) chitin-g-P4VP.....	51
Figure 18: XRD spectrum for (a) chitin and (b) chitin-g-P4VP.....	53
Figure 19: TGA thermogram for (a) chitin (b) chitin-g-P4VP.....	54
Figure 20: DSC analysis for chitin-g-P4VP.....	55
Figure 21: DSC analysis for chitin.....	55
Figure 22: Swelling behaviours for blank chitin beads (ch) and grafted chitin beads (g-ch) with respect to t (min) at pH 7.0.....	57
Figure 23: Swelling behaviours for blank chitin beads (ch) and grafted chitin beads (g-ch) with respect to t (min) at pH 1.4.....	57
Figure 24: Swelling behaviours for blank chitin beads (ch) and grafted chitin beads (g-ch) with respect to t (min) at pH 7.4.....	58
Figure 25: SEM micrograph of the blank chitin beads, (a) is X 50, (b) X 100, (c) is X 500, (d) is X 1.000, (e) is X 5.000, (f) is X 10.000.....	59
Figure 26: SEM micrograph of the grafted chitin beads, (a) is X 50, (b) X 100, (c) is X 500, (d) is X 1.000, (e) is X 5.000, (f) is X 10.000.....	60

Figure 27: Fe <sup>3+</sup> adsorption (mg Fe <sup>3+</sup> /g bead) for chitin beads in (a) 5.0 mM Fe <sup>3+</sup> , (b) 1.0 mM Fe <sup>3+</sup> with respect to time.....	63
Figure 28: Fe <sup>3+</sup> adsorption (mg Fe <sup>3+</sup> /g bead) for chitin-g-P4VP beads (G%=226%) in (a) 5.0 mM Fe <sup>3+</sup> , (b) 1.0 mM Fe <sup>3+</sup> with respect to time.....	64
Scheme 1: Adsorption mechanism onto chitin and chitin-g-P4VP beads.....	64
Figure 29: Cholesterol adsorption for chitin-g-P4VP beads with respect to time (a) 5.0 mg/mL, (b) 1.0 mg/mL, (c) 0.5 mg/mL cholesterol concentration.....	66
Figure 30: Quaternization of Chitin-g-P4VP Beads with 2-Chloroacetamide.....	67
Figure 31: SEM micrograph of the quaternized chitin-g-P4VP beads, (a) is X 100, (b) X 500, (c) is X 500, (d) is X 1.000, (e) is X 5.000, (f) is X 10.000.....	67
Figure 32: Binding of Mercury Ions on Quaternized Chitin-g-P4VP.....	68
Figure 33. SEM micrograph of the chitin beads (a) and (d) nongrafted chitin beads, (b) and (e) P4VP grafted chitin beads, (c) and (f) for quaternized P4VP grafted chitin beads.....	69
Figure 34: Variation of trace mercury concentration during interaction with the quaternized chitin-g-P4VP (0.25 g) with 50mL Hg <sup>2+</sup> (100ppm) solution.....	70
Figure 35: Equilibrium adsorption of Hg <sup>2+</sup> ions on the quaternized chitin-g-P4VP (0.25 g) with 50 mL Hg <sup>2+</sup> (100ppm) solution.....	71
Figure 36: Hg <sup>2+</sup> ions adsorption on qP4VP-g-Chitin through pseudo-first order kinetic models.....	72
Figure 37: Hg <sup>2+</sup> ions adsorption on qP4VP-g-Chitin through pseudo second-order kinetic models.....	73
Figure A1.1: Calibration Curve for Naproxen.....	88



Figure A1.2: Calibration Curve for Ibuprofen.....	89
Figure A1.3: Calibration Curve for Acetyl Salicylic Acid.....	90
Figure A1.4: Drug Encapsulated Chitin Beads.....	91
Figure A2.1: FTIR Spectrum for Chitin (d) and P4VP Grafted Chitin in Organic Solvents.....	92
Figure A3.1.1: Water Purified Grafted (Left Side) Chitin and Water Purified non-grafted Blank Chitin Beads (Right Side).....	93
Figure A3.1.2: Water Purified Filtered non-grafted Blank Chitin Beads (Wet).....	93
Figure A3.1.3: Chitin-g-P4VP while Drying.....	93
Figure A3.1.4: Chitin-g-P4VP Beads after the Soxhlet Purification in Et-OH, before Water Purified.....	94
Figure A3.1.5: Chitin-g-P4VP during the Water Purification.....	94
Figure A3.1.6: Chitin-g-P4VP in Water.....	94
Figure A3.2.1: FTIR spectroscopy of P4VP grafted chitins compared to (a) non-grafted blank chitin (non-grafted blank: without 4VP, under same conditions as grafted).....	95
Figure A4.1: Different Chitin and Chitosan SEM Microstructures.....	96
Figure A6.1: Chitin-g-P4VP quaternized with 2-chloroacetamide in DMF.....	99
Figure A6.2: FTIR for (a) chitin-g-P4VP, (b) quaternized chitin-g-P4VP, (c) chitin.....	99
Figure A6.3: SEM for Quaternized Chitin-g-P4VP Beads.....	100
Figure A6.4: SEM for Quaternized Chitin-g-P4VP Beads.....	101
Figure A6.5: Hg <sup>2+</sup> ions adsorption on qP4VP-g-Chitin through pseudo-first order kinetic models including statistical results.....	102

Figure A-6.6. Hg <sup>2+</sup> ions adsorption on qP(4-VP)-g-Chitin through pseudo-first order kinetic models including statistical results (first 15 minutes).....	102
Figure A-6.7: Hg <sup>2+</sup> ions adsorption on qP4VP-g-Chitin through pseudo second-order kinetic models including statistical results.....	103
Figure A-7.1: Burning Test for Chitin in DMAc and NMP with Weak Acids (MA, OA, AA) (See the Matlab program for the detail).....	104
Figure A-7.2: Burning Test for Chitin in DMAc and NMP with Weak Acids (MA, OA, AA) (See the Matlab program for the detail).....	104
Figure A-7.3: Burning Test for Chitin in DMAc with Weak Acids (MA, OA, AA). See the Matlab program for the detail.....	105
Figure A-7.4: Burning Test for Chitin in NMP with Weak Acids (MA, OA, AA). See the Matlab program for the detail.....	105
Figure A-8.1: Swelling Tests for DMAc+Chitin Gells (wet) for Nonsolvent Gelation and Thermoreversible Gelation. Note is True for the Whole Rest Figures.....	108
Figure A-8.2: Swelling Tests for DMAc+Chitin Gells (dried) for Nonsolvent Gelation and Thermoreversible Gelation.....	109
Figure A-8.3: Swelling Tests for NMP+Chitin Gells (dried) for Nonsolvent Gelation and Thermoreversible Gelation.....	110
Figure A-8.4: Swelling Tests for NMP+Chitin Gells (Wet) for Nonsolvent Gelation and Thermoreversible Gelation.....	111
Figure A-8.5: Swelling Tests for DMAc+AA+Chitin Gells (dried) for Nonsolvent Gelation and Thermoreversible Gelation.....	112

Figure A-8.6: Swelling Tests for DMAc+AA+Chitin Gells (Wet) for Nonsolvent Gelation and Thermoreversible Gelation.....	113
Figure A-8.7: Swelling Tests for DMAc+MA+Chitin Gells (Wet) for Nonsolvent Gelation and Thermoreversible Gelation.....	114
Figure A-8.8: Swelling Tests for DMAc+OA+Chitin Gells (Wet) for Nonsolvent Gelation and Thermoreversible Gelation.....	115
Figure A-8.9: Swelling Tests for DMAc+MA+Chitin Gells (dried) for Nonsolvent Gelation and Thermoreversible Gelation.....	116
Figure A-8.10: Swelling Tests for DMAc+OA+Chitin Gells (dried) for Nonsolvent Gelation and Thermoreversible Gelation.....	117
Figure A-8.11: Swelling Tests for NMP+AA+Chitin Gells (Wet) for Nonsolvent Gelation and Thermoreversible Gelation.....	118
Figure A-8.12: Swelling Tests for NMP+MA+Chitin Gells (Wet) for Nonsolvent Gelation and Thermoreversible Gelation.....	119
Figure A-8.13: Swelling Tests for NMP+OA+Chitin Gells (Wet) for Nonsolvent Gelation and Thermoreversible Gelation.....	120
Figure A-8.14: Swelling Tests for NMP+AA+Chitin Gells (Dried) for Nonsolvent Gelation and Thermoreversible Gelation.....	121
Figure A-8.15: Swelling Tests for NMP+MA+Chitin Gells (Dried) for Nonsolvent Gelation and Thermoreversible Gelation.....	122
Figure A-8.16: Swelling Tests for NMP+OA+Chitin Gells (Dried) for Nonsolvent Gelation and Thermoreversible Gelation.....	123
Figure A-9.1: Calibration Curve for Fe <sup>3+</sup> .....	125

# Chapter 1

## INTRODUCTION

### 1.1 Chitin and Chitosan

Chitin is the most abundant amino polysaccharide which is a component of the shells of crustaceans such as crabs and shrimps, the cuticles of the insects and the cell walls of fungi. Chitin is substantially composed of 2-acetamido-2-deoxy-D-glucopyranose (N-acetyl-D-glucosamine, GlcNAc) units linked by  $\beta$ -(1 $\rightarrow$ 4) linkage. Chitosan is the N-deacetylated derivative of chitin. Although a definite distinction is not available, usually samples with a N-acetylation higher than 60% are referred as chitin. Chitosan obtained from chitin mainly by N-deacetylation with an alkaline hydrolysis is chiefly composed of 2-amino-2deoxy-D-glucopyranose (D-glucosamine, GlcN) units. Most of the naturally occurring polysaccharides, e.g. cellulose, dextran, pectin, alginic acid, agar, agarose and carragenans, are neutral or acidic in nature, whereas chitosan is an example of highly basic polysaccharides [Kumar, 2000]. Figure 1 shows chemical structures of chitin, chitosan and cellulose.

Deacetylation of chitin produces chitosan as illustrated in Figure 2. The reverse process shown in Figure 3, acetylation of chitosan is also reported in literature [Vachoud, 1997]. This method allows better control of the acetylation degree of the aimed product.

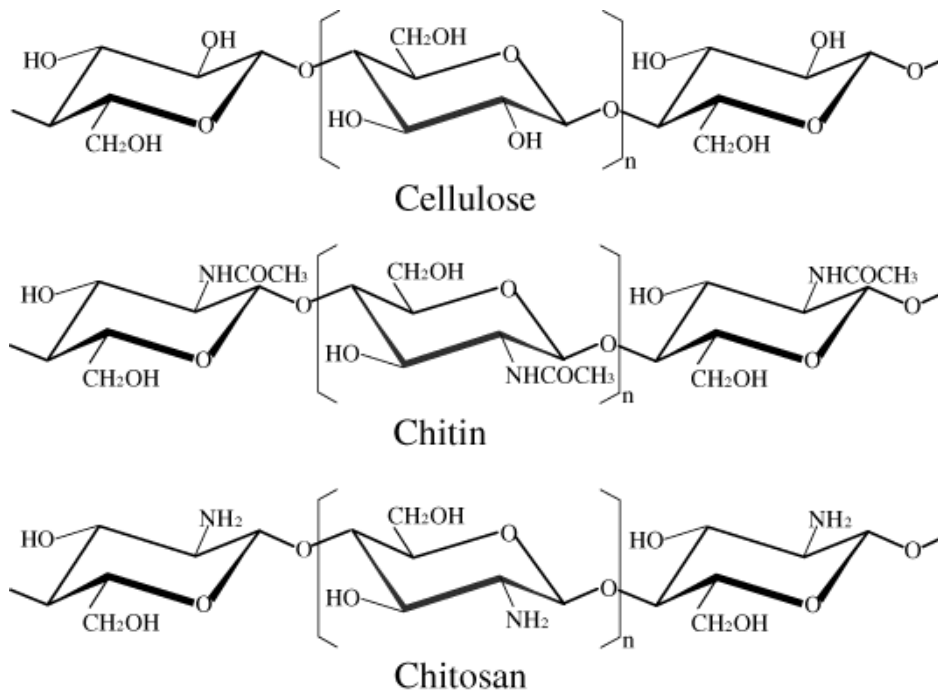


Figure 1. Cellulose, Chitin and Chitosan.

There is a growing tendency to replace, wherever possible, synthetic polymers with biodegradable, biocompatible and non-toxic polymers of biological origin. Therefore, physical properties of chitin are worth studying since chitin, cellulose and other similar natural polymers are expected to find increasing biotechnological applications in the near future.

Some investigated application areas for chitin and chitosan are; biomedicine, paper and textile industries, and waste water treatment [Smith, 2000]. Chitin and chitosan are of commercial interest due to their high nitrogen (6.89 %) which makes chitin a useful chelating agent [Kumar, 2000]. Chitin and chitosan are natural polymers which are considered to be biocompatible, biodegradable, non-toxic [Kumar, 2000]. The

degradation behavior of chitin and chitosan substrates is very important for biomedical applications such as controlled drug release, tissue engineering [Khor, 2003].

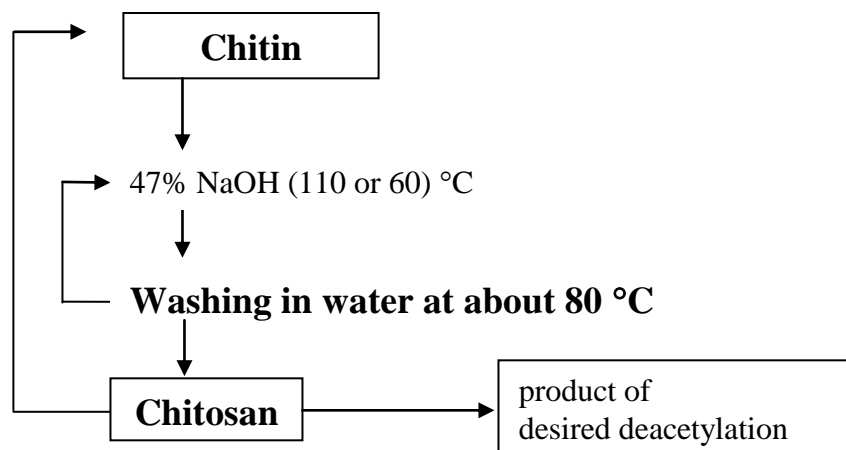


Figure 2. Conversion of Chitin to Chitosan

Enzymatic degradation of chitin is interesting as an alternative to acid hydrolysis, used commercially to obtain amino sugars such as N-acetylglucosamine (NAG) and glucosamine [Bengisu, 2004], which are believed to possess therapeutic potential [Donzelli, 2003], [Sashiwa, 2003]. Chitin has been shown to increase wound healing [Farkas, 1990], [Fleet & Phaff, 1981] in animals and humans. Sulfate esters of chitin were shown to be non-thrombogenic. Chitin and chitosan, on the other hand, were found to enhance blood coagulation [Okamoto, 2003].

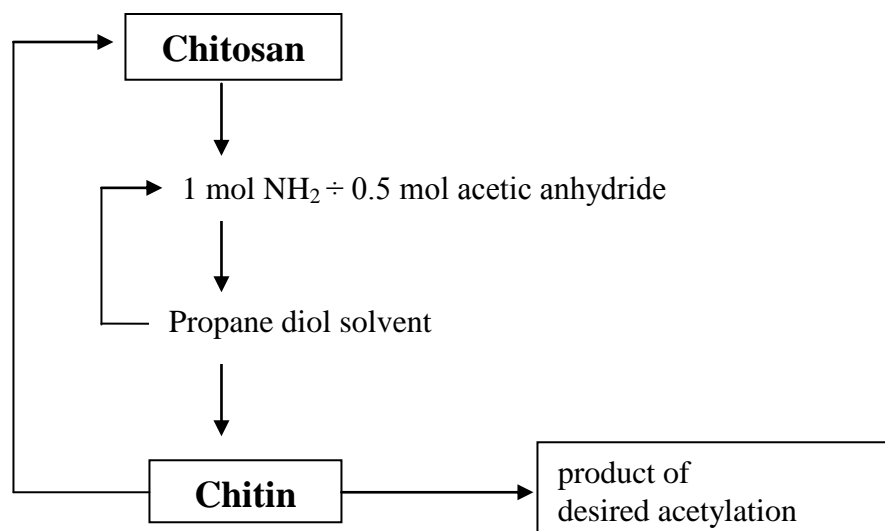


Figure 3. Conversion of Chitosan to Chitin

## 1.2 Solution Properties of Chitin

### 1.2.1 Dissolution of Chitin

Chitosan, the deacetylated derivative of chitin has widely been studied for its modification and potential applications, but reports about chitin are scarce in the literature. The main reason for this is the intractable nature of chitin. This biopolymer, is a highly crystalline polysaccharide, which resists dissolution in common organic and inorganic solvents. It is insoluble in aqueous or common organic solvents. Some specific solvents for chitin are, hexafluoroisopropanol, hexafluoroacetone, chloroalcohols in conjugation with aqueous solutions of mineral acids [Kumar, 2000], dimethylacetamide containing 5% lithium chloride and N-methyl-2-pyrrolidone NMP/LiCl5%. Chitosan, on the other hand is soluble in dilute acids such as acetic acid, formic acid, etc.

In polar aprotic solvents, LiCl will form ion pairs [Morgenstern, 1996], which are characterized by the fact that their constituents are linked electrostatically rather than by covalent bonds. Moreover, anions are poorly solvated while cations are strongly solvated

by solvent molecules. Frequently, solvation of the small lithium cation by DMAc or other tertiary amide molecules is interpreted as complex formation mediated chiefly through interaction of the  $\text{Li}^+$  ion and the carbonyl oxygen of DMAc. Many papers provide experimental evidence for the existence of these LiCl-DMAc complexes. [Morgenstern, 1996] and similar complexes with other dipolar aprotic solvents (HMPTA, DMF, NMP and DMSO) [Morgenstern, 1996], although different views exist on their detailed structure. Some of the proposed structures of the DMAc- $\text{Li}^+$  complexes are shown in Figure 4 (a): proposed by Mc Cormick et al [Mc Cormick, 1985], (b): proposed by El-Kafrawy [El-Kafrawy, 1982], (c): proposed by Turbak [Turbak, 1984], (d): proposed by Morgenstern et al [Morgenstern, 1996].

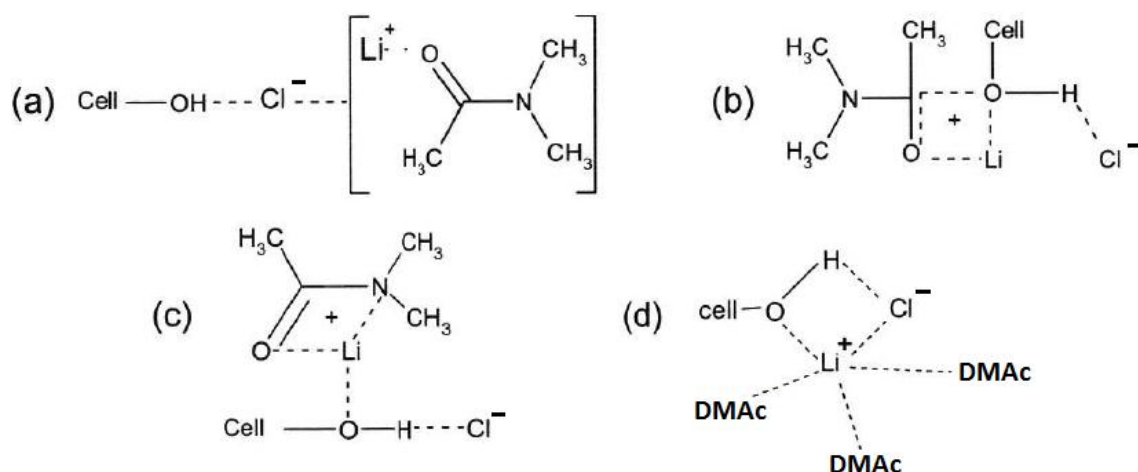


Figure 4. Proposed structures of Chitin DMAc-LiCl complexes (Cell: cellulose or chitin).

The complex formation of LiCl in five amidic solvents, DMAc, NMP, DMF, dimethylpropylene urea (DMPU) and tetramethyl urea (TMU), was studied by  $^{13}\text{C}$ -NMR spectroscopy [Morgenstern, 1996]. Small downfield shifts were observed for the chemical shift of the carbonyl carbons in solutions containing LiCl, Which indicates



reduced shielding of these carbons when LiCl is present. These shifts could be arranged in the following series:



which reflects decreasing strength of interaction between LiCl and amide from DMAc to TMU, that is, reduced complex stability. Solvation of polysaccharides like cellulose and chitin take place via an ion-dipole interaction between polymer and  $[\text{DMAc-Li}]^+$  complex as shown in Figure 5.

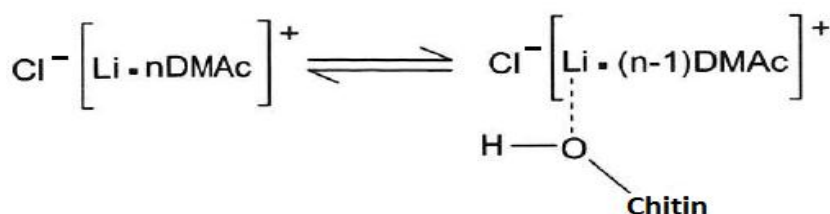


Figure 5. Solvation of chitin by  $[\text{DMAc-Li}]^+$  complex.

## 1.2.2 Characterization of Chitin Solution

### 1.2.2.1 Dilute Solution Viscometry

Viscometry is a simple and rapid method for the determination of molecular weight and polymer conformation in solution. The relative viscosity  $\eta_{\text{rel}}$  of a polymer solution can be calculated by taking the ratio of the viscosity of the polymer solution to the viscosity of the pure solvent.

$$\eta_{\text{rel}} = t / t_0 \tag{1.1}$$

where,

$t$  = efflux time of solution

$t_0$  = efflux time of solvent

$\eta_{rel}$  = relative viscosity

The specific viscosity of a polymer solution is the difference in the efflux times of the solution and the pure solvent, relative to the efflux time of the pure solvent.

$$\eta_{sp} = (t - t_0) / t_0 \quad (1.2)$$

When specific viscosity is divided by the concentration of the solution, then the reduced viscosity is obtained as:

$$\eta_{red} = \eta_{sp} / c \quad (1.3)$$

where,

$\eta_{sp}$  = specific viscosity

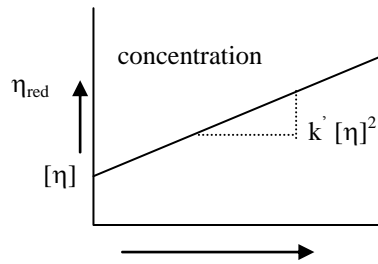
$c$  = concentration

$\eta_{red}$  = reduced viscosity

Table 1. Dilute Solution Viscometry – Definitions

Common name	IUPAC Name	Symbol and definition
Relative viscosity	Viscosity ratio	$\eta_{rel} = \eta / \eta_0 = t / t_0$
Specific viscosity	-----	$\eta_{sp} = \eta_{rel} - 1$
Reduced viscosity	Viscosity number	$\eta_{red} = \eta_{sp} / c$
Inherent viscosity	Logarithmic viscosity number	$\eta_{inh} = \ln(\eta_{rel}) / c$
Intrinsic viscosity	Limiting viscosity number	$[\eta] = \lim_{c \rightarrow 0} (\eta_{red})$

$\eta_0$  = viscosity of the solvent,  $\eta$  = viscosity of a polymer solution



A plot of reduced viscosity vs. concentration. The y-intercept  $[\eta]$ , or the intrinsic viscosity. The slope is related to  $[\eta]$ , it's equal to  $k' [\eta]^2$

$\eta_{rel}$  and  $\eta_{sp}$  depend on the polymer concentration, so to extract the “intrinsic” properties of the polymer chain itself, one must extrapolate to zero concentration. A typical plot is as shown below. The slope of the plot is  $k'$ . The extrapolated back to zero concentration and the y-intercept is the intrinsic viscosity. The intrinsic viscosity is a hypothetical construct. As viscosity varies with concentration, the intrinsic viscosity is the hypothetical viscosity at a hypothetical “zero concentration”. The equation in slope intercept form,  $y = a + bx$ , where  $b$  is the slope of the line and  $a$  is the y-intercept:

$$y = a + bx$$

$$\eta_{red} = [\eta] + b c \tag{1.4}$$

This is known as the Huggins equation in which,

$$b = k_H [\eta]^2 \tag{1.5}$$

where  $b$ , the slope of the line; and  $[\eta]$  is the, the y-intercept.  $k_H$  is the Huggins coefficient . Inherent viscosity is obtained when the natural logarithm of the relative viscosity is taken, and divided into the concentration of the solution.

inherent viscosity =  $\ln(\text{relative viscosity}) / \text{concentration}$

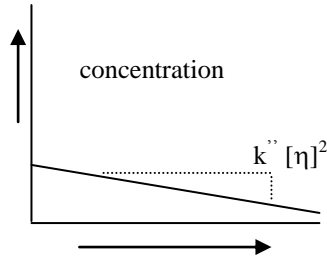
$$\eta_{inh} = \ln \eta_{rel} / c$$

(1.6)

By plotting viscosity on the y-axis, and the concentration on the x-axis,  $[\eta]$  is obtained

according to:  

$$\frac{\eta_{inh}}{[\eta]}$$



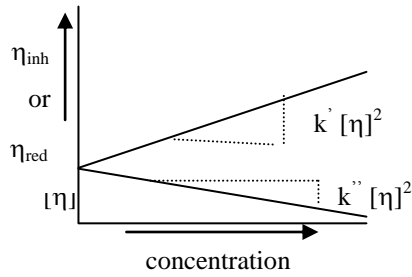
A plot of reduced viscosity vs. concentration. The y-intercept  $[\eta]$ , or the intrinsic viscosity, just like in the plot of reduced viscosity vs. concentration . The slope is again related to  $[\eta]$ , this time it's equal to  $k''$

$$\ln \eta_{rel} / c = [\eta] + k'' [\eta]^2 c$$

(1.7)

where,  $[\eta]$  is the intercept, and the slope is  $k'' [\eta]^2$  .

Intrinsic viscosity is found by using both methods. We usually put the plots from both methods together to get a plot that looks like this, with the two lines meeting at their common intercept:



The data are considered reliable if  $k_H - k''$  is around 0.5.

The polymer solution has to be dilute to measure its viscosity by using the viscometric method. For the concentrated solutions, the polymer molecules might interact with each other. This prevents the accurate measurement and characterization of polymer solution.

For non-electrolyte dilute polymer solutions, a plot of  $\eta_{sp}/c$  versus  $c$  should yield a straight line with intercept and gradient corresponding to  $[\eta]$  and  $b$ , respectively. Theoretically, the parameter  $[\eta]$  measures the effective hydrodynamic-specific volume of an isolated polymer, whereas the quantity  $b$  reflects the binary interactions between polymer segments.

Mark-Houwink-Sakurada (MHS) equation gives the relationship between the intrinsic viscosity and the molecular weight of a polymer sample:

$$[\eta] = K M_v^\alpha \quad (1.8)$$

where,  $K$  and  $\alpha$  are MHS constants for a given polymer at a given temperature in a given solvent.

#### **1.2.2.2 Dilute Solution Properties of Chitin/Chitosan**

Literature reports on dilute solution properties of chitin are scarce. The deacetylated derivative chitosan has been studied in detail because of the ease of dissolution of chitosan in dilute organic or mineral acids. Several studies exist in literature reporting methods to determine molecular weight and size of chitosan samples. Different sets of  $K$  and  $\alpha$  values have been proposed for chitosan samples of given degree of deacetylation in given solvents at constant temperature [Majeti 2000], [Terbojevich 1997]. Chitosan has been reported to assume an extended chain conformation in dilute acid solutions. Chitosan samples with a broad range of degree of acetylation and molecular weights were studied at pH 4.5. It was reported that the degree of ionization does not change significantly with varying ionic strength. Higher N-acetyl content increases the stiffness of the chain. Polyelectrolyte effect exerts a higher influence on the conformation at lower ionic strengths.

Chitin is insoluble in common organic solvents and soluble under highly acidic conditions. NMR spectroscopy studies show that non-degradative solubilization occurs with DMAc-LiCl system so the system is a true solvent for chitin. A higher temperature (around 100 °C) decreasing solvent power of DMAc-LiCl cause gelation. Chitin is partially soluble in DMAc-LiBr solution. NMP-LiCl is also a good solvent for chitin. MHS constants determined for chitin in DMAc/LiCl5% solution are given in Table 2.

Table 2. MHS constants for chitin in DMAc/LiCl5%

Research Group	$\alpha$	K (dL/g)	$M_w$ range ( $\times 10^{-3}$ g mol <sup>-1</sup> )	Temperature (°C)
Terbojevich et al 1988	0.69	$2.4 \times 10^{-3}$	90-510	25
Terbojevich et al 1996	0.88	$2.1 \times 10^{-4}$	120-1200	25
Poirier, Charlet 2002	0.95	$7.6 \times 10^{-5}$	80-710	30

### 1.3 Gel Formation in Polymeric Systems

Chitin solutions result in physical gels upon heating or upon contact with nonsolvents [Yilmaz, 2003], [Yilmaz, 2004]. Formation of a polymer network occurs during gelation. A network polymer is defined as crosslinked polymer where there is a high enough number of crosslinks for all the polymer molecules, or molecular segments to be joined to each other. A polymer gel is a crosslinked network polymer, which is insoluble and is only swollen on contact with solvating liquids. A hydrogel or water-containing gel is a polymer, which is hydrophilic but insoluble in water. In water it swells to an equilibrium volume, but preserve its shape. While insolubility and stability of shape is due to three-dimensional network structure, hydrophilicity is due to the presence of polar groups such as -OH, -COOH, SO<sub>3</sub>OH etc.

A polymer gel may be obtained either by chemical or physical means. Chemical crosslinks are formed between polymerizing species in non-linear step polymerization, for example a rapid change from the fluid state (sol state) to the gel-state occurs during polymerization at a critical conversion  $p_c$ , as the branched polymer molecules begin to join up. Polymer network is also form in addition polymerization of divinyl monomers or in the presence of difunctional (or multifunctional) cross-linking agents. In the case of chemical crosslinking, gelation is an irreversible process.

Physical junction points may also result in a three-dimensional network of polymer chains, several factors may be responsible from physical gel formation. For example, the physical bonds, such as H-bonding, dipole-dipole interaction, that form between the chains may lead to physical aggregations and the aggregates may act as a gel. The junction points may be hydrogen-bonding type of associations of polymer chains. For partly crystalline polymers crystalline micro regions may act as well as cross-linking points. Another phenomenon that may lead to physical gelation is liquid-liquid demixing (spinodal mechanism). This is due to the competition between polymer-polymer and the polymer-solvent interactions such as hydrogen-bonding and hydrophilic interactions. Physical gel formation is usually reversible.

Thermoreversible gelation is due to the formation of a three-dimensional polymer network cross-linked by physical junctions. The thermoreversible gelation of a polymer solution is an equilibrium phenomenon. Normally gelation occurs with decreasing temperatures. In other words, a phase transition from a sol state to a gel state occurs on cooling and a phase transition from a gel state to sol-state (gel melting) on heating. The reverse is also possible depending on whether the solvent power decreases or increases on lowering the temperature.

Whatever the mechanism of gel formation is, a gel exhibits both solid-like and liquid like properties. In a system where the polymer network and the solvent exist together, the network structure prevents the liquid (solvent) from flowing away. It has a shear modulus so it retains its shape. The solvent, on the other hand, prevents the polymer network from collapsing into a compact mass (Collapsed state to swollen state).



Gels have found many technological applications such as disposable diapers, sanitary napkins, as sheets to keep food fresh, as molecular sieves for molecular separation, in drug delivery systems or as actuators or sensors in switching devices on or off.

### **1.3.1 Gelation of Chitin Solutions**

Gel forming materials are needed as dressing for the treatment of ulcers in elderly people, since these materials allow frequent replacement without disturbing the tissues. Also, gel forming materials are useful in drug delivery systems, surgical devices, and in tissue engineering [Muzzarelli, 1998; Mi, 2002; Vachoud, 2000].

Gelation of chitin solutions is possible in three ways: Thermo reversible gelation [Bianchi, 1997], nonsolvent coagulation [Bianchi, 1990; Yusof, 2001], and via chemical modification of chitin or chitosan [Hirano, 1989; Hirano, 1990; Vachoud, 1997]. Thermoreversible gelation of chitin solutions [Bianchi, 1997], coagulation from an alcoholic solution [Khor, 1997] ,[Vachoud, 1997], or gelation by nonsolvent addition [Yilmaz, 2003] is well documented in the literature. Gelation of chitin occurs on decreasing the solvent power by destroying the  $[\text{DMAc-Li}]^+$  or  $[\text{NMP-Li}]^+$  complex that solubilizes chitin.

During thermo reversible gelation, the solvent power decreases on increase in temperature because the complex between LiCl and DMAc is destroyed. Intramolecular hydrogen bonding among chitin chains is reestablished leading to gelation. Bianchi et al. argue that gelation occurs due to the development of side-to-side aggregation. A given chitin chain may participate in the aggregation at different points and when a partial crystallization occurs the three-dimensional network becomes stable. The fact that

transparent gels are formed indicates that the dimensions of the crystalline areas are small.

During gelation by nonsolvent coagulation method, the complex between the [DMAc-Li]<sup>+</sup> ion and the chitin molecule is broken down due to reduced solvent power by the addition of water, ethanol or acetone. As a result, segment-segment interactions namely intra- and inter- molecular hydrogen bonding predominate over segment-solvent interactions to form a network of chains which phase-separate from solution. Crystalline domains also develop, which assist in network formation.

Chemical cross-links are formed between polymerizing species in non-linear step polymerization, for example a rapid change from the fluid state (sol state) to the gel-state occurs during polymerization at a critical conversion  $p_c$ , as the branched polymer molecules begin to join up. Polymer network is also form in addition polymerization of divinyl monomers or in the presence of difunctional (or multifunctional) cross-linking agents. In the case of chemical crosslinking, gelation is an irreversible process.

In the literature blend of 1% chitin poly(D,L-lactide-co-glycolide 50:50) was dissolved in DMAc/LiC5% w/w and chlorambucil(anti-cancer drug) is added stirred and dissolved in it, microspheres have been formed and may be used as a special drug delivery system[Mi, 2002].

## 1.4 Heavy Metal Adsorption by Chitin/Chitosan Gels

Industrial waste waters are contaminated with toxic and hazardous substances especially heavy metals harmful to living things. A few examples are metal finishing, electroplating, painting, dyeing, and printed circuit board manufacture. Adsorption is a widely used and efficient technique applied for waste water treatment for cleaning of the heavy metal pollutants. Heavy metals such as cadmium, cobalt, chromium, copper, lead, mercury, nickel, zinc, arsenic, molybdenum etc., which are highly toxic and dangerous, deserve special attention. Removal of these ions from solution by chitin and chitosan and their derivatives have been studied by many researchers [Guibal, 2004], [Varma, 2004]. One example to these studies is the adsorption of  $Pb^{2+}$ ,  $Cd^{2+}$ ,  $Cu^{2+}$  from an aqueous solution on the cellulose/chitin beads formed by coagulating a blend of cellulose and chitin [Zhou, 2004]. Chitin/Chitosan/Cellulose like naturally abundant materials exhibit a limitation in their reactivity and processability when applied as adsorbents [Amass, 1998], [Illum, 1998]. These polymers have excellent properties such as biocompatibility, biodegradability, non-toxicity, adsorption properties. Modification of these materials with suitable functional groups would increase their applicability as heavy metal adsorbents. Since it is known that removal of mercury from aqueous solution especially drinking water is very important in hydrometallurgical and waste water treatment [Fu, 2011] and since chitin and chitosan are known as cholesterol [Maezaki, 1993; Sreenivasan, 1998; Kim, 1999; Chiu, 2004; Tong, 2005; Zhang, 2008] and heavy metal adsorbents, [Yang, 1984; Hoshi, 1997; Hein, 2005; Wu, 2010; Zhou, 2004] the P4VP grafted chitin beads prepared as a part of this thesis work were tested for their cholesterol,  $Fe^{3+}$  and  $Hg^{2+}$  adsorption properties and were compared to chitin.

## 1.5 Present Work

The aims of this study are; preparation of chitin gels in the form of beads by thermo reversible gelation, nonsolvent coagulation, via chemical modification of chitin, the comparative study of cholesterol and  $\text{Fe}^{3+}$  adsorption behavior on the beads, quaternization of crosslinked P4VP-g-chitin beads with 2-chloroacetamide and their mercury uptake properties.

Thermo reversible gelation of DMAc and NMP has been studied. Here the physical gelation is formed upon contact with heating up to a certain temperature. The effects of the type of solvent, the mechanical tests for the gels, and how the additions of organic acids effects on gelation temperature and mechanical properties, have been studied.

In this study, physical properties of chitin gels obtained by nonsolvent addition and gels prepared by heating to the gelation point followed by nonsolvent addition were investigated. The effects of the type of solvent and the addition of organic acids to the solvent were also studied.

This thesis mainly focusses on chemical modification of chitin via grafting with poly(4-vinyl pyridine) (P4VP). Redox initiator potassium per sulphate ( $\text{K}_2\text{S}_2\text{O}_8$ ) has been used in the reaction medium. The effect of monomer concentration on the extent of grafting (G%), and the efficiency of grafting were studied. Grafting percentages up to 226% were obtained. The capability of chitin to form physical gels has been used to form gel beads of modified chitin by using P4VP. Grafted chitins have been formed under argon gases to prevent humidity within two hours, and then coagulated from the nonsolvent ethanol

in the form of beads. Beads were purified with ethanol in soxlet for a few days then pure water has been used to carry out the removal of impurities and excess 4VP. The product has been characterized by FTIR, TGA, XRD and SEM analyses. The swelling behavior of the beads has been studied in aqueous solution (neutral, acidic and basic medium). By this modification on the chitin backbone with P4VP functional group has been managed to be added so that more uniform beads are formed and the gel network of the chitin is improved to develop more applications such as potential heavy metal adsorbents. These chitin based gel beads which are furnished with additional chemical functionality of the pyridine ring are potential tools for solid phase extraction, or as biosensors.

## Chapter 2

### EXPERIMENTAL

#### 2.1 Chitin, Solvent System, Chitin Solution, Thermoreversible Gelation, Dilute Solution Viscometry

Chitin was purified, and then the solvent systems and chitin solutions were prepared carefully. The prepared solutions were used for thermoreversible gelation and dilute solution viscometry.

##### 2.1.1 Materials

Chitin (Sigma), N, N-Dimethylacetamide, DMAc (Aldrich), N-Methyl-2-Pyrrolidone, NMP (Aldrich), Dimethylformamide, DMF (Aldrich), LiCl, LiBr, NaOH, HCl, EtOH, ascorbic acid, maleic acid, oxalic acid, acetone and molecular sieves (400 Å) were used in the experiments.

##### 2.1.2 Purification of Chitin Powder

Purification process has been applied to the received chitin powder in order to remove the excess proteins and lipids to make it soluble. Chitin was treated with 1 M NaOH for 3 hours at 80°C, and neutralized with water (Checked with litmus paper). 1 M HCl solution is prepared and chitin is digested in it for 12 hours. These processes have been repeated twice. (20.0 g of raw chitin is taken and 11.0 g is obtained.) Chitin powder recovered was soluble in DMAc/LiCl5% w/w or in NMP/LiCl5% w/w solutions.

### **2.1.3 Preparation of Solvent Systems**

The solvent DMAc was dried for 48 h over molecular sieves of 400 Å activated at 280°C for at least 4 h. LiCl salt was dried at 130°C for 3-4 h. The optimum solvent/salt system was prepared by weighing the salt and adding the solvent such that a 5% w/w solution is obtained. Complete dissolution was possible by stirring the solutions overnight (12-16 h). NMP-LiCl and DMF-LiCl solutions were prepared in a similar manner.

### **2.1.4 Preparation of Chitin Solutions**

After preparing the DMAc/LiCl5% solution for dissolving chitin, the problem was to find out the best working concentration. First, 1 % w/v chitin solution has been prepared in DMAc/LiCl5% solution. It was a highly viscous solution, and was not practical to dissolve ascorbic acid, maleic acid or oxalic acid in it. Different chitin concentrations have been prepared (0.1 % chitin DMAc/LiCl5%, 0.3 % chitin DMAc/LiCl5%, 0.5 % chitin DMAc/LiCl5%, and 1.0 % chitin DMAc/LiCl5%) to find out best working concentration. The suitable concentration was 0.5 % chitin DMAc/LiCl5%. Gelation of chitin has been studied in DMAc/LiCl5%, DMAc/LiCl5% + ascorbic acid (AA) (for 0.5 % chitin 0.005 g, for 0.1 % 0.001g AA, etc.), DMAc/LiCl5% + maleic acid, DMAc/LiCl5% + oxalic acid, respectively. By using similar methods, NMP/LiCl5% solution has been prepared. Gelation experiments were carried out using 0.5 % solution of chitin in NMP/LiCl5% alone and in the presence of ascorbic acid, maleic acid or oxalic acid. Similarly the DMF solution for chitin has also been prepared but solubility of chitin in DMF/LiCl5% is very limited. The effect of the organic acids on the pH of the chitin solution was also followed, by using PH meter.

### 2.1.5 Thermoreversible Gelation

Chitin solutions should be protected from humidity or contact with water because chitin gels easily in the presence of water. Two mL of solutions of chitin were placed in 10 mL glass test tubes and heated in an oil bath at a rate of  $2^{\circ}\text{C} / \text{min}$ . The test tubes were turned upside down to test for the completion of gelation. Gelation is considered complete when no flow of solution is observed. Gelation experiments were repeated for chitin solutions containing ascorbic acid (AA), maleic acid (MA) and oxalic acid (OA).

### 2.1.6 Dilute Solution Viscometry

Viscosities for the chitin/DMAc/LiCl were determined using a suspended-level Ubbelohde viscometer (Figure 6) equipped with three bulbs situated at different heights (h) above the bottom of the capillary.



Figure 6. Multigradient Ubbelohde viscometer.



The viscometer is placed in a constant-temperature bath regulated to  $25.0 \pm 0.1^\circ\text{C}$ . The solvent flow times are preferably greater than 100 s for bulbs having a volume about 1 mL. A stopwatch is necessary, having 0.1 s subdivision marks.

Multiple measurements have been carried out and the average efflux time,  $t$ , for each solution concentration was measured. The results were compared to the efflux time of the pure solvent. The efflux time of the pure solvent is given as  $t_0$ .

## **2.2 Preparation and Characterizations of Chitin-Organic Acid Gels**

DMAc/LiCl5% and NMP/LiCl5% solutions of chitin have been prepared. Thermoreversible gelation is used on these solutions and the effect of gelation temperature by additions of organic acids to the solutions has been calculated and after the thermoreversible gelation. The gels are stabilized at room temperature by nonsolvent (ethanol, water, and acetone) addition methods. Later on the gels are characterized by analyzing their FTIR spectra, mechanical properties and swelling properties.

### **2.2.1 Preparation of Chitin-Organic Acid Solutions**

Chitin solutions with 0.5% (w/w) concentration were formed in DMAc/LiCl5% and NMP/LiCl5% solvent systems. Ascorbic acid (AA), maleic acid (MA) and oxalic acid (OA) were added to these solutions at a concentration of 0.005 % (w/w).

### **2.2.2 Preparation of Chitin-Organic Acids Gels**

In the first method, gels were formed by heating the solutions to the gelation temperature and then adding the nonsolvent ethanol. In the second method, gelation was induced by ethanol addition at room temperature.

### **2.2.3 FTIR Spectrum of Chitin-Organic Acids Gels**

FTIR spectra of the dried gels were taken using a Mattson 5000 Satellite FTIR spectrophotometer.

### **2.2.4 Mechanical Tests of Chitin-Organic Acids Gels**

Mechanical analysis of the gels swollen in ethanol was carried out using a Lloyd LRX 5K instrument with a 5000 N cell. The gels whose diameter to length ratio (D/L) was 0.75 were compressed in ethanol at 2 mm/min.

### **2.2.5 Swelling Tests for Chitin-Organic Acids Gels**

The swelling tests were carried out on gels (D/L = 0.33) in ethanol and in pH=7.4 phosphate buffer solution at 37°C. The swelling ratio (Q) was calculated as the ratio of the swollen weight to the dry weight.

## **2.3 Preparation and Characterization of P4VP Grafted Chitin Beads**

Chemical modification of chitin via grafting with P4VP has been carried out. Redox initiator potassium persulphate ( $K_2S_2O_8$ ) has been used in the reaction medium. The effect of monomer concentration on the extent of grafting degree (G%), and the efficiency of grafting were studied. Grafting percentages up to 226% were obtained. The capability of chitin to form physical gels has been used to form gel beads of modified chitin by using P4VP [Yilmaz, 2003]. Grafted chitin has been formed under argon gas to prevent humidity within two hours, and then coagulated from the nonsolvent ethanol in the form of beads. Beads were purified with ethanol in soxhlet for a few days then pure water has been used to carry out the removal of impurities and excess 4VP. The grafting reaction was confirmed by FTIR spectrophotometry. The swelling behaviour of the beads has been studied in aqueous solution (neutral, acidic and basic medium).

### **2.3.1 Materials**

Chitin (Sigma, Germany), DMAc (Aldrich, Germany), LiCl (Sigma, Germany), potassium persulphate ( $K_2S_2O_8$ ) (KPS) (Aldrich, Germany), 4VP (Aldrich, Germany), were purified as described later. Food grade ethanol (Sema, Northern Cyprus) was used as received.

### **2.3.2 Purification of Chitin**

Purification process has been applied to the received chitin powder in order to remove the excess proteins and lipids to make it soluble. Chitin was treated with 1 M NaOH for 3 hours at 80°C, and then it is neutralized with water (Checked with litmus paper). 1 M HCl solution is prepared and chitin is digested in it for 12 hours. These processes have been repeated twice. (20.0 g of raw chitin is taken and 11.0 g is obtained.) Chitin powder recovered was soluble in DMAc/LiCl 5% w/w or in NMP/LiCl 5% w/w solutions.

### **2.3.3 Preparations of Solvent System**

The solvents DMAc was dried for 48 h over molecular sieves of 400 Å activated at 280°C for at least 4 h. LiCl salt was dried at 130°C. The optimum solvent/salt system was prepared by weighing the salt and adding the solvent such that a 5% w/w solution is obtained. Complete dissolution was possible by stirring the solutions overnight.

### **2.3.4 Preparations of Chitin Solution**

Chitin solutions with concentration 1.0% w/v were prepared by dissolving appropriate amounts of chitin in DMAc/LiCl solution. Clear, transparent chitin solutions were obtained after stirring the solutions for at least 48 h at room temperature. The amount of undissolved, swollen material was negligible. The redox

initiator KPS, 1.2 g was dissolved in the 30 mL of DMAc/LiCl15% solvent system, by stirring for 2 minutes, so the final concentration of the chitin is reduced to 0.5%.

### **2.3.5 Purification of 4VP**

The raw 4VP was purified by distillation. The distillation apparatus was setup, oil bath was used in order to get a uniform heat rate at a time, maximum of 120°C is used for the oil bath, steam temperature should not exceed 60°C, small ceramic pieces were used to prevent anti bumping, distillation should be done under vacuum, vacuum pump should be adjustable, magnetic stirrer should be used for uniform heat distribution, vacuum pump should be connected to fume cupboard because of the foul smelling. Pure colorless 4VP was collected under vacuum and stored in the freezer. The color of 4VP could be changed as time passes so redistillation is necessary for the efficient grafting.

### **2.3.6 Preparation of Chitin-Grafted P4VP Solution**

30 mL of 1% clear and transparent chitin in DMAc/LiCl15% solution was taken, and then 1.2 g of KPS was dissolved in the prepared DMAc/LiCl15% solvent system and added to the solution. In order to calculate the effect of monomer concentration to the percent grafting blank, 0.3, 0.9, 1.5 and 4.5 mL of purified 4VP was added to the solution for grafting. For the prepared solution magnetic stirrer with a rate of 50 rpm was used for at 70°C water bath for 2 h under argon atmosphere to prevent humidity were used for grafting. The color changing occurs on the solution as follows; light blue color after 20 minutes, colorless (cream color) after 50 minutes and again light blue color after 110 minutes. The color changing does not occur on the blank solution only cream color within 2 h.

### **2.3.7 Preparations of P4VP Grafted Chitin Beads**

Nonsolvent ethanol (~150 mL) is added into a beaker, magnetic stirrer is used to form more regular beads, and grafted chitin solution was taken into 3 mL plastic transfer pipette and slowly dropped into the nonsolvent. Chitin solution gels in the form of a bead instantaneously. These processes were repeated on blank, 0.3, 0.9, 1.5 and 4.5 mL of 4VP solutions.

### **2.3.8 Purification of P4VP Grafted Chitin Beads**

After the forming P4VP grafted chitin beads, the beads were left for a while in ethanol for color changing (light blue to white). The beads were taken into a cellulose extraction thimble for solvent exchange with ethanol. After two days alcohol rains in soxhlet and 4-5 days ethanol bath in shaker, beads were left into pure water; here the solvent exchange has turned out the white colors of the beads, to a transparent color. After a few days later beads were filtered and placed into the oven to be dried at 60°C for two days.

### **2.3.9 Grafting Percent of P4VP onto Chitin Solution**

After the preparation of chitin-g-P4VP solution as described in section 2.3.6 the product has been coagulated in ethanol by pouring slowly over the magnetic stirrer, so the uniform thin worm like gelation has been formed. Then the product has been purified and dried as described in section 2.3.8. The gravimetric analysis has been done for the calculation of grafting % of chitin as follows:

$$\text{Grafting}\% = \frac{\text{Graft Copolymer (g)} - \text{Chitin (g)}}{\text{Chitin (g)}} \times 100 \quad (2.1)$$

### 2.3.10 FTIR Spectroscopy Analysis

After purifying and drying of the grafted products with different amounts of 4VP and processed non-grafted blank chitin, they were powdered and their KBr pallets were used for FTIR analysis. FTIR analysis was carried out using a Mattson 5000 Satellite FTIR Spectrometer.

### 2.3.11 X-Ray Diffraction (XRD)

X-ray diffraction (XRD) analysis was applied to detect the crystallinity of chitin beads. Shimadzu XRD-6000 diffractometer with Cu-X ray tube ( $\lambda=1.5405 \text{ \AA}$ ) was used. Crystallinity percentage was calculated using the method proposed by Focher et al [Focher, 1990]. The maximum intensity,  $I_{110}$  at  $2\theta$  angle of  $19.28^\circ$  was determined for purified chitin and  $19.46^\circ$  for the grafted product and the amorphous diffraction,  $I_{am}$ , at  $2\theta$  angle of  $16^\circ$  are measured and the crystallinity index is calculated using the formula,

$$CI_{peak} = \frac{I_{110} - I_{am}}{I_{110}} \quad (2.2)$$

### 2.3.12 Thermal Analysis (DSC and TGA)

Differential scanning calorimetry (DSC) and thermal gravimetric analysis (TGA) were done to understand the thermal behaviour of the purified chitin and the grafted products. DSC was performed with a Perkin-Elmer/Pyris-1 calorimeter. The samples were studied under nitrogen atmosphere. Temperature from  $20^\circ\text{C}$  to  $440^\circ\text{C}$  at a heat rate of  $10^\circ\text{C}/\text{min}$  was used. TGA was performed with a Perkin-Elmer/Pyris-1 instrument. The samples were studied under nitrogen atmosphere. Temperature from  $20^\circ\text{C}$  to  $840^\circ\text{C}$  at a heat rate of  $10^\circ\text{C}/\text{min}$  was used.

### 2.3.13 Swelling Behaviour

The swelling behaviour of the processed blank chitin beads without grafted 4VP and P4VP grafted chitin beads has been studied in aqueous solution under neutral, acid and phosphate buffers with a pH values of 7.0, 1.4 and 7.4 respectively at 37°C. The amount of water absorbed was determined gravimetrically and the swelling ratio,  $Q$ , was calculated with respect to time. The formula was used to calculate the swelling ratio:

$$Q = \frac{w_s}{w_d} \quad (2.3)$$

where  $w_s$  is weight of the swollen material,  $w_d$  is weight of dry material.

### 2.3.14 SEM Analysis

Blank and grafted chitin beads were Au (gold) coated using Quorum Technologies SC7640 Sputter Coater Au/Pd instrument. SEM (scanning electron microscope) was performed with a model of JEOL 6335F SEM.

### 2.3.15 Fe<sup>3+</sup> Adsorption onto the Beads

A 50 mg sample of beads was placed in a 50 mL aqueous Fe<sup>3+</sup> solution at pH=1.2 and stirred at 50 rpm at 30°C for 6 h. The initial Fe<sup>3+</sup> concentrations used for the adsorption studies are; 1 and 5 mM. 1 mL of solution was taken at 1 hour intervals and analyzed for Fe<sup>3+</sup> concentration by visible spectrophotometry. The amount of Fe<sup>3+</sup> adsorbed was calculated from the difference between the initial and final concentrations of the solution. Each experiment was repeated twice to get reliable data within ±5% error.

### **2.3.16 Determination of Fe<sup>3+</sup> in Solution**

1 mL Fe<sup>3+</sup> solution was mixed with 1 mL of sulfosalicylic acid dehydrate, (10% w/v) and diluted to 10 mL with a buffer solution of pH=1. The amount of Fe<sup>3+</sup> in solution was determined by visible spectrophotometry at 505 nm using a UV-1201 V spectrophotometer. By using the initial and final absorbance values, the amount of Fe<sup>3+</sup> adsorbed onto the beads was determined as Fe<sup>3+</sup>/g bead. The calibration curve shown in appendix A-10 for the Fe<sup>3+</sup> concentration with respect to absorbance (at  $\lambda=505$  nm) vs. concentration was drawn and a linear equation was obtained within a concentration range of 0.1–5.0 mM Fe<sup>3+</sup>.

### **2.3.17 Cholesterol Adsorption onto the Beads**

Beads was placed into 50 mL aliquets of 5.0 mg/mL, 1.0 mg/mL and 0.5 mg/mL cholesterol solutions in acetone and stirred at 60 rpm at 37°C for 3 h. At one hour intervals, 0.01 mL aliquots were mixed with 1.0 mL cholesterol reagent to analyse cholesterol concentration by the model of BTS 310 spectrophotometer at 505 nm. Cholesterol adsorption was calculated from the difference between the initial and final concentrations of the solution. The calibration curve for the cholesterol concentration with respect to absorbance at  $\lambda=505$  nm was drawn. The calculations were made by using the linear equation obtained. The amount of cholesterol adsorbed was calculated as mg cholesterol/g bead.

## **2.4 Quaternization of P4VP Grafted Chitin Beads**

After the preparation (2.3.7.) and purification (2.3.8.) of P4VP grafted chitin beads, the product is quaternized with 2-chloroacetamide as follows in section 2.4.1.



#### **2.4.1 Quaternization of Crosslinked P4VP Beads**

P4VP-g-Chitin beads (5g) of 420–590  $\mu\text{m}$  size were soaked into the solution of 7.00 g 2-chloroacetamide in 25 mL dimethyl formamide. The mixture was shaken by a continuous shaker for 3 days at room temperature, and then heated to 60°C in a constant temperature bath for 2 h. The light green beads were filtered and transferred into 250 mL water. The product was washed with excess of water (2×250 mL) and left to stand in 50 mL acetone for 3 h. The nearly-white product was filtered, washed with methanol (20 mL) and ether (20 mL). The vacuum-dried sample weighed 7.26g.

#### **2.4.2. Chloride Analysis**

The quaternization yield was followed by analysis of the chloride ions of the final product. Thus 0.3 g of the quaternized beads was boiled in 20 mL of 20% NaOH solution for 3 h. The mixture was filtered and washed with 30 mL distilled water. The filtrate and washings were combined and neutralized with 3 M HNO<sub>3</sub>. The solution was transferred in a 100 mL volumetric flask. Analysis of the chloride ions solution was performed by the mercuric thiocyanate method as described in the literature [Helfferich,1962]. Experimentally 2.48 mmol g<sup>-1</sup> of chloride content was obtained for the quaternized product.

#### **2.4.3 Mercury Adsorption**

The mercury uptake experiments were performed in non-buffered conditions. In these experiments a weighed quantity (0.2 g) of the quaternized polymer first wetted with 5 mL distilled water and 20 mL HgCl<sub>2</sub> solution (0.22 M) was added to the mixture (so that the final concentration was 0.18 M). The mixture was shaken (on a continuous shaker) for 24 h. After filtration and dilution of the filtrate to 100 mL in

volumetric flask, 10 mL of the solution was used for colorimetric analysis of residual mercury by the diphenyl carbazide method [Singh, 1999]. This analysis gave 2.67 mmol g<sup>-1</sup> mercury loading capacity.

#### **2.4.4 Kinetics of the Mercury Adsorption**

Batch kinetic experiments were carried out with highly diluted Hg<sup>2+</sup> acetate solutions to inspect efficiency of the polymer for low mercury concentrations. Thus, 0.25 g polymer sample was mixed with 50 mL of Hg<sup>2+</sup> acetate (100 ppm mercury) and stirred (350–400 rpm) with a magnetic stirring bar. Variation of the mercury concentration was followed by analysis of samples (5 mL) taken at appropriate time intervals. The results were plotted as time in minutes, with respect to adsorbed Hg<sup>2+</sup> concentration in ppm.

## Chapter 3

### RESULTS AND DISCUSSION

#### 3.1 Solution Properties of Chitin

Dilute solution viscometry and thermoreversible gelation of chitin DMAc/LiCl5% and NMP/LiCl5% results are given in sections 3.1.1 and 3.1.2

##### 3.1.1 Dilute Solution Viscometry

Viscosity measurements have been carried out for chitin in DMAc/LiCl5% and in NMP/LiCl5% solutions at 25°C. Flow times of the solvents and the chitin solutions studied are given in Table 3. Each viscosity measurement experiment was repeated at least twice. The results agree with each other within  $\pm 0.2$  second.

Table 3. Flow times of the solvents and the chitin solutions

Chitin concentration (g/dl)	Flow time (s)	Flow time(s)
	Solvent=DMAc/LiCl5%	Solvent= NMP/LiCl5%
-	281.8	456.0
0.050	554.4	954.9
0.033	447.4	770.2
0.025	399.8	684.8
0.020	374.3	630.8
0.017	356.6	602.8
0.014	344.7	586.7

$\eta_{red}$  and  $\eta_{inh}$  values of the chitin solutions given in Table 4 were calculated using the equations 1.1 – 1.3 and 1.6. Intrinsic viscosity values of the chitin solutions were then determined according to equations 1.4 and 1.7 as shown in Figure 7 and Figure 8.

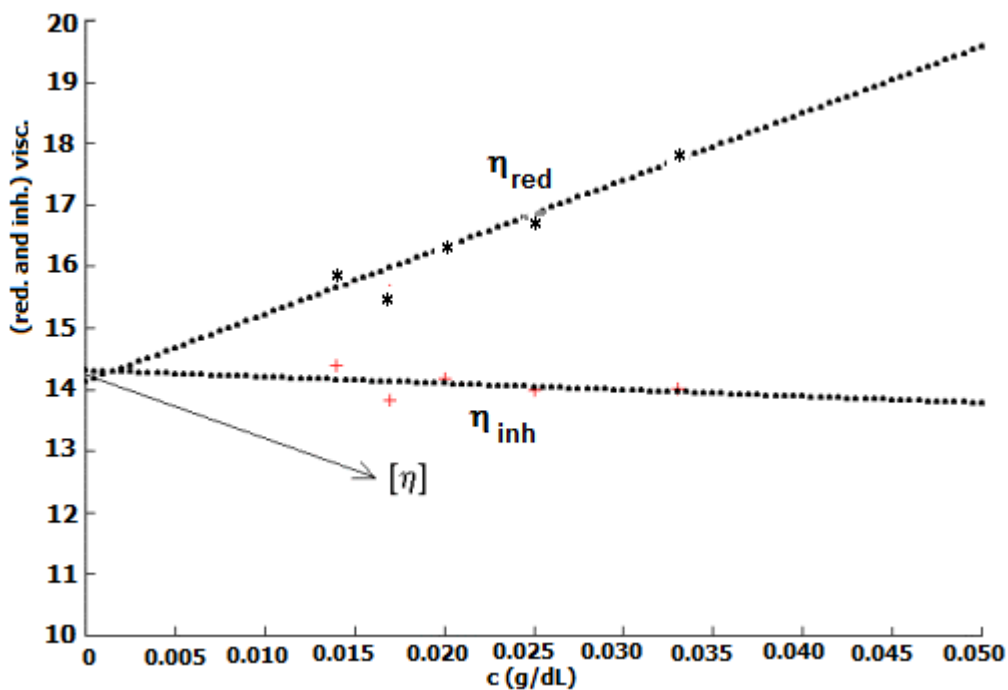


Figure 7.  $\eta_{inh}$  and  $\eta_{red}$  values for Chitin DMAc/LiCl5% solutions as a function of concentration

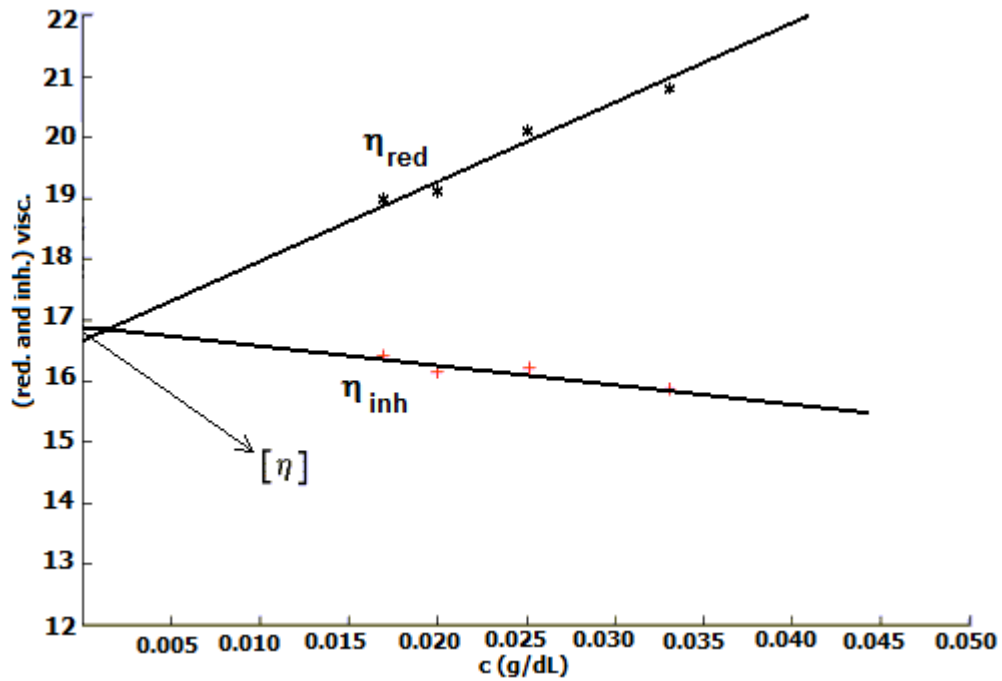


Figure 8.  $\eta_{inh}$  and  $\eta_{red}$  for Chitin NMP/LiCl5% solution as a function of concentration.

Table 4. Reduced viscosity and inherent viscosity of chitin solutions studied

c(g/dL)	$\eta_{red}$ (DMAc)	$\eta_{inh}$ (DMAc)	$\eta_{red}$ (NMP)	$\eta_{inh}$ (NMP)
0.033	17.81	14.01	20.88	15.88
0.025	16.75	14.00	20.07	16.27
0.020	16.41	14.18	19.17	16.22
0.017	15.61	13.83	18.94	16.42
0.014	15.94	14.38	20.47	18.00

The linear regression of the data in Figure 7 ( $\eta_{red} \Rightarrow y = 14.13 + 108.95x$ ,  $\eta_{inh} \Rightarrow y = 14.31 - 10.59x$ ) gives the average intercept as **14.22**, which is the intrinsic viscosity  $[\eta]$  for the chitin in DMAc/LiCl5% solution. The slope is 108.95, which gives the  $k_H$  value as 0.55. On the other hand the intrinsic viscosity  $[\eta]$  for chitin in NMP/LiCl5% solution can be obtained from Figure 8 ( $\eta_{red} \Rightarrow y = 16.76 + 126.2x$ ,  $\eta_{inh} \Rightarrow y = 16.91 - 30.01x$ ) as an average of **16.84** and  $k_H = 0.45$ .

Using the Mark-Houwink-Sakurada equation (1.8) and taking  $K$  and  $\alpha$  values as  $2.1 \times 10^{-4}$  dL/g and 0.88 respectively [Terbojevich, 1997] molecular weight of chitin can be calculated as  $3.1 \times 10^5$  g/mol.

### 3.1.2 Thermoreversible Gelation of Chitin

Gelation temperatures do not vary much, by changing chitin concentration within the range studied. 0.1 %, 0.3 % and 0.5 % chitin with DMAc/LiCl5% solutions has gelation temperatures of 113°C, 113°C and 115°C (Each gelation temperature experiment was repeated at least twice. The results agree with each other within  $\pm 1^\circ\text{C}$ ) respectively. Since the solutions studied are dilute, there is not much difference in the balance between intermolecular interactions between chitin and [solvent-Li]<sup>+</sup> complex and intramolecular chitin-chitin interactions. Therefore, gelation temperature is independent of concentration in the dilute regime studied. At higher concentrations a decrease in  $T_{\text{gel}}$  has been reported [Bianchi, 1996]. This must be due to the presence of more chitin-chitin interactions. Gelation temperatures of chitin in DMAc/LiCl5% and in NMP/LiCl5% solutions in the presence of ascorbic acid, maleic acid and oxalic acid are given in Table 5.

Table 5. Gelation temperatures of DMAc and NMP solutions

DMAc/LiCl5%	Gel T(°C)	NMP/LiCl5%	Gel T(°C)
0.5 % Chitin	115	0.5 % Chitin	134
0.5 % Chitin+AA	97-109*	0.5 % Chitin+AA	128
0.5 % Chitin+MA	112-119*	0.5 % Chitin+MA	142
0.5 % Chitin+OA	110	0.5 % Chitin+OA	Precipitated

$T_{\text{gel}}$  for NMP solution is much higher than that of DMAc solution. This suggests that NMP-Li complex is stronger than DMAc-Li complex. Addition of organic acids to chitin solution lowers the gelation temperature. On addition of 0.01 g of ascorbic acid (AA) to the solution,  $T_{\text{gel}}$  is lowered from 115°C to 97°C, a decrease of 18°C. Addition of the same amount of MA or OA lowers  $T_{\text{gel}}$  to 112°C and 110°C respectively. Lowering of  $T_{\text{gel}}$  on addition of organic acids may be attributed to the competition that arises between the organic acid and the chitin molecules to form a complex with the  $[\text{DMAc-Li}]^+$ . The complex between chitin and  $[\text{solvent-Li}]^+$  complex becomes weaker due to this competition and decomposes at lower temperatures leading to lower gelation temperatures.

The effect of AA on the gelation temperature of 0.5 % chitin-NMP solution is less pronounced than that on chitin-DMAc solution.  $T_{\text{gel}}$  decreases from 134°C to 128°C on addition of 0.01 g of AA. This observation suggests that the  $[\text{NMP-Li}]^+$  complex should be a stronger one than  $[\text{DMAc-Li}]^+$ . This possibility is supported by the colors of the solutions after the heating process. While DMAc/AA solution is yellow, NMP/AA solution is black as shown in Table 6.

Table 6. Colors of DMAc and NMP solutions

Chitin Solution	No Acid	AA	MA	OA
DMAc (before heated)	Colorless	Colorless	Colorless	Colorless
DMAc (after heated)	Colorless	Yellow	Brownish	Brownish
NMP (before heated)	Yellow	Yellow	White	White
NMP (after heated)	Yellow	Black	Black	Black

The gel obtained by heating the chitin/DMAC/LiCl/AA solution was kept around 150°C.

The gel could not be permanently stabilized upon prolonged heating.

Once gelation occurs chitin gel is stable on decreasing the temperature until the gel melting temperature is reached as shown in Table 7.

Table 7. Gel forming and melting temperatures of Chitin/DMAc/LiCl system in the presence of Ascorbic Acid and Maleic Acid.

Solution	Gelation T(°C)	Gel Melting T(°C)
0.5% Chitin + DMAc + AA	109	57
0.5% Chitin + DMAc + MA	119	68

pH values of the solvent systems used for chitin are given in Table 8. Each pH measurement experiment was repeated at least twice. The results agree with each other within  $\pm 0.1$ .

Table 9 summarizes the pH values for different solutions of chitin before and after the gelation, where time t1 is: time required for gelation at a fixed temperature (140°C), and time t2 is: time required for the melting of the gel on cooling to room temperature. Each time measurement experiment was repeated at least twice. The results agree with each other within  $\pm 2$  seconds.



Table 8. pH values of the solvent systems used for Chitin

Solution	pH
DMAc/LiCl5%	6.5
NMP/LiCl5%	6.4
DMAc/LiCl5% + AA	6.2
NMP/LiCl5% + AA	5.8
DMAc/LiCl5% + AA (heated – cooled)	5.6
NMP/LiCl5% + AA (heated – cooled)	5.0

Table 9. pH Values, gelation times of solutions and melting times of gels

Solution	pH	pH (gelled-cooled)	time(second)	
			t1	t2
DMAc LiCl+ 0.5 % Chitin	6.8	6.9	80	130
DMAc LiCl+ 0.5 % Chitin + AA	6.6	6.5	55	165
DMAc LiCl+ 0.5 % Chitin + MA	4.6	5.4	75	135
DMAc LiCl+ 0.5 % Chitin + OA	4.5	4.7	45	125
NMP LiCl+ 0.5 % Chitin	6.3	5.9	155	180
NMP LiCl+ 0.5 % Chitin + AA	5.5	6.6	170	180
NMP LiCl+ 0.5 % Chitin + MA	5.2	5.7	195	130
NMP LiCl+ 0.5 % Chitin + OA	5.1	4.3	No Gel	

The pH values of 0.5 % chitin solution formed in DMAc/LiCl and NMP/LiCl solvent systems are given in Table 9. Addition of AA, MA or OA increases the acidity of the solutions as shown in Table 9. This could be an advantage in future uses of thermo reversible gelation of chitin under acidic conditions. Addition of mineral acids to chitin solution should be avoided since aqueous systems induce gelation of chitin through coagulation out of solution.

## **3.2 Preparation and Characterizations of Chitin-Organic Acid Gels**

Chitin/DMAc/LiCl and Chitin/NMP/LiCl solutions have been gelled upon contact with heating and the gels are stabilized by nonsolvent addition. Gels are characterized by FTIR, mechanical test (Young's modulus was measured) and swelling behaviors.

### **3.2.1 Gel Formation**

Gelation of chitin solutions by nonsolvent addition was studied and the effect of polymer concentration and the type of nonsolvent on gel and bead formation was reported in detail [Yilmaz, 2003].

In this study, gels were formed from chitin solutions at room temperature upon ethanol addition. As a second approach, chitin solutions were heated to the gelation temperature and then further treated with ethanol to obtain stable gels at room temperature as shown in Figure 9. Gels formed by two different methods were compared to each other with respect to their FTIR spectra, mechanical strength, and swelling properties.

Table 10 gives Young's Modulus (E) values, swelling indices (Q) and the gelation temperatures ( $T_{gel}$ ) of chitin gels formed by heating to the gelation temperature followed by ethanol addition. The gelation temperature (134°C) for the NMP-LiCl solution of chitin is much higher than that of the DMAc/LiCl solution of the biopolymer (115°C). This suggests that the  $[NMP-Li]^+$  complex is a stronger one than the  $[DMAc-Li]^+$  complex since gelation of chitin solutions is believed to arise from the decomposition of

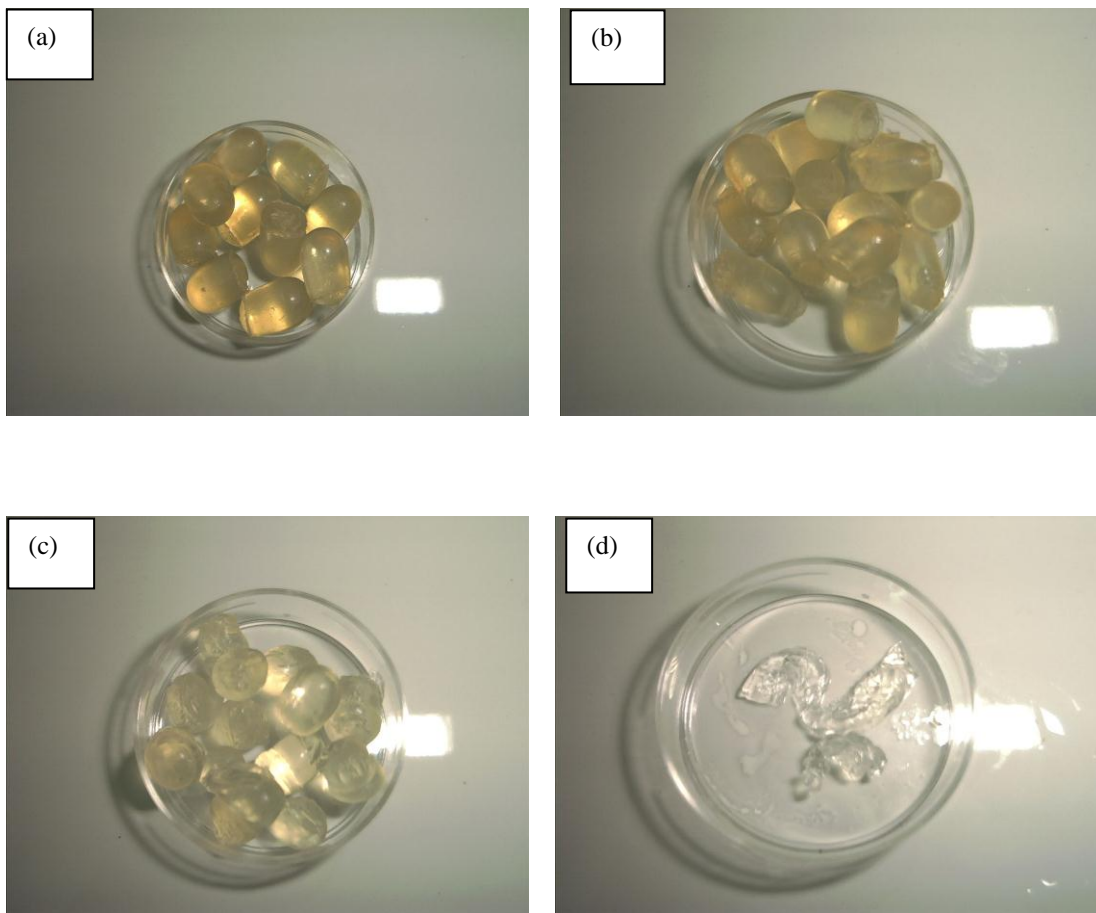


Figure 9. Photograph of the chitin gel formed from ((a) 0.5, (b) 1.0, (c) 1.5) %w/w solution of DMAC/LiCl5% by heating to gelation temperature followed by ethanol addition, (d) chitin gel formed from 0.5 % w/w solution of DMAC/LiCl5% by nonsolvent gelation.

the solvent complex and hence decrease of the solvent power. Addition of organic acids to the gelation system resulted in lower gelation temperatures Table 10. This is related to the complexation ability of the organic acid with the  $[\text{DMAC-Li}]^+$  system. The competition of the carbonyl group of the acid with that of DMAC weakens the  $[\text{DMAC-Li}]^+$  complex, so it decomposes at a lower temperature. The color change in the solutions is an evidence for the complex formation between the organic acid and the solvent during heating. While all chitin solutions in DMAC/LiCl, whether containing an organic acid or not were colorless before the heat treatment, the ones containing an acid change color and form a colored gel at the gelation temperature. The gel formed in the

presence of AA was yellow, and the others were brownish. After the gels were treated with ethanol, they all became transparent as a result of solvent exchange.

### 3.2.2 FTIR Spectroscopy

Chitin gels obtained were characterized by FTIR spectroscopy. Figure 9 shows FTIR spectra of (c) raw chitin, (b) chitin gel regenerated from DMAc/LiCl solution and (a) chitin gel regenerated from NMP/LiCl. In the FTIR spectrum of raw chitin, free O-H groups absorb strongly at  $3450\text{ cm}^{-1}$ , and H-bonded O-H groups are observed to absorb at  $3264\text{ cm}^{-1}$  forming a shoulder.

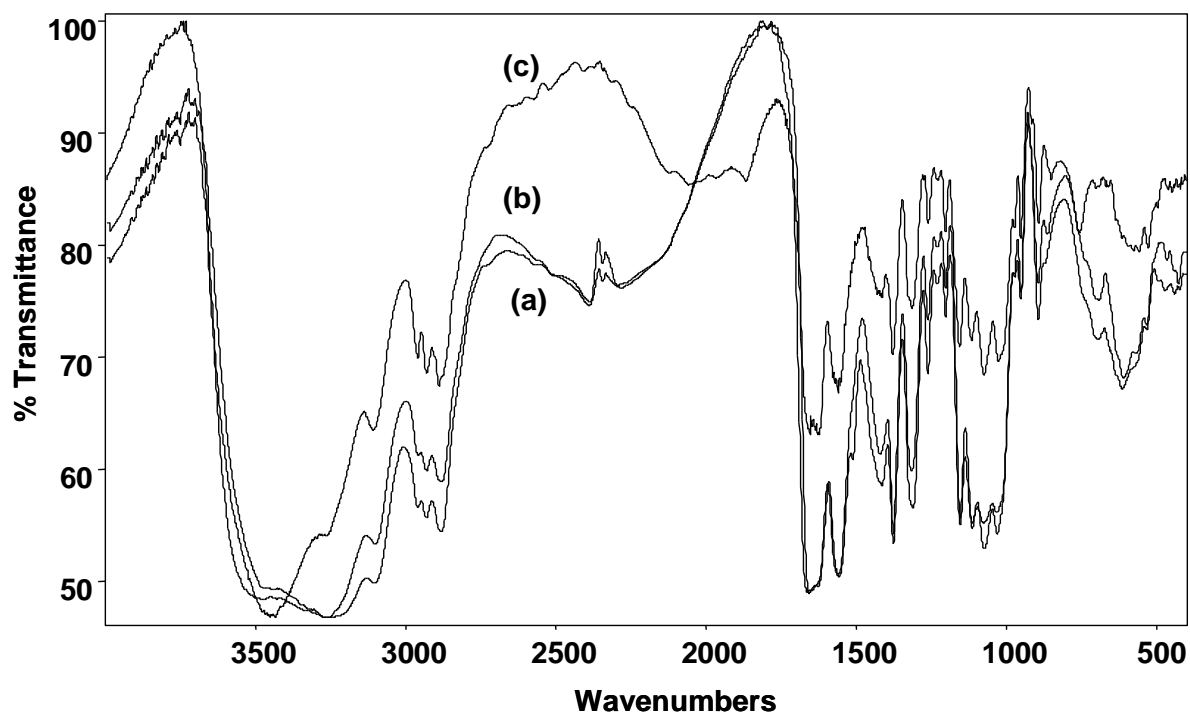


Figure 10. FTIR spectrum of the chitin gel formed from 0.5% w/w solution of (a) Chi/NMP/LiCl5% (b) Chi/DMAc/LiCl5% and (c) original chitin sample.

In the FTIR spectra of the gels regenerated either from DMAc/LiCl or NMP/LiCl solutions, it can be observed that absorption of intermolecularly hydrogen bonded O-H group increases at the expense of the free hydroxyl band, as a consequence of gel formation. FTIR spectra of gels prepared in the presence of organic acids were identical with those of gels obtained in their absence, indicating no chemical change upon treatment with organic acids.

### **3.2.3 Mechanical Analysis**

Gels formed by nonsolvent addition only and without any heat treatment did not have as regular shapes as the ones formed by heating to the gelation temperature. Therefore, no compression tests could be applied on these samples. The gels formed by heating, followed by nonsolvent addition, could easily be obtained in the form of regular cylinders in ethanol. The presence of MA in the DMAc/LiCl5% solvent system led to the formation of a stronger network. This gel had the highest Young's modulus,  $E=0.068$  MPa. The presence of AA, on the other hand, resulted in a weaker gel with  $E= 0.028$  MPa. When mechanical stabilities and gelation temperatures of acid containing DMAc-LiCl based systems are compared to each other, it can be noted that a higher gelation temperature results in a more stable gel, indicating a more compact network formation. This, in turn should be related to the degree and the nature of intermolecular interactions and the amount of polymer taking part in gel formation. The system with AA has the lowest gelation temperature. This indicates that AA has the highest complexation ability with the  $[\text{DMAc-Li}]^+$  system. This could have led to a smaller fraction of chitin molecules to participate in gel formation leading to a weaker gel. When two different solvent systems, NMP/LiCl and DMAc/LiCl, are compared to each other a

similar trend to exhibit a better mechanical strength with higher gelation temperature can be observed.

### 3.2.4 Swelling Properties

Chitin gel obtained from NMP/LiCl solution swells considerably more than the one derived from DMAc/LiCl system as shown in Table 10. Each swelling experiment was repeated at least twice. The results agree with each other within  $\pm 0.1$ . When the gels formed in acid containing solvents are compared to each other, it can be observed that the gel formed in the MA containing system resulted in a gel swelling more than the others both in ethanol and in phosphate buffer. The gel from the AA containing system swells the least. The swelling tests confirm the above given discussion that a smaller amount of polymer is involved during the formation of the mechanically weaker gels. The network elasticity of the gel-AA, for example, should be less than the others due to the smaller amount of polymer involved in the gel formation. A similar observation was made with the swelling behavior of chitin beads formed from different concentrations of chitin solutions [Yilmaz, 2003].

Table 10. Young's Modulus (E) Values and Swelling Indices (Q) and Gelation Temperatures ( $T_{gel}$ ) of chitin gels formed by heating to gelation temperature followed by ethanol addition.

Sample	Chi/NMP LiCl5%	Chi/DMAc/ LiCl5%	Chi/DMAc/ LiCl5%/MA	Chi/DMAc/ LiCl5%/OA	Chi/DMAc/ LiCl/5% AA
$E^*$ (MPa)	0.051	0.042	0.066	0.041	0.028
$T_{gel}$ ( $^{\circ}$ C)	134	115	112	110	97
$Q_{ethanol}$	1.4	1.3	1.8	1.5	1.5
$Q^{**}_{PB}$	2.6	2.1	2.8	2.4	2.2

\* E values determined in ethanol

\*\* Q in phosphate buffer pH=7.4

### **3.3 Formation and Characterization of P4VP Grafted Chitin Beads**

The P4VP grafted chitin beads have been managed to be formed and purified. The gravimetric analysis has been done for the calculation of grafting %. Beads have been characterized by FTIR, Thermal analysis, XRD, Swelling behavior under acid buffer, neutral and phosphate buffer and microstructural analysis.

#### **3.3.1 The Formation of P4VP Grafted Chitin Beads**

Chitin dissolved in an appropriate solvent is known to undergo physical gelation via nonsolvent addition [Bianchi, 1997; Hirano, 1989; Khor, 1997; Vachoud, 1997]. Sol-gel transition may result in bulk gel, [Yilmaz, 2003; Yilmaz, 2005; Bengisu, 2005] bead [Yusof, 2001] or fiber [Kumar, 2000] formation under given conditions. Optimum conditions for strong, spherical, chitin gel beads with a homogeneous surface were established by our group and reported earlier [Yilmaz, 2003; Yilmaz, 2005; Bengisu, 2005]. On the other hand chemical modification of chitin with 4VP followed by beads formation has not been addressed. In this research project we managed to modify the chitin solution by grafting with 4-VP, then followed by the simple and instant method; beads formation via nonsolvent addition [Yilmaz, 2003], so that P4VP grafted chitin beads have been managed to be formed. The Figure 11 is summarizes the whole processes.

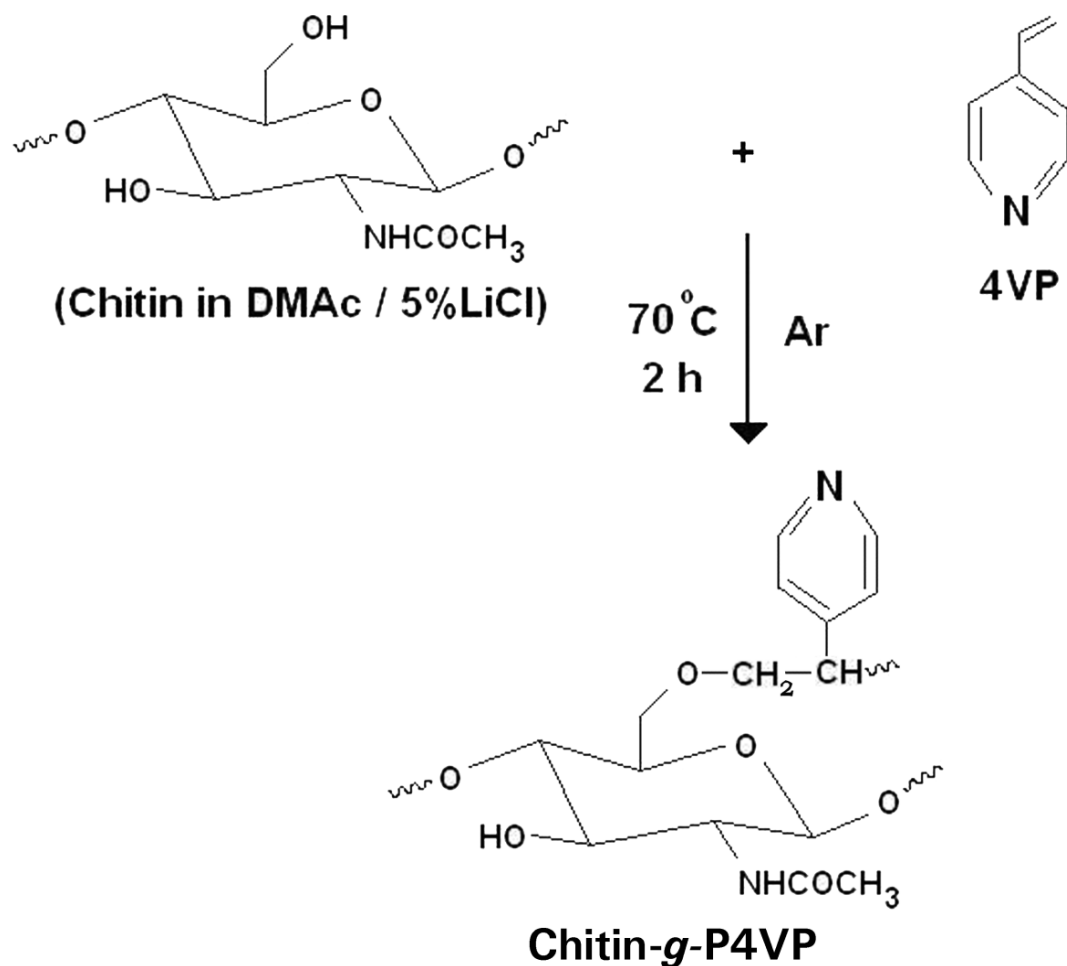


Figure 11. Chemical modification followed by nonsolvent gelation on chitin solution to form beads.

Heating the chitin solution, before the nonsolvent addition, results in stronger gels than by preparing similar gels at room temperature [Yilmaz, 2005]. This is also true for the chemically modified chitin with 4VP.

On the chemical modification process (Figure 12) the blue color occurs due to the addition of 4VP onto the 0.5 % chitin DMAc/LiCl5% solution and upon heating under argon gas, to prevent humidity, and during the nonsolvent gelation process with ethanol. This color is removed in a short period of time by solvent exchange with DMAc/LiCl5%



with nonsolvent ethanol. Here the blue color shows that the chitin solvent DMAc/LiCl5% with 4VP upon heating under argon gas forms a complex, without 4VP this blue color does not exist. This color changing was a light for us on grafting process. The grafted product is coagulated with ethanol to form uniform beads. After the purification processes as described uniform transparent beads have been formed (Figure 13, Figure 14, and Figure 15). Figure 15 (a) is for P4VP-g-chitin beads purified in ethanol followed by water purification. Figure 15 (b) is only ethanol purified; (c) is for ethanol purified blank beads and (d) is blank chitin beads, ethanol purified followed by water purification.

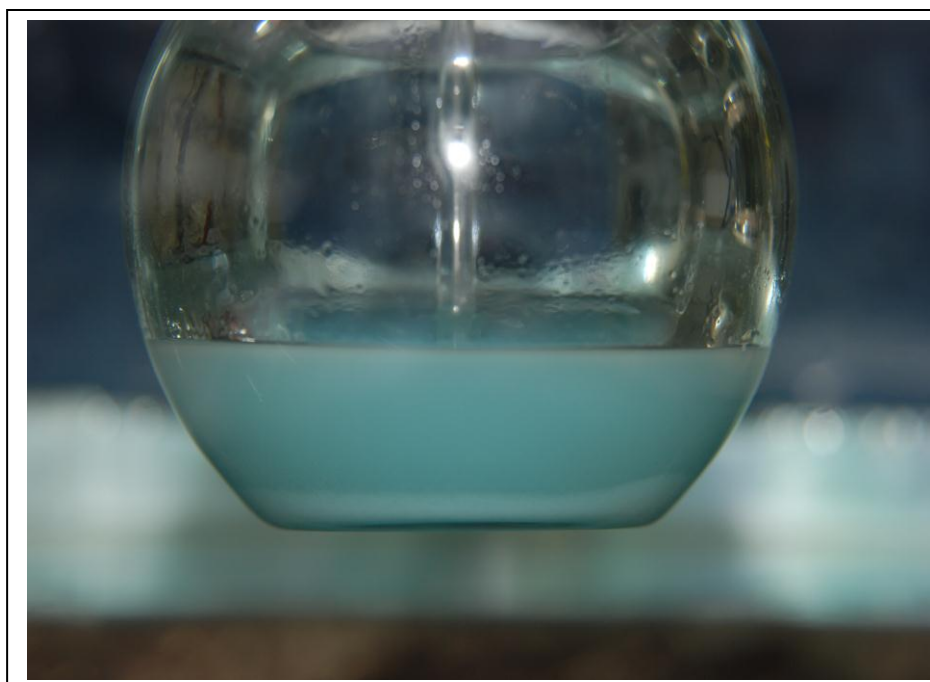


Figure 12. Chemical Modification, chitin-g-P4VP formation.



Figure 13. Optical picture of P4VP grafted chitin beads formed by nonsolvent addition.

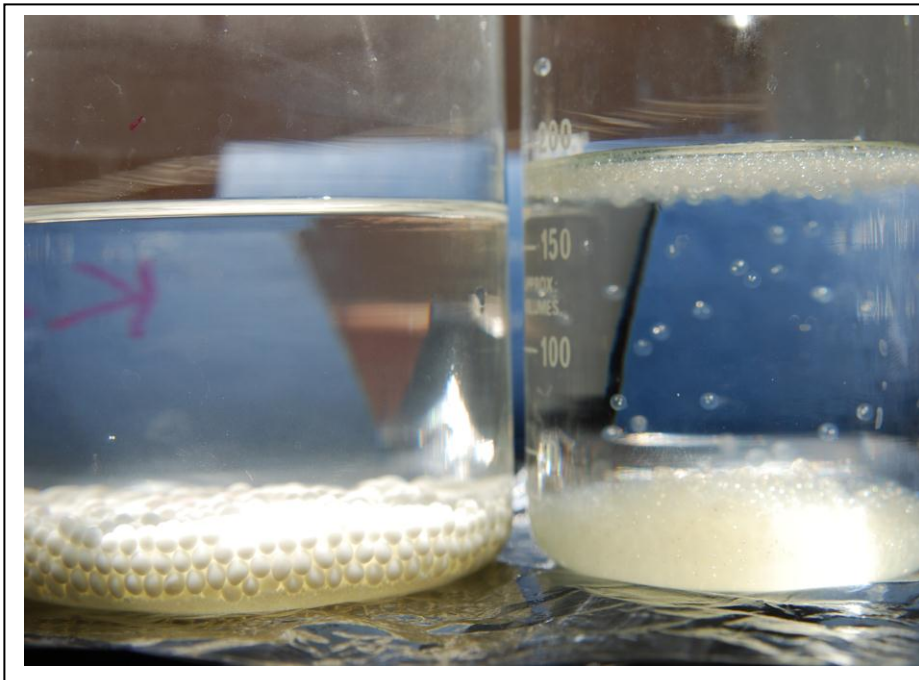


Figure 14. Purification (Et-OH (left), H<sub>2</sub>O (right)), P4VP grafted chitin beads

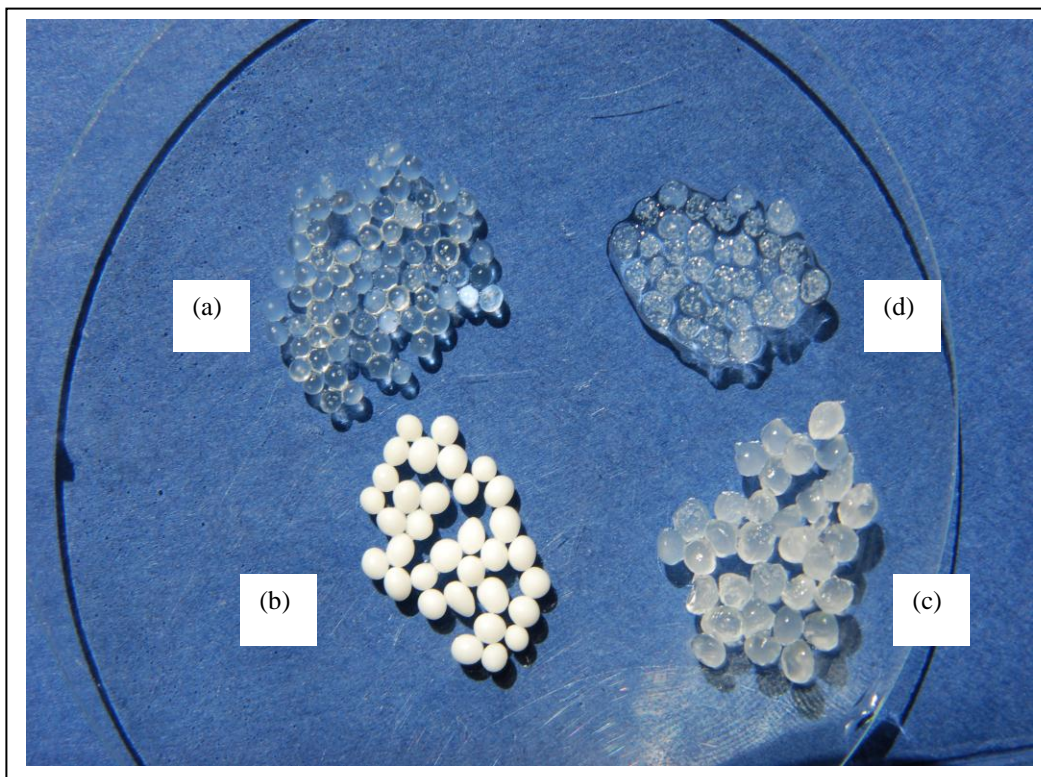


Figure 15. Purified beads, (a) Et-OH, H<sub>2</sub>O purified-grafted, (b) Et-OH purified-grafted, (c) Et-OH, purified-blank processed, (d) Et-OH, H<sub>2</sub>O purified-blank processed

### 3.3.2 Grafting Yield

The equation (2.1) is used experimentally in order to calculate the grafting % of the Figure 12. Each grafting experiments was repeated at least twice, the results agree with each other within  $\pm 1\%$ . The grafting yield was calculated as in Table 11 and Figure 16.

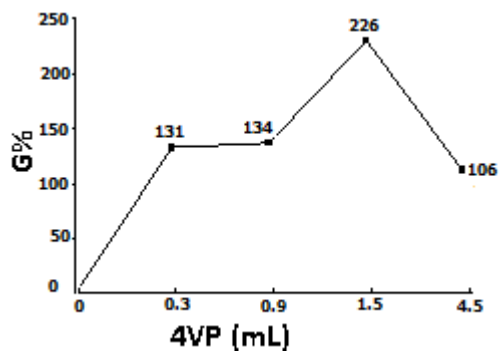


Figure 16. Percent grafting of P4VP grafted chitin with respect to amount of 4VP (KPS 1.2 g).

Table 11. Percent grafting values for different initial amounts of 4VP.

Sample	4-VP (ml)	Grafting %
1	0.3	131
2	0.9	134
3	1.5	226
4	4.5	106

As shown in Table 11 up to 226 grafting % is obtained. At the same time, this was the most uniform and strongest gel compared to others. There is not too much grafting % difference on 0.3 ml and 0.9 ml of 4VP amounts as shown in Table 11. This is only 3%. On the other hand, this difference is 92 % between 0.9 and 1.5 mL. Finally the excess amount of 4VP is not increasing the grafting % linearly, grafting % is even less than 0.3 mL of 4VP by 25%.

A chitin solution with 0.5% (w/v) polymer concentration is viscous enough to lead to strong and spherical gel beads and relatively dilute to be handled easily. Percent grafting value is almost constant up to addition of 0.9 mL 4VP. Then a maximum value of 226 %

is obtained using 1.5 mL monomer. When color changes observed during grafting reaction are considered together with the fact that % grafting value remains the same even if the amount of the monomer is tripled. It can be suggested that a complex formation mechanism is involved in the process. Percent grafting decreases in the presence of 4.5 mL 4VP since probability of homopolymerization increases at higher monomer concentrations [McDowall, 1984].

In this study, the effect of monomer concentration on the grafting yield was studied at a fixed amount of polymer (60 ml 0.5% DMAc/LiCl15% = 0.3 g chitin) at a fixed temperature (70°C is the best grafting temperature for chitosan 4VP, [Caner, 1997]), and at a constant time interval 2 h. The highest grafting is 226 % with 1.5 ml of 4VP amount.

### **3.3.3 FTIR Analysis**

Chitin-*g*-P4VP samples were analyzed by FTIR spectroscopy. The FTIR spectra are shown in Figure 17. The spectrum given in Figure 17(a) and 17(b) belongs to chitin and chitin-*g*-P4VP, respectively. The characteristic amide bands of chitin at 1660, 1626 (Amide I) and 1561 cm<sup>-1</sup> (Amide II) and 1255 cm<sup>-1</sup> (Amide III), the doublets at 1415 and 1561 cm<sup>-1</sup> due to the stretching of C-N and C-C bonds, the C-H and O-H stretchings in the 1400-1200 cm<sup>-1</sup> region, the C-O stretching of the pyranose ring and the etheric linkage between the N-acetylglucosamine units in the 1160-900 cm<sup>-1</sup> are available in the spectrum of chitin. The Amide II band shifted to 1549 cm<sup>-1</sup> with reduced intensity, the C-CH<sub>3</sub> stretching at 1379 cm<sup>-1</sup> appearing as a weak shoulder, new C-N stretchings of C-N-C linkage at 1650 cm<sup>-1</sup> and the aromatic C-H stretching band of 4VP at 824 cm<sup>-1</sup> can be observed in the spectrum of the grafted product. In the 1350-1000 cm<sup>-1</sup> region, the C-

O and O-H stretchings are not as distinctly observable as in the spectrum of chitin. When this analysis is compared to FTIR data on other grafted chitins [Tanodekaew, 2004; Jayakumar, 2008; Filho, 2004] together with proposed reaction mechanisms available in the literature, the synthesis of chitin-g-P4VP can be illustrated as shown in Figure 11.

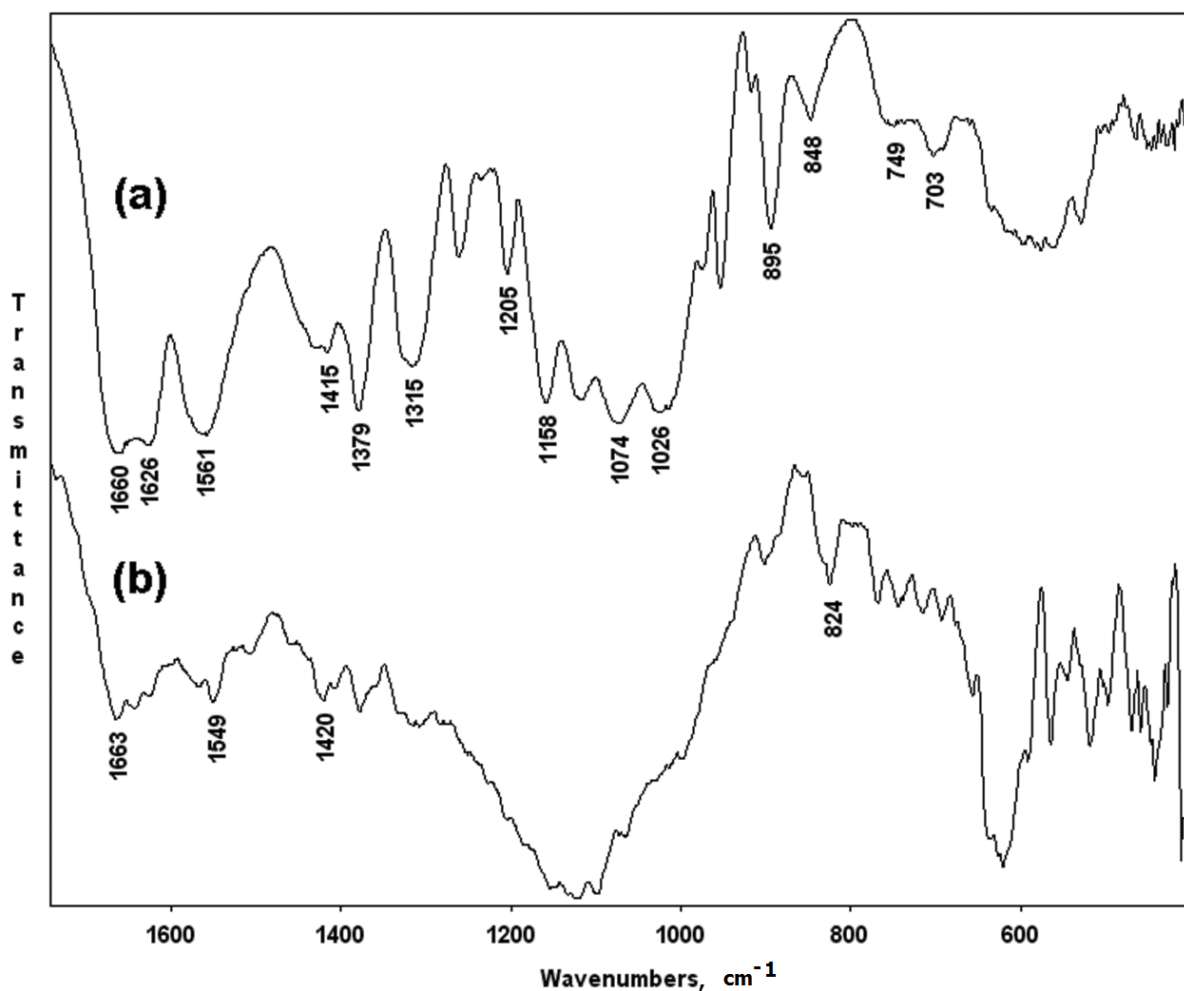


Figure 17. FTIR spectrum of (a) chitin (b) chitin-g-P4VP.



### 3.3.4 XRD Analysis

Crystallinity of chitin and chitin-g-P4VP beads were determined by XRD analysis. Figure 18 (a) and Figure 18 (b) shows the XRD patterns of chitin and chitin-g-P4VP bead (G%=226). Percent crystallinity was calculated using the method proposed by Focher et al using equation (2.2) and Figure 18. Table 12 and Table 13 show the angles at  $2\theta$  for purified and grafted chitins. The maximum intensity,  $I_{110}$  at  $2\theta$  angle of  $19.28^\circ$  measured for chitin was 4250. The corresponding  $2\theta$  angle of the grafted chitin was slightly shifted to  $19.46^\circ$  with a maximum intensity of 2150.

The amorphous diffraction,  $I_{am}$ , at  $2\theta$  angle of  $16^\circ$  was measured as 350 and 550 for chitin and grafted chitin respectively. The crystallinity index was calculated by using Equation 2.2. The calculations revealed that % crystallinity of chitin decreases from 92% to 74% when grafted with P4VP to a grafting extent of 226%.

Table 12. XRD Data

<i>Samples</i>	$2\theta$ ( $^\circ$ )	$d(A)$	$I/I$	<i>FWHM</i>	<i>Intensity</i> (Counts)	<i>Integrated</i> <i>Int(Counts)</i>
<b>ch</b> *	19.28	4.6	100	1.53	1504	111481
	9.29	9.5	41	1.15	616	39885
	26.18	3.4	17	1.16	253	19052
<b>g-ch</b> *	19.46	4.56	100	2.86	581	88531
	9.16	9.65	58	1.62	338	29144
	26.28	3.39	40	1.07	235	15000

**ch**\*: purified chitin, **g-ch**\*: grafted chitin.

Table 13. Crystallinity index calculated by using equation (2)

<i>Samples</i>	$2\theta$ at $I_{110}$ ( $^\circ$ )	$2\theta$ at $I_{am}$ ( $^\circ$ )	$I_{110}(CPS)$	$I_{am}(CPS)$	$Cr I_{peak}(\%)$
<b>ch</b>	19.3	16	4250	350	92
<b>g-ch</b>	19.5	16	2150	550	74

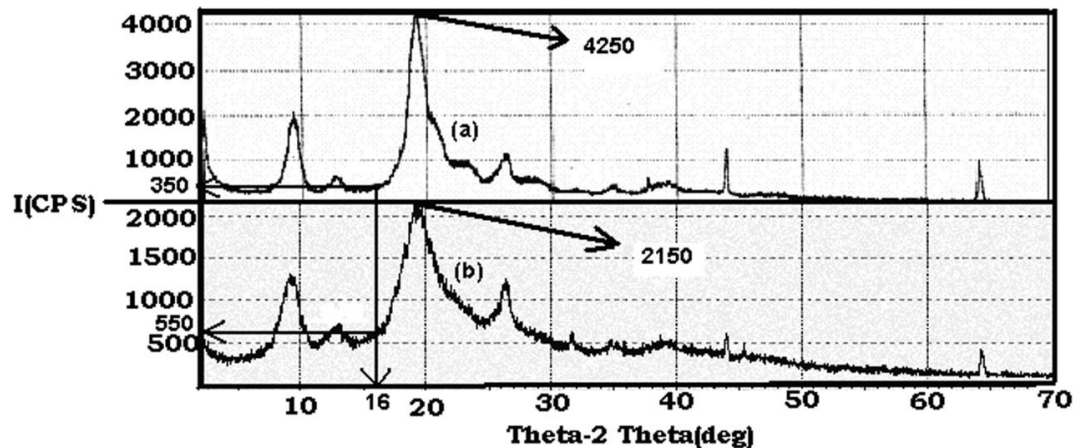


Figure 18. XRD spectrum for (a) chitin and (b) chitin-g-P4VP.

### 3.3.5 Thermal Analysis

TGA and DSC analysis results are shown in Figure 19, Figure 20 and Figure 21, for purified chitin powder and grafted chitin powder. Figure 19(a) shows that chitin has a maximum decomposition temperature of 380°C. On the other hand, this is 305°C for the grafted chitin. At a reference temperature of 500°C, pure chitin has a weight loss of around 75% while the grafted product loses 90% of the initial weight. At 840°C, 87% weight loss is observed. This value is 99.5% for the grafted products. Hence, the grafted products have lower thermal stability than chitin. Lower thermal stability after grafting can mainly be attributed to the disruption of crystallinity to a certain extent as revealed by XRD analysis.

The DSC analysis of Figure 20 and Figure 21 show that water loss occurs at 68°C with a  $\Delta H$  value of 138.7 J/g. This peak shifts to 106°C and 313.2 J/g for chitin-g-P4VP. The second peak of chitin is at 252°C, 8.6 J/g; for chitin-g-P4VP this is at 268°C, with 10.5 J/g. So we can say that the grafted products are more heat stable than chitin up to 300°C.



At higher temperatures (above 300°C) the situation is reversed, chitin has a third peak at 392°C with a 165.9 J/g, but chitin-g-P4VP has an exothermic decomposition around 300°C. So we can say that at higher temperatures chitin is more heat stable than the chitin-g-P4VP due to its higher crystallinity.

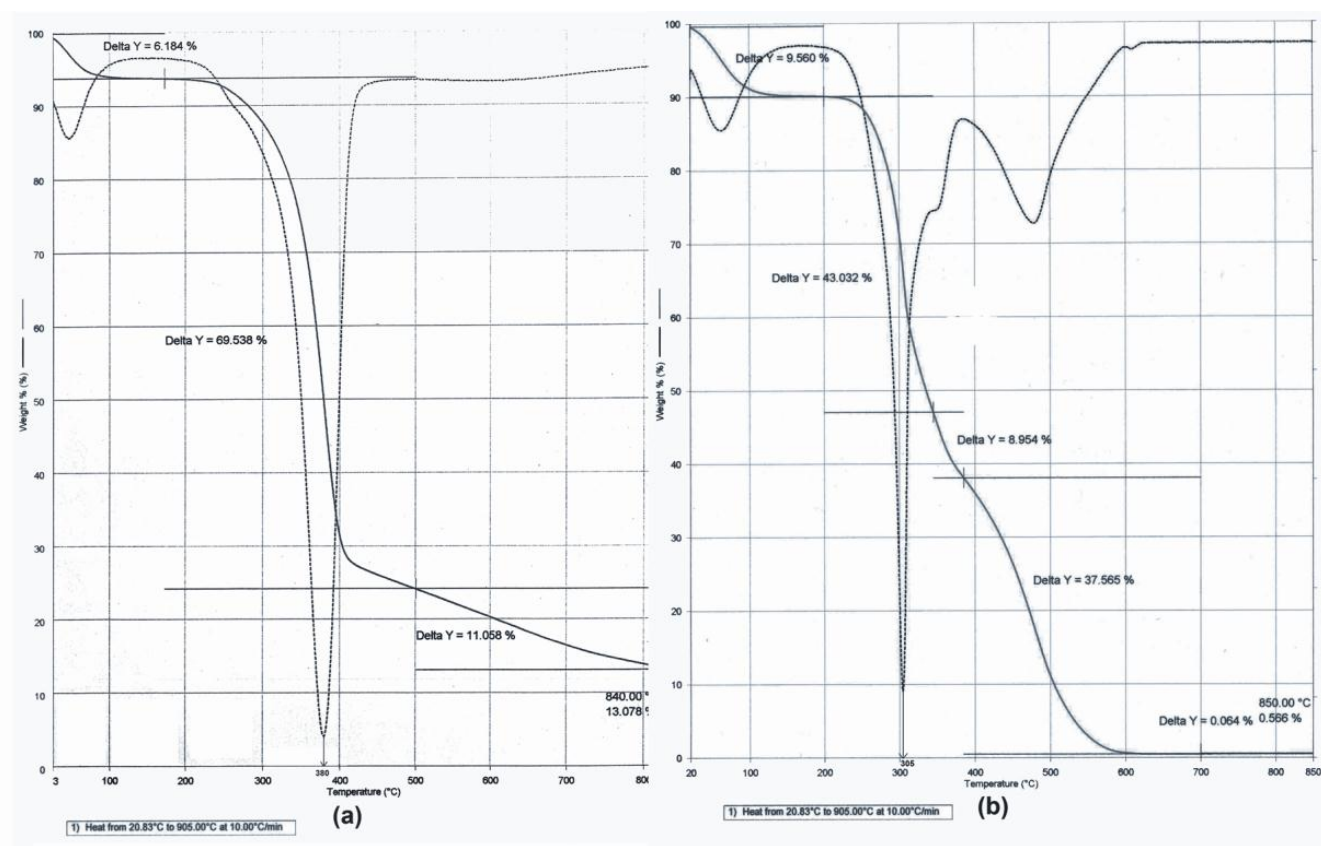


Figure 19. TGA thermogram for (a) chitin (b) chitin-g-P4VP.

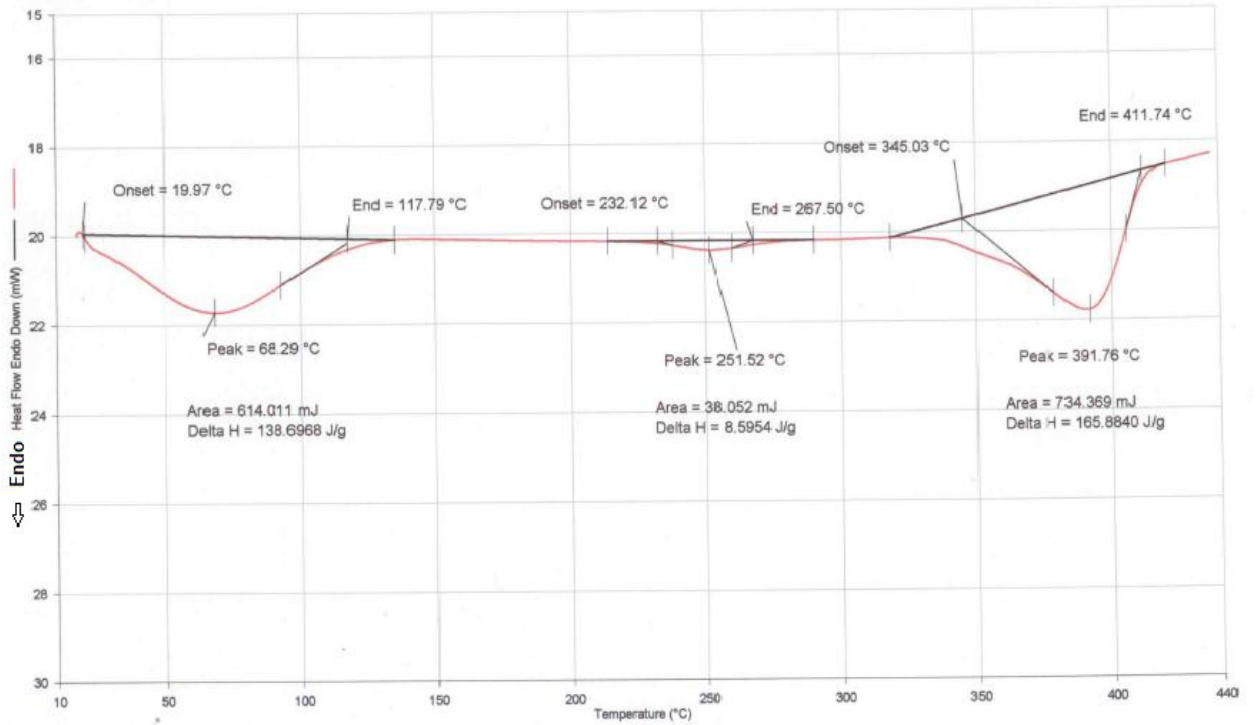


Figure 20. DSC analysis for chitin-g-P4VP.

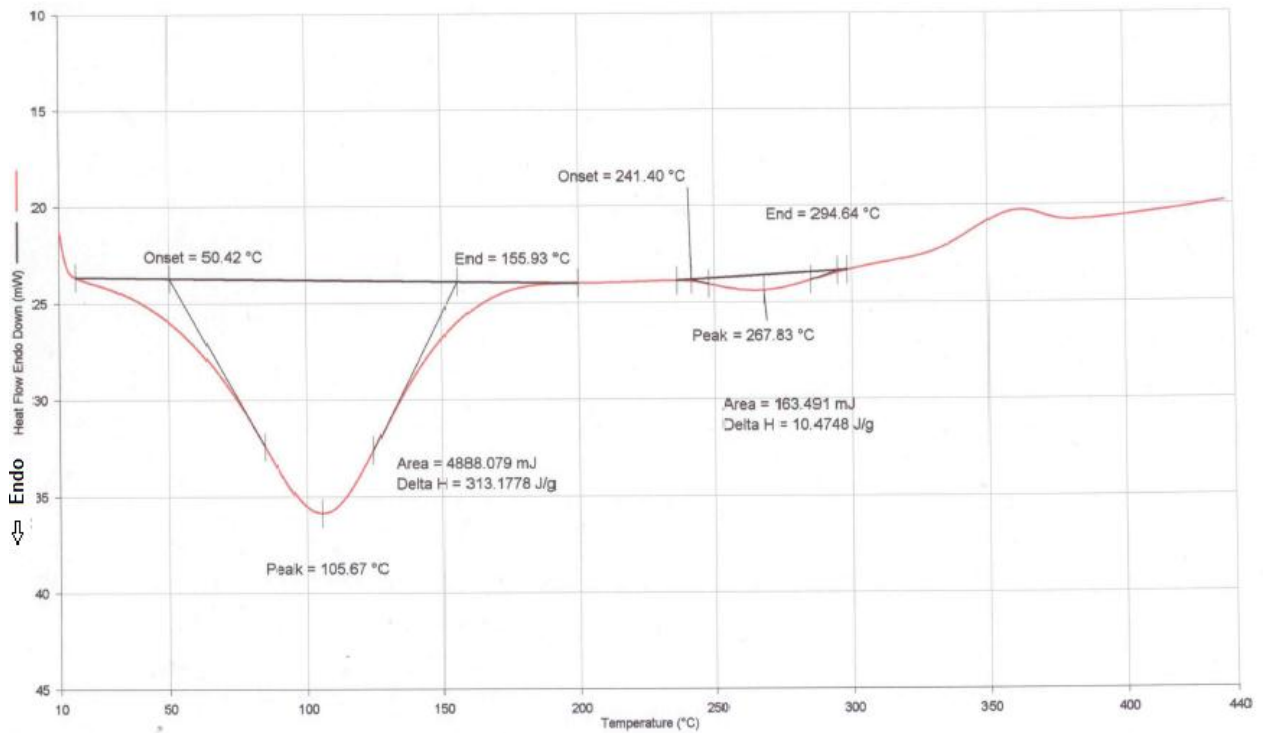


Figure 21. DSC analysis for chitin.

### 3.3.6 Swelling Behavior

The swelling behaviour of the processed blank chitin beads and grafted chitin beads have been studied in aqueous solution under neutral, acid and phosphate buffers with pH values of 7.0, 1.4 and 7.4 respectively at 37°C.

Figure 22 shows that there is not a big swelling ratio difference between chitin and chitin-g-P4VP. At equilibrium the grafted product has a swelling ratio of ~2.7 while chitin beads has a value of ~2.5 at pH 7.0. Figure 23 shows the swelling ratios of chitin and grafted chitin with respect to time in minutes at pH 1.4 acid buffer. Result in Figure 23 shows that again there is not a measurable difference between the swelling ratios (~2.7 to ~2.6 at equilibrium) between the chitin and grafted chitin in acid buffer at pH 1.4. Figure 24 shows that blank and grafted products, have the same swelling ratio value of ~2.5 at pH 7.4 phosphate buffer. Slightly higher swelling capacity of the grafted chitin beads in acidic medium can be attributed to the presence of pyridine group which becomes protonated under the given condition.

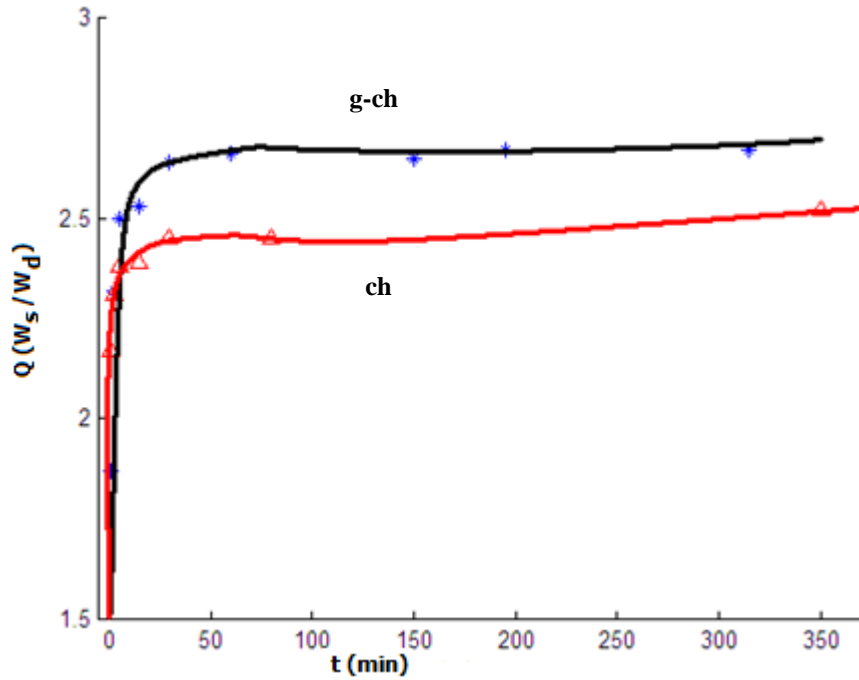


Figure 22. Swelling behaviours for blank chitin beads (ch) and grafted chitin beads (g-ch) with respect to t (min) at pH 7.0.

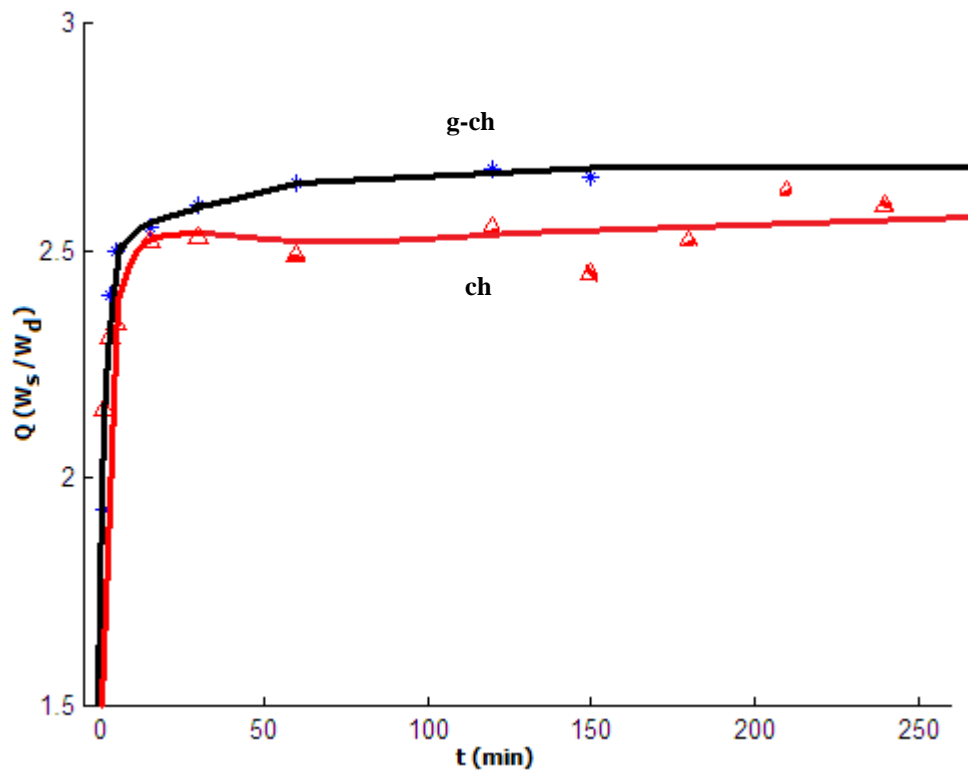


Figure 23. Swelling behaviours for blank chitin beads (ch) and grafted chitin beads (g-ch) with respect to t (min) at pH 1.4.

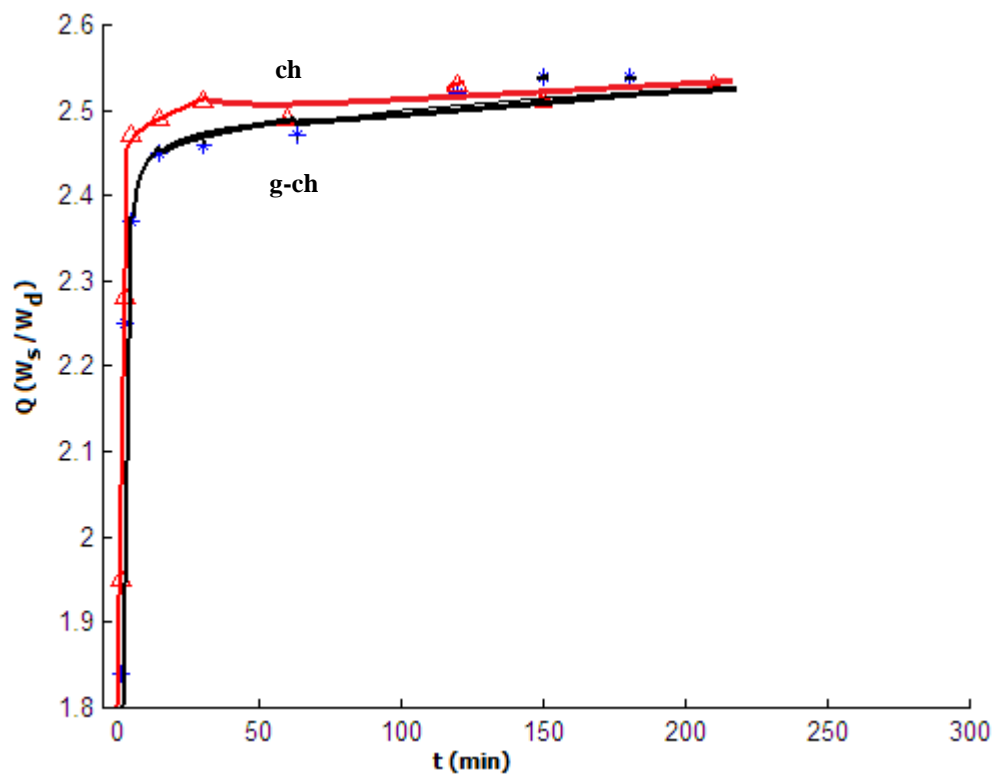
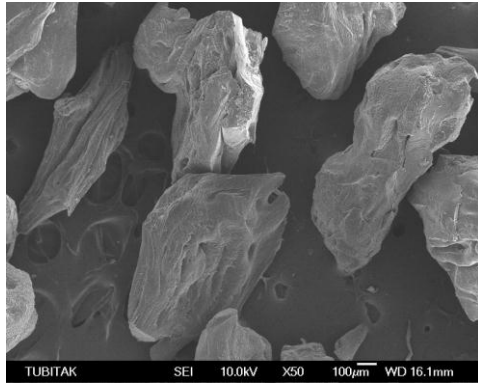


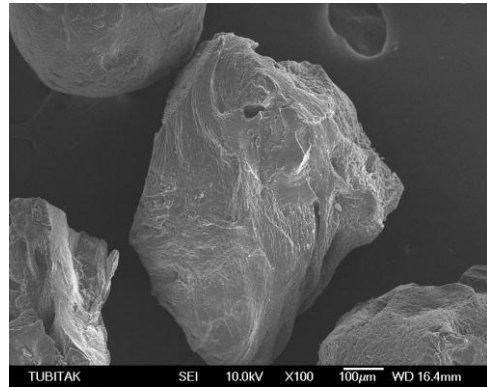
Figure 24. Swelling behaviours for blank chitin beads (ch) and grafted chitin beads (g-ch) with respect to t(min) at pH 7.4.

### 3.3.7 Beads Morphology (SEM)

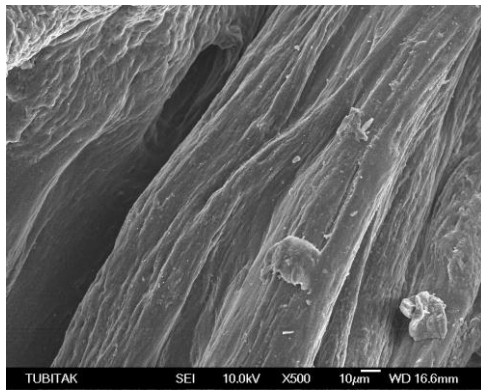
SEM micrographs of the non-grafted and chitin-g-P4VP (G%=226) beads are given in Figure 25 and Figure 26, respectively.



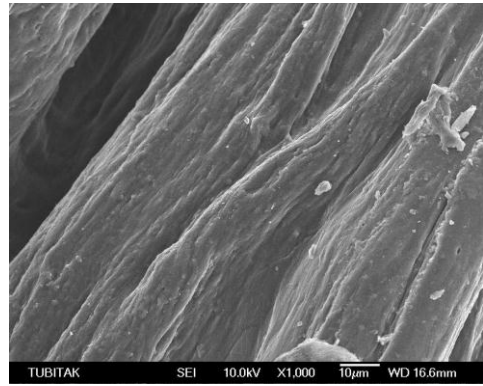
(a)



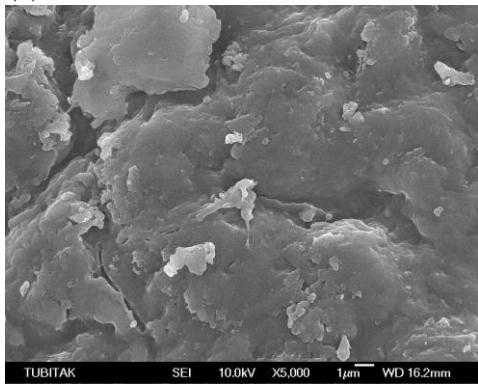
(b)



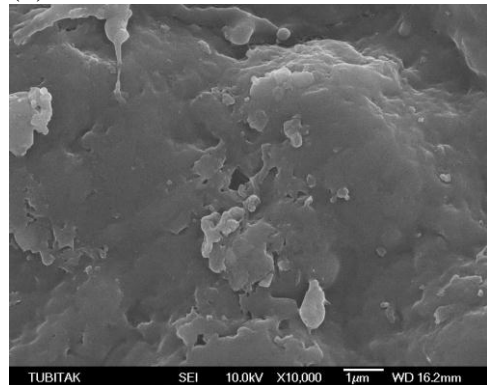
(c)



(d)

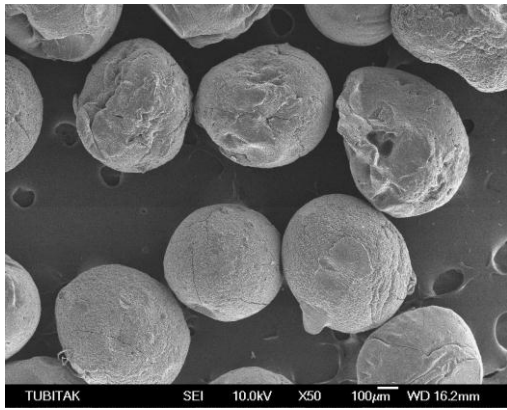


(e)

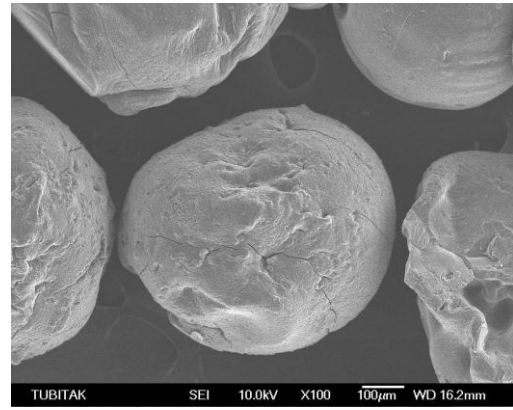


(f)

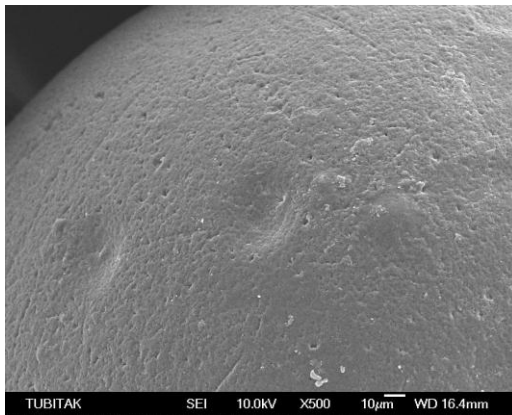
Figure 25. SEM micrograph of the blank chitin beads, (a) is X 50, (b) X 100, (c) is X 500, (d) is X 1,000, (e) is X 5,000, (f) is X 10,000



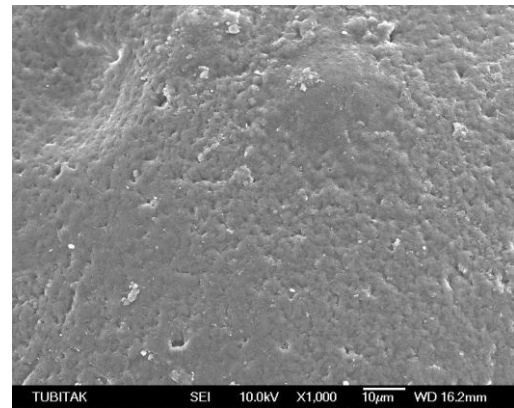
(a)



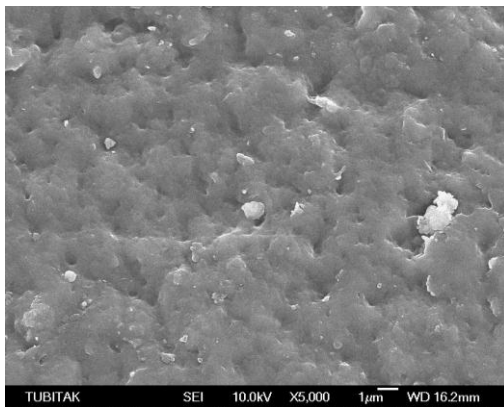
(b)



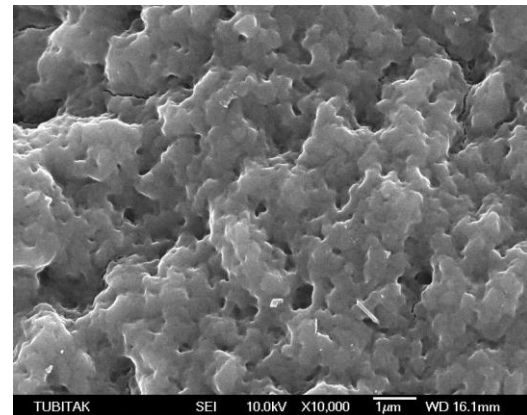
(c)



(d)



(e)



(f)

Figure 26. SEM micrograph of the chitin-g-P4VP beads, (a) is X 50, (b) X 100, (c) is X 500, (d) is X 1.000, (e) is X 5.000, (f) is X 10.000

The beads morphology of the grafted chitin is much more spherical compared to the non-grafted blank chitin beads. The shape of the grafted chitin is much more spherical compared to the non-grafted blank chitin beads. The bead diameters are approximately around 600 $\mu$ m. SEM micrographs with 10.000 magnification shows that gel network structure of the grafted products have a more microporous surface compared to the non-grafted ones, and this is also supporting the XRD, TGA and swelling behaviour data.

### **3.3.8 Fe<sup>3+</sup> Adsorption Behavior**

It can be observed from Figure 27 and Figure 28 that chitin based beads exhibit an initial adsorption-desorption behavior clearly observed in the 5mM Fe<sup>3+</sup> solution. In Table 14 surface adsorption behaviour of the processed blank chitin beads and grafted chitin beads for 1 mM of prepared Fe<sup>3+</sup> solution can be compared. Each adsorption experiment was repeated at least twice. The results agree with each other within  $\pm 0.5$ mg/g. Chitin beads have negligible Fe<sup>3+</sup> adsorption capacity (0-2 mg/g) at equilibrium as shown in Figure 27. Although these beads adsorb a considerable amount of Fe<sup>3+</sup> within the first 3 h in 5 mM solution, the adsorbed ion is desorbed and equilibrium is reached after 3 h with a negligible amount of ion left on the adsorbent (2 mg/g). The concentration gradient is a driving force for the migration of the ions towards chitin beads resulting in temporary adsorption. When the solute concentration is higher, there is a higher probability of having Fe<sup>3+</sup> ions in close vicinity of the beads resulting in adsorption of a given amount of the ion on the bead surface. Since non-grafted (chitin) beads have non-porous surfaces (Figure 25), diffusion of the ions into the inner parts in the bead structure is restricted. Hence, binding is expected to occur only on the bead surface which later allows easier desorption. Desorption is observed in between second and third contact h which is more



pronounced in higher concentration adsorption media (5mM Fe<sup>3+</sup> solution) rather than in 1mM solution since a higher amount had been adsorbed initially. This behavior indicates that there is a competition between the ions in the adsorbed state and in the dissolved state. Since there are no specific chemical interactions such as complex formation between Fe<sup>3+</sup> and chitin which may hold the adsorbed ions on the bead surface, Fe<sup>3+</sup> adsorbed on chitin beads via physical interactions only, prefer to migrate back to the solution to restore the chemical potential and reach a thermodynamically more stable state. On the other hand, in the case of the chitin-g-P4VP beads, the weak desorption process that takes place between the first and second contact h is followed by resorption and equilibrium. Chitin-g-P4VP beads reach equilibrium adsorption capacity (20 mg/g) within first 30 min in 1 mM Fe<sup>3+</sup> solution whereas an equilibrium adsorption capacity of 60 mg/g is attained after 3 h contact in 5.0 mM solution (Figure 28). Hence, Fe<sup>3+</sup> adsorption capacity of chitin based gel beads has significantly been improved by P4VP grafting. In addition to the chemical affinity of the pyridine group towards Fe<sup>3+</sup> ion, the fact that chitin-g-P4VP beads have microporous morphology enhances their adsorption capacity. It can be proposed that the micropores allow diffusion of the ions in solution into the bead structure. Hence, binding to the chemically modified sites both on the outer and inner surface is achieved. The proposed adsorption mechanism onto non-grafted and grafted chitin beads in aqueous solution is described in Scheme 1.

Table 14. Fe<sup>3+</sup> adsorption onto, chitin-g-P4VP and processed blank chitin beads in 1mM Fe<sup>3+</sup> solution.

Time (hr.)	Fe <sup>3+</sup> adsorption onto chitin-g-P4VP (mg/g-bead)	Fe <sup>3+</sup> adsorption onto processed blank chitin (mg/g-bead)
0.25	20.90	2.13
0.50	21.92	1.33
0.75	21.12	0.71
1.00	16.89	1.29
2.00	20.24	0.33
3.00	19.47	1.33
4.00	20.01	0.92
5.00	20.18	0.01
6.00	18.48	0.29

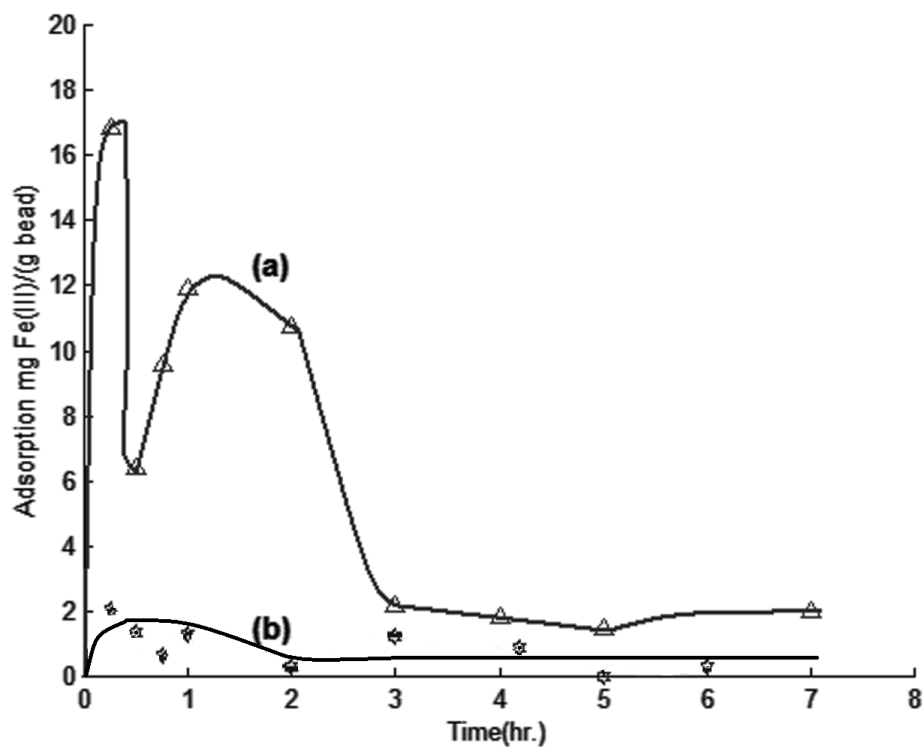


Figure 27. Fe<sup>3+</sup> adsorption (mg Fe<sup>3+</sup>/g bead) for chitin beads in (a) 5.0 mM Fe<sup>3+</sup>, (b) 1.0 mM Fe<sup>3+</sup> with respect to time.

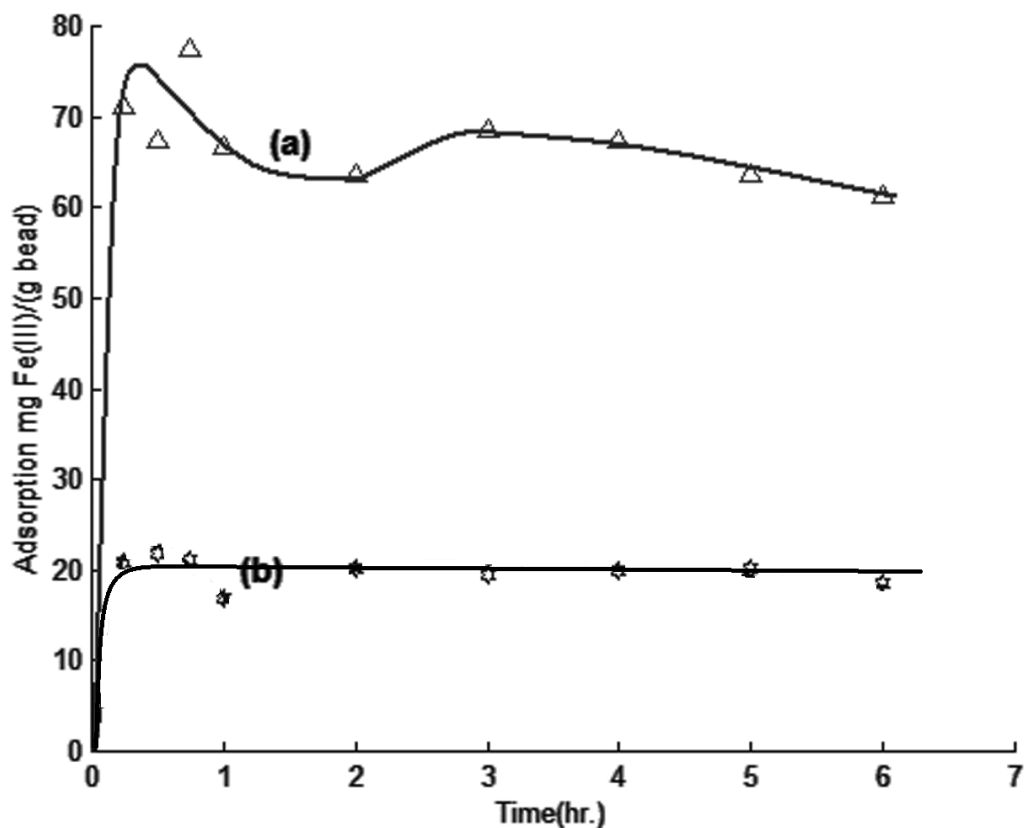
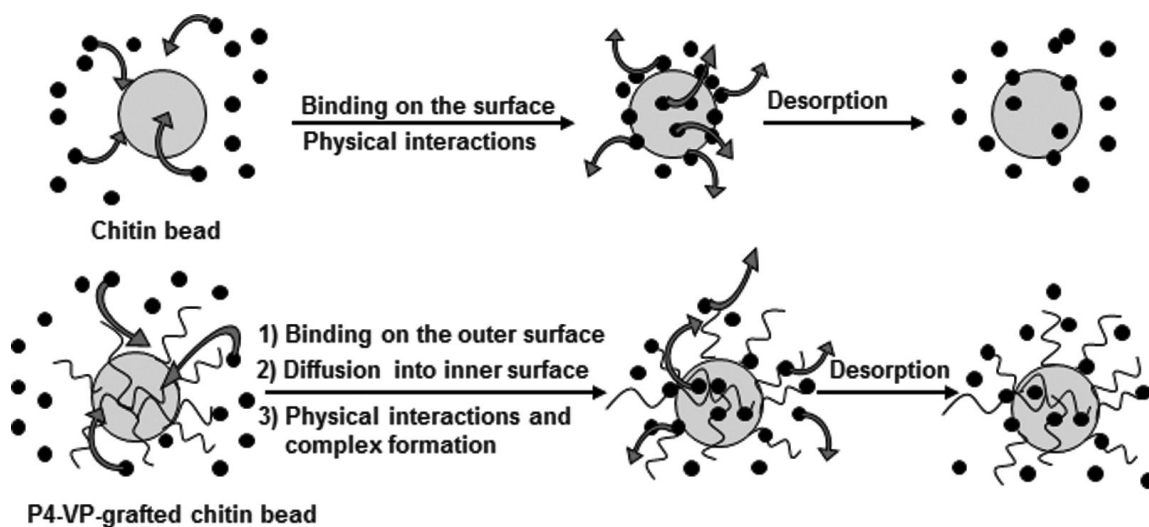


Figure 28.  $\text{Fe}^{3+}$  adsorption ( $\text{mg Fe}^{3+}/\text{g bead}$ ) for chitin-g-P4VP beads ( $G\%=226\%$ ) in (a)  $5.0 \text{ mM Fe}^{3+}$ , (b)  $1.0 \text{ mM Fe}^{3+}$  with respect to time.



Scheme 1. Adsorption mechanism onto chitin and chitin-g-P4VP beads.

### 3.3.9 Cholesterol Adsorption Behavior

Table 15 compares the cholesterol adsorption capacities of chitin-*g*-P4VP beads ( $G\%=226$ ) and chitin beads. Grafting P4VP on to chitin gel beads leads to an increased cholesterol adsorption capacity. Cholesterol adsorption of chitin gel beads has been increased by 30% when grafted with P4VP. The increase in the cholesterol adsorption capacity can be attributed to both chemically and physically modified bead surface which leads to an improved physicochemical interaction with cholesterol. The beads remain unswollen in acetone solution; therefore cholesterol adsorption must mainly occur on the bead surface. The cholesterol adsorption behavior of chitin-*g*-P4VP beads are shown in Figure 29. In 0.5 mg/mL cholesterol solution in acetone, the amount of cholesterol adsorbed increases with time and reaches equilibrium within an hour. The equilibrium adsorption capacity of the chitin-*g*-P4VP bead is 433 mg/g bead in 0.5 mg/mL solution. In more concentrated cholesterol solutions of 1.0 mg/mL and 5 mg/mL concentration, an adsorption-desorption-resorption process which is pronounced in the 5 mM solution is observed, as explained above. An equilibrium adsorption capacity of 577 mg/g bead and 744 mg/g bead in 1.0 mg/mL and 5 mg/mL solutions respectively has been achieved after 2 h of contact with the cholesterol solution. Each experiment was repeated at least twice. The results agree with each other within  $\pm 5$  mg/g.

Table 15. Cholesterol adsorption onto, chitin-g-P4VP and chitin beads in 1mg/ml cholesterol solution.

Time (min)	Cholesterol adsorption onto chitin-g-P4VP (mg/g-bead)	Cholesterol adsorption onto chitin (mg/g-bead)
30	405	384
60	425	368
120	314	292
180	577	235

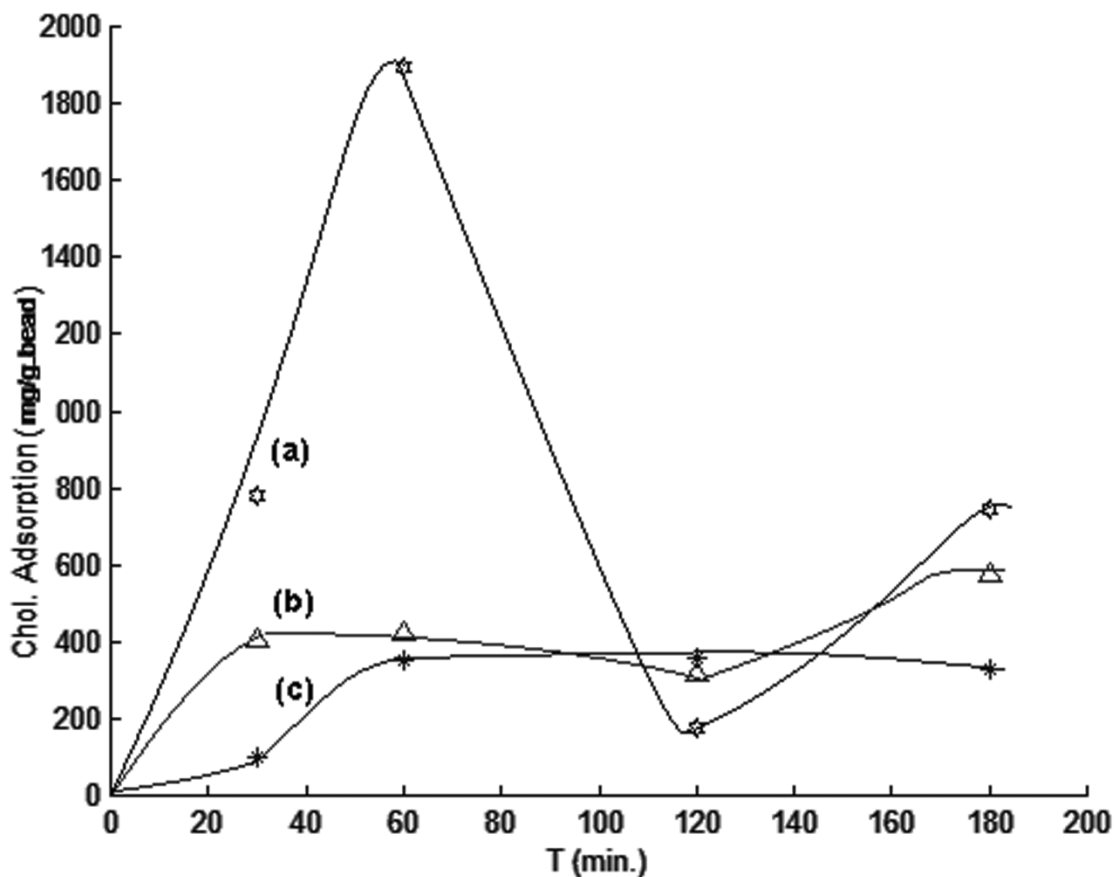


Figure 29. Cholesterol adsorption for chitin-g-P4VP beads with respect to time (a) 5.0 mg/ml, (b) 1.0 mg/ml, (c) 0.5 mg/ml cholesterol concentration.

### 3.4 Quaternization of Chitin-g-P4VP Beads

In the literature, quantitative quaternization of P4VP with active halogen compounds [Nunez, 1998], 1-chloroacetone and 2-chloroacetamide, has been described. In the present work, chitin-g-P4VP beads with 2-chloroacetamide has been successfully quaternized. Figure 30 shows the whole process (grafting followed by quaternization). Figure 32 gives the SEM pictures of the quaternized P4VP grafted chitin beads. Figure 33 compares the SEM pictures of the blank, the grafted and the quaternized chitin beads.

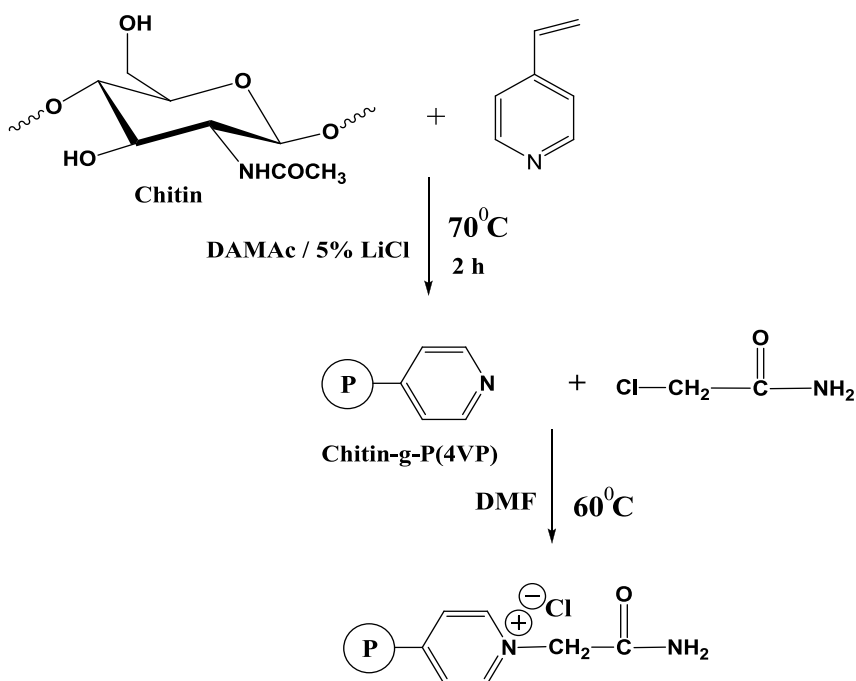


Figure 30. Quaternization of Chitin-g-P4VP Beads with 2-Chloroacetamide.

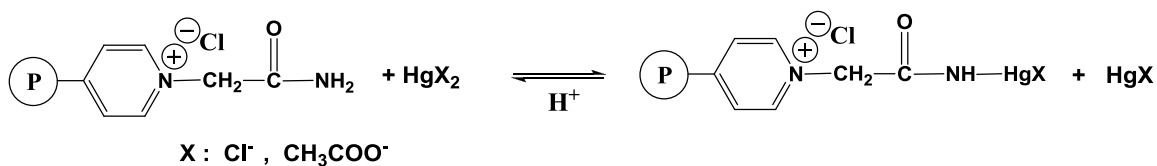


Figure 31. Binding of Mercury Ions on Quaternized Chitin-g-P4VP.

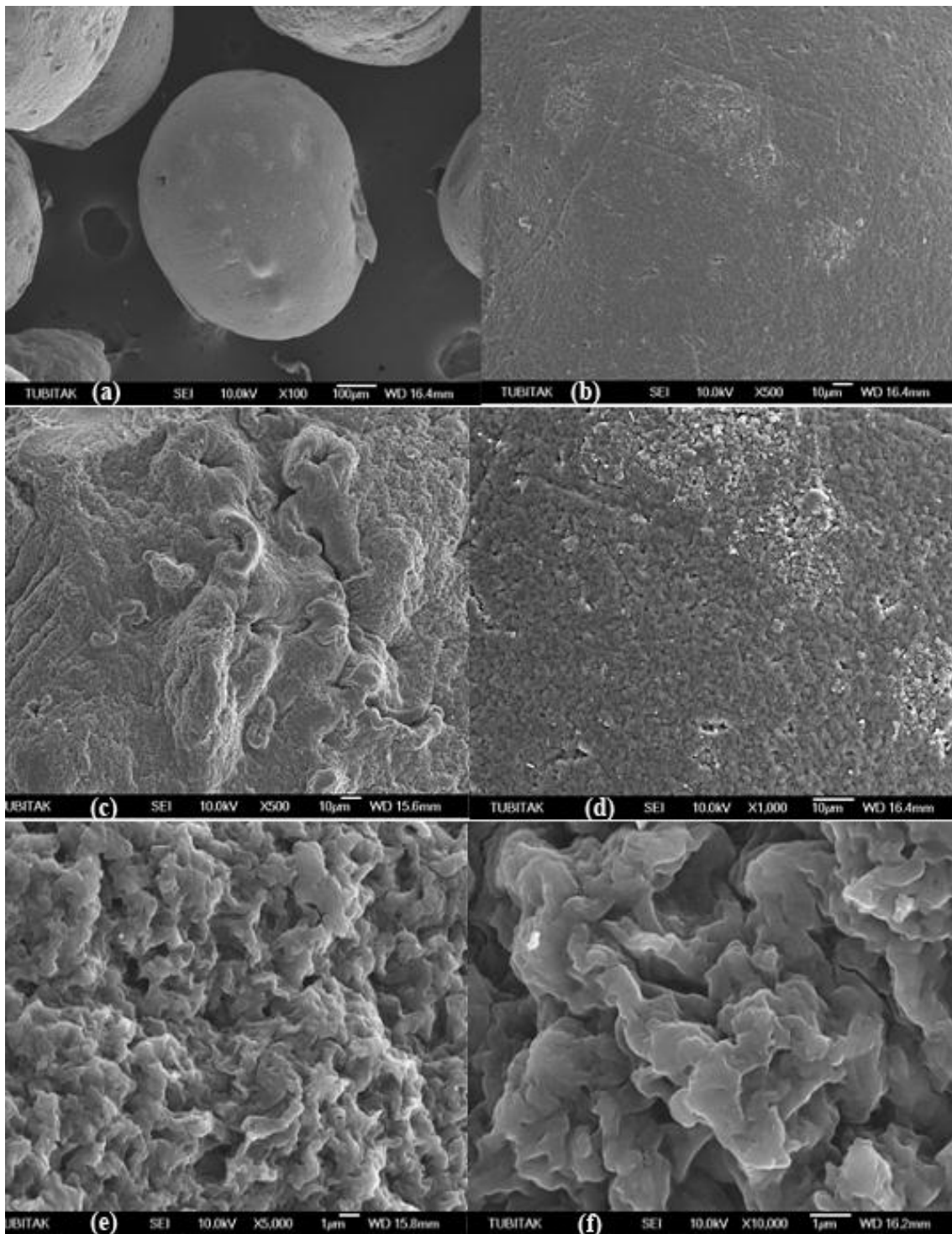


Figure 32. SEM micrograph of the quaternized chitin-g-P4VP beads, (a) is X 100, (b) X 500, (c) is X 500, (d) is X 1,000, (e) is X 5,000, (f) is X 10,000.

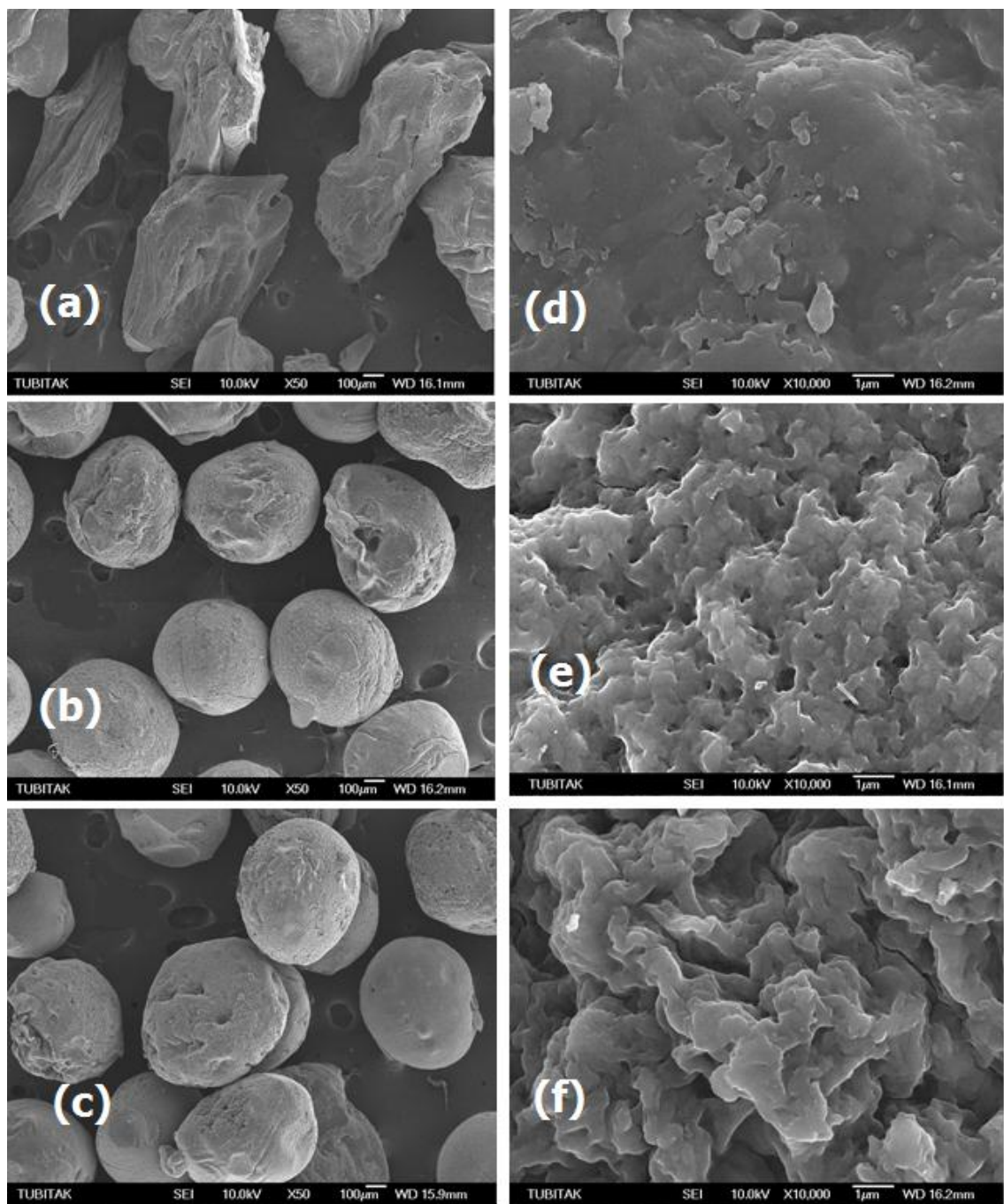


Figure 33. SEM micrograph of the chitin beads (a) and (d) non-grafted chitin beads, (b) and (e) P4VP grafted chitin beads, (c) and (f) for quaternized P4VP grafted chitin beads.



The quaternized beads are mercury-selective sorbents, which bind mercury through the amide groups. Mercuric ions reaction with amide groups of quaternized beads, yielding covalent mercury–amide linkages [Dujardin, 2000], is shown in Figure 31.

### 3.4.1 Extraction of Trace Mercury

To examine extractability of trace quantities, the resin samples were brought into contact with dilute mercury solutions whose initial concentration was 100 ppm. A very rapid decrease in the mercury concentration, within first 15-20 minutes, indicates both efficiency of the sorbent, and reasonably fast mercury extractions from solution (Figure 34). See also Figure 35 for equilibrium mercury adsorption in mg/g. Pseudo-first order and pseudo-second order sorption kinetics of  $\text{Hg}^{2+}$  acetate on the quaternized chitin-g-P4VP beads were also studied.

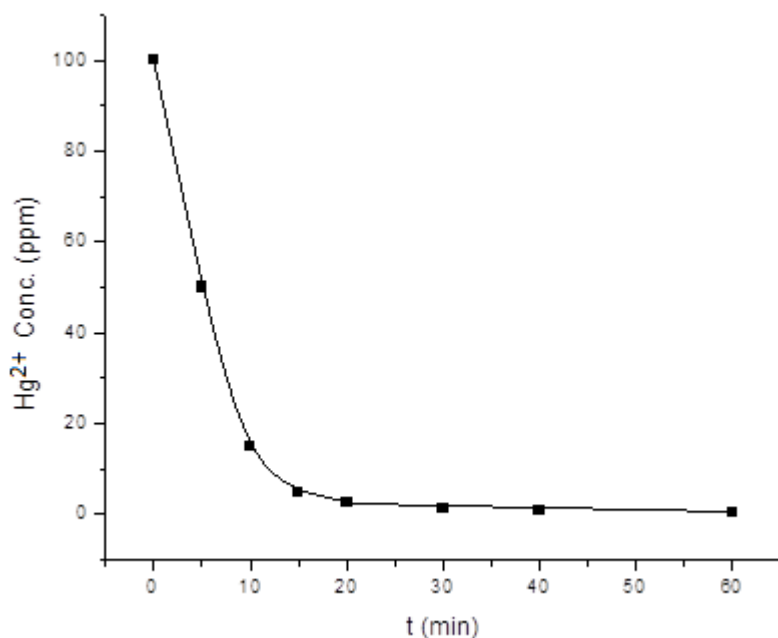


Figure 34. Variation of trace mercury concentration during interaction with the quaternized chitin-g-P(4VP) (0.25 g) with 50ml  $\text{Hg}^{2+}$  (100ppm) solution.

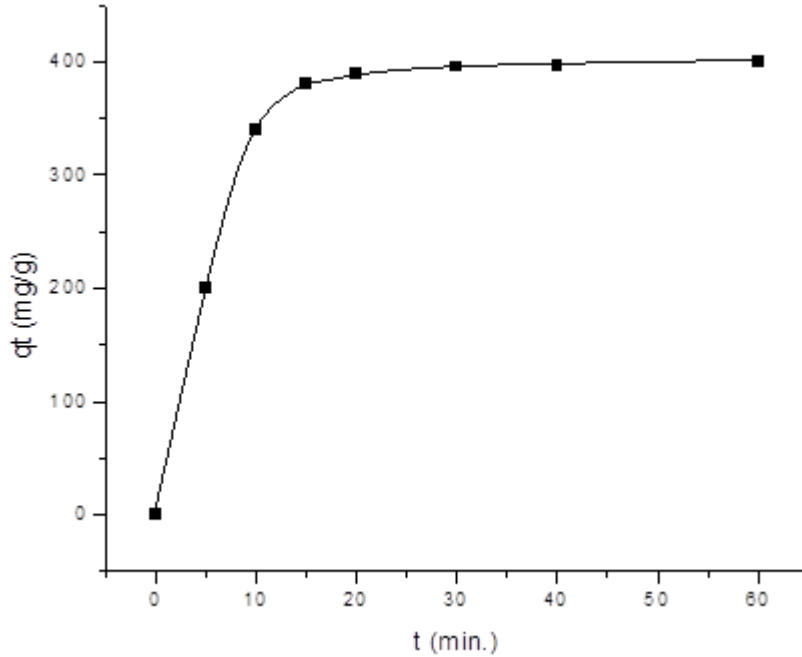


Figure 35. Equilibrium adsorption of  $\text{Hg}^{2+}$  ions on the quaternized chitin-g-P4VP (0.25 g) with 50ml  $\text{Hg}^{2+}$  (100ppm) solution.

### 3.4.2 Pseudo-First Order Kinetic Model

Lagergren pseudo first order equation for the adsorption of solid-liquid systems expressed as in equation (3.1).

$$\frac{dq}{dt} = k_1(q_e - q_t) \quad (3.1)$$

where,  $q_e$  and  $q_t$  are the adsorption capacities at equilibrium and at time  $t$  respectively (mg/g).  $k_1$  is the rate constant of pseudo-first order adsorption ( $\text{min}^{-1}$ ). After integration and applying boundary conditions,  $t = 0$  to  $t = t$  and  $q_t = 0$  to  $q_t = q_t$ , the integrated form of equation (3.1) becomes:

$$\ln(q_e - q_t) = \ln(q_e) - k_1 t \quad (3.2)$$

This equation is verified if the plot of  $\ln(q_e - q_t)$  as a function of time gives a straight line.  $k_1$  is deduced from the slope of the line and  $q_t$  gives the vertical intercept as shown in Figure 36. As can be observed from this analysis shown in Figure 36 linearity is not obeyed. The results of linear regression analysis are given in Table 16.

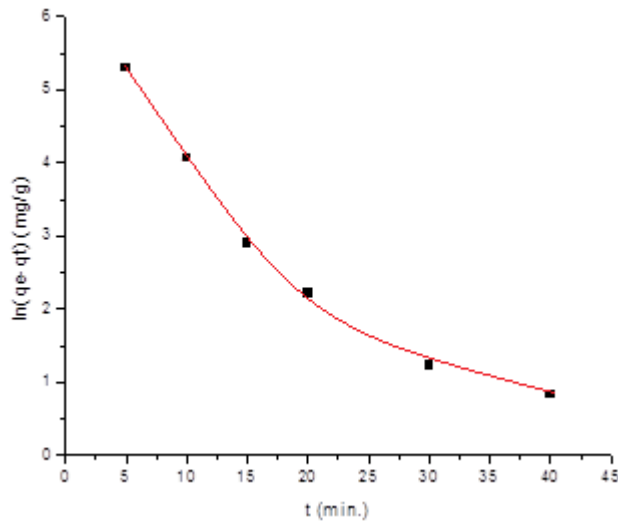


Figure 36.  $\text{Hg}^{2+}$  ions adsorption on QP(4-VP)-g-Chitin through pseudo-first order kinetic models.

### 3.4.3 Pseudo-Second-Order Model

The pseudo second-order adsorption kinetic rate equation is expressed as:

$$\frac{dq}{dt} = k_2 (q_e - q_t)^2 \quad (3.3)$$

Where  $k_2$  ( $\text{mg}^{-1} \text{min}^{-1}$ ) is the rate constant of pseudo second order adsorption. From the boundary conditions  $t = 0$  to  $t = t$  and  $q_t = 0$  to  $q_t = q_t$ , the integrated form of equation (3.3) becomes:

$$\frac{1}{q_e - q_t} = \frac{1}{q_e} + k_2 t \quad (3.4)$$

This is the integrated rate law for a pseudo second order reaction. Equation (3.4) can be rearranged to obtain equation (3.5) which has a linear form:

$$\frac{t}{q_t} = \frac{1}{k_2 q_e^2} + \frac{t}{q_e} \quad (3.5)$$

If the initial adsorption rate  $h_0$  (mg/(g. min)) is:

$$h_0 = k_2 q_e^2 \quad (3.6)$$

Then, equations (3.5) and (3.6) become:

$$\frac{t}{q_t} = \frac{1}{h_0} + \frac{t}{q_e} \quad (3.7)$$

Thus, from equation (3.7), plots of  $(t/q_t)$  versus  $t$  give values of  $q_e$  and  $k_2$  from the slopes and intercepts respectively, (See Figure 37).

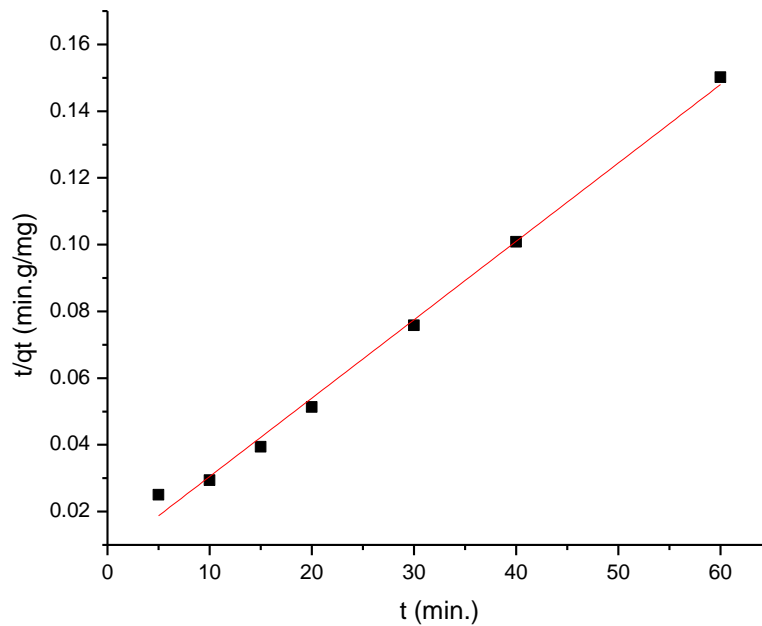


Figure 37.  $Hg^{2+}$  ions adsorption on qP4VP-g-Chitin through pseudo second-order kinetic models.

Experimental  $q_e$  value, at equilibrium, is obtained as 399.6 mg/g from Figure 33. As summarized in Table 16, pseudo-first order kinetics are not suitable for this set of data. Because experimentally 189.3 mg/g does not agree with the theoretical value 399.6 mg/g. Also the R-square value of 0.882 shows that, the data is not linear, on the other hand, second order kinetics are obeyed with an R-square value of 0.994. Calculated  $q_e$  value, which is 425.5 mg/g agrees with the experimental value of 399.6 mg/g within  $\pm 1.0$  mg/g. So we can easily say that kinetics of qP4VP-g-chitin beads mercury sorption shows second order profiles.

Table 16. Comparison of pseudo-first order and pseudo-second order rate constants, correlation coefficients and equilibrium adsorptions ( $q_e$ ).

$q_{e,exp}$ (mq/g)	Pseudo-First Order			Pseudo-Second Order		
	$q_e$ (mq/g)	$k_1 10^{-1}$ (min <sup>-1</sup> )	$R^2$	$q_e$ (mq/g)	$k_2 \times 10^{-4}$ (g/mg.min)	$R^2$
399.6	189.3	1.25	0.882	425.5	7.89	0.994

### 3.4.4 Regeneration

Amide groups are not stable enough to the acid and base hydrolysis. Hence, regeneration with mineral acids is not suitable for the sorbed mercury removal. In the literature, reports are available for mercury regeneration [Bıçak, 2002; Bıçak & Gazi, 2003], more than 20 times without hydrolysis of the amide groups. The same procedure was followed in this work for back extraction of mercury from the qP4VP-g-chitin. Experimentally recovered mercury with hot acetic acid is about 0.95 mmol g<sup>-1</sup>. This amount can be increased by using soxhlet type of continuous extracting system for the large scale separation processes. The mercury-free polymer obtained by this regeneration procedure can be recycled to be used again and again.

## Chapter 4

### CONCLUSION

Gelation temperatures does not vary much, by changing chitin concentration within the range studied. 0.1 %, 0.3 % and 0.5 % chitin with DMAc/LiCl5% solutions has gelation temperatures of 113°C, 113°C and 115°C respectively. Since the solutions studied are dilute, there is not much difference in the balance between intermolecular chitin and [solvent-Li]<sup>+</sup> complex interactions and intramolecular chitin-chitin interactions. Therefore, gelation temperature is independent of concentration in the dilute regime studied.

T<sub>gel</sub> for Chitin/NMP solution is much higher than that of Chitin/DMAc solution. This suggests that NMP-Li complex is stronger than DMAc-Li complex. Addition of organic acids to chitin solution lowers the gelation temperature. On addition of 0.01 g of ascorbic acid (AA) to 2 ml of solution, T<sub>gel</sub> is lowered from 115°C to 97°C, a decrease of 18°C. Addition of the same amount of MA or OA lowers T<sub>gel</sub> to 112°C and 110°C respectively. Lowering of T<sub>gel</sub> on addition of organic acids may be attributed to the competition that arises between the organic acid and the chitin molecules to form a complex with [DMAc-Li]<sup>+</sup>. The complex between chitin and [solvent-Li]<sup>+</sup> become weaker due to this competition and decomposes at lower temperatures leading to lower gelation temperatures.

The effect of AA on the gelation temperature of 0.5 % Chitin/NMP solution is less pronounced than that on Chitin/DMAc solution.  $T_{gel}$  decreases from 134°C to 128°C on addition of 0.01 g of AA. This observation suggests that the  $[NMP-Li]^+$  complex should be a stronger one than the  $[DMAc-Li]^+$  complex.

The gel obtained by heating the chitin/DMAC/LiCl/AA solution was kept around 150°C. The gel could not be permanently stabilized upon prolonged heating. Once gelation occurs chitin gel is stable on decreasing the temperature until the gel melting temperature is reached.

Heating the chitin solution to the gelation temperature, before nonsolvent addition, results in stronger gels than by preparing similar gels at room temperature. Addition of an organic acid causes the  $T_{gel}$ , E, and Q values of the gels to decrease in the order gel-MA>gel-OA>gel-AA. Experimental results indicate that the gelation mechanism in the presence of these acids involve complex formation between the acids and the  $[DMAc-Li]^+$  system which plays a role in the amount of polymer forming the gel. A smaller amount of chitin involved in gel formation results in weaker gels having lower Young's Modulus (E) values and smaller swelling indices (Q).

Mild and inexpensive grafting conditions used are suitable for industrial applications. On the other hand, purification processes requires time and need to be improved for commercial use.

Under organic conditions by using redox initiator, modification of the chitin solution by grafting with 4VP followed by the beads formation via nonsolvent addition, so that P4VP grafted chitin beads were formed. After two days under alcohol rains in

soxhlet and 4-5 days ethanol bath in shaker, beads were left into pure water, so that DMAc/LiCl 5%, the excess 4VP and KPS have been taken out to get purified homopolymer of P4VP grafted chitin beads.

The effect of monomer concentration to the fixed amount of polymer at a fixed temperature with a constant time interval was studied and the highest and lowest efficient grafting is calculated as 226 % with 1.5 mL and 106 % with 4.5 mL of 4VP amounts.

Based on the FTIR analysis the aromatic C-H stretching bond of 4VP at  $824\text{ cm}^{-1}$  does not exist in blank chitin but on the other hand this band exist in all other grafted product. This is taken as evidence of P4VP grafting onto chitin.

XRD analysis shows that crystallinity% decreases in the grafted product compared to chitin from 92 % to 74 %. So, modified chitin has a more amorphous structure compared to chitin.

The TGA analysis of the purified chitin powder and grafted chitin powder show that; maximum decomposition temperature of chitin is reduced from  $380^{\circ}\text{C}$  to  $305^{\circ}\text{C}$  after grafting. At a reference temperature of  $500^{\circ}\text{C}$ , pure chitin has a weight loss of around 90% but grafted product has 75% weight loss. At  $840^{\circ}\text{C}$  13 % of the chitin sample remains; this is only 0.5% for the grafted products. Hence, grafted products are less heat stable than the purified chitin. XRD analysis results support this observation, since higher crystallinity results in higher heat stability. DSC results are in accordance with TGA results.



The swelling behaviour of the processed blank chitin beads and grafted chitin beads have been studied in aqueous solution under neutral, acid and phosphate buffers with pH values of 7.0, 1.4 and 7.4 respectively at 37°C. The swelling ratio difference between chitin and grafted chitin at pH 7.0 does not have a big difference ~2.7 and ~2.5, respectively. The swelling ratios at pH 1.4 acid buffer do not show a considerable difference between the grafted chitin and chitin. At equilibrium the swelling ratios are ~2.7 and ~2.6 respectively. The swelling ratio at pH 7.4 phosphate buffer does not have any difference between the blank and grafted product; at equilibrium ~2.5.

SEM micrographs of the processed blank chitin beads and 226 % grafted chitin beads show that; beads morphology of the grafted chitin is much more spherical compared to the non-grafted blank chitin beads. SEM micrographs magnified by 10.000 shows that gel network structure of the grafted products are more heterogenous and more microporous compared to non-grafted ones.

Chitin beads have negligible  $\text{Fe}^{3+}$  adsorption capacity (0-2 mg/g) at equilibrium; on the other hand Chitin-g-P4VP beads reach equilibrium adsorption capacity (20 mg/g) within first 30 min in 1 mM  $\text{Fe}^{3+}$  solution whereas an equilibrium adsorption capacity of 60 mg/g is attained after 3 h contact in 5.0 mM solution.

Cholesterol adsorption onto chitin bead at equilibrium is 235 mg/g bead. On the other hand, the equilibrium adsorption capacity of the chitin-g-P4VP bead is 433 mg/g bead in 0.5 mg/mL solution, this is 577 and 744 mg/g bead in 1.0 mg/mL and 5 mg/mL solutions respectively at equilibrium.

Surface adsorption of cholesterol and  $\text{Fe}^{3+}$  onto the beads shows that this new polymer, chitin-g-P4VP, has improved functionality when compared to the precursor polymer chitin, and is a potential candidate for cholesterol and  $\text{Fe}^{3+}$  removal/detection, and feasible to be used for environmental protection or biomedical applications.

Quaternization process is also a good candidate for the removal of heavy metals, such as mercury uptake. Experimentally a maximum  $2.67 \text{ mmol g}^{-1}$  mercury loading capacity was obtained. Simple regeneration process with hot acetic acid allowed  $0.95 \text{ mmol g}^{-1}$  mercury to be recovered. Amide groups on the quaternary pyridine resin provide highly selective mercury extraction to be used for environmental protection. Kinetic experiments shows the pseudo-second order type of release. Pseudo-first order kinetic can be suitable within first 20 minutes.

P4VP grafted chitin is a potential heavy metal adsorbent which can be applied for environmental cleaning. I hope this work contributes to chitin research and may provide a starting point for more elaborate contributions to the literature.

## REFERENCES

- [Bianchi, 1996] E. Bianchi, E. Marsano, A. Tacchino, Carbohydrate Polymers, 32, 23-26 (1996).
- [Hirano, 1989] S. Hirano and K. Horiuchi, Int. J. Biol. Macromol., 11, 253-254 (1989).
- [Hirano, 1990] S. Hirano, R. Yamaguchi, N. Fukui, and M. Iwata, Carbohydrate Research, 201, 145-149 (1990).
- [Kumar, 2000] M.N.V.R. Kumar, Reactive and Functional Polymer , 46, 1-27 (2000).
- [Mima,1983] S. Mima, M. Miya, R. Iwamoto, S. Yoshikawa, Journal of Applied Polymer Science, 28, 1909-1917 (1983).
- [Morgenstern,1996] B. Morgenstern, H.-W. Kammer, TRIP, 4, 87-91 (1996).
- [El-Kafrawy, 1982] El-Kafrawy, A. J Appl. Polym. Sci., 27, 2435-2443 (1982).
- [Mc Cormic, 1985] C.L. Mc Cormick, P.A. Callais, B.H. Hutchinson Jr, Macromolecules, 18, 2394-2401 (1985).

- [Turback, 1984] A.F. Turback, J. Tappi, 67(1), 94-96 (1984).
- [Peter, 1995] M. G. Peter, J.M.S.-Pure Appl. Chem., A32(4), 629-940(1995).
- [Smith, 2000] <http://www.eos.ncsu.edu/bea/cours...5-projects/bake/smith/index1.html> , 14.09.(2000).
- [Terbojevich, 1997] M. Terbojevich, A. Cosani, Chitin Handbook, European Chitin Society, Italy, 87-91 (1997).
- [Vachound, 2000] L. Vachound, N. Zydowicz, A. Domard, Carbohydrate Research, 326, 295-304 (2000).
- [Yusof, 2001] N. L. B. M. Yusof, L. Y. Lim, E. Khor, Journal of Biomedical Materials Research, 54(1), 59-68 (2001).
- [Mi, 2002] F.-L. Mi, Y.-M. Lin, Y.-B. Wu, S.-S. Shyu, Y.-H. Tsai, Biomaterials, 23, 3257-3267 (2002).
- [Bianchi, 1997] E. Bianchi, E.Marsano and A.Tacchino, Carbohydrate Polymers, 50, 23-26 (1997).
- [Khor, 1997] E. Khor, A.C.A. Wan, C.F. Tee, G.W. Hastings, J.Polym.Sci., Part A: Polym. Chem., 35, 2049-2053 (1997).

- [Vachoud, 1997] L.Vachoud, N. Zydowich and A. Domard, Carbohydrate Research, 302(3-4), 169-177 (1997).
- [Muzarelli, 1998] R.A.A. Muzarelli and S. Mancini, In: S. Mancini, Editor, Trattato di Flebologia, UTET, Torino, Italy (1998).
- [Maezaki, 1993] Y. Maezaki, K. Tsuji, Y. Nakagawa, Y. Kawai, M.T. Akimoto, T. Sugita, Biosci. Biotechnol. Biochem., 57, 1439-1444 (1993).
- [Sreenivasan, 1998] K. J. Sreenivasan, Appl. Polym. Sci., 69, 1051-1055 (1998).
- [Kim, 1999] C.H. Kim, H.Chun, J. Polym. Bull., 42(1), 25-32 (1999).
- [Chiu, 2004] S.H. Chiu, T.W. Chung, R. Giridhar, W.T. Wu, Food Res. Int., 37(3), 217-223 (2004).
- [Tong, 2005] Y. Tong, S. Wang, J. Xu, B. Chua, C. He, Carbohydr. Polym., 60(2), 229-233 (2005).
- [Zhang, 2008] J. Zhang, J. Liu, L. Li, W. Xia, Nutr. Res., 28(6) , 383-390 (2008).
- [Yang, 1984] T.C. Yang, R. R. Zall, Ind. Eng. Chem. Prod. Res. Dev., 23, 168-172 (1984).

- [Hoshi, 1997] S. Hoshi, K. Kanuma, K. Sugamara, M. Uto, K. A. Talanta, 44(8), 1473-1478 (1997).
- [Hein, 2005] N.Q. Hien, D.V. Phu, N.N. Duy, H.T. Huy, Nucl. Inst. Meth. in Phys. Res., Section B: Beam Int. Mater. Atoms, 236(1-4), 606-610 (2005).
- [Wu, 2010] F.C. Wu, R.L. Tseng, R.S. Juang, J. Env. Mgmt., 91(4), 798-806 (2010).
- [Farkas, 1990] V. Farkas, Acta Biotechnologica, 10, 225–238 (1990).
- [Fleet, & Phaff 1981] G. H. Fleet, H. Phaff, J. Fungal, Encyclopedia of Plant Physiology New Series, 13B, 416–440 (1981).
- [Okamoto, 2003] R. Okamoto, K. Yano, I. Miyatake, Y. Tomohiro, S. Shigemasa and S. Minami, Carbohydrate Polymers, 53(3), 337-342 (2003).
- [Khor, 2003] E. Khor and L. Y. Lim, Biomaterials, 24, 2339-2349 (2003).
- [Donzelli, 2003] B. G. G. Donzelli, G. Ostroff, and G. E. Harman, Carbohydrate Research, 338, 1823-1833 (2003).

- [Sashiwa, 2003] H. Sashiwa, S. Fujishima, N. Yamano, N. Kawasaki, A. Nakayama, E. Muraki, M. Sukwattanasinitt, R. Pichyangkura, and S. I. Aiba, *Carbohydrate Polymers*, 51, 391-395 (2003).
- [Oylum, 2004] H. Oylum, E. Yılmaz, M. Bengisu, *Biomed 2004-11. International Biomedical Science and Technology Days, September 6-10 (2004)*.
- [Bengisu, 2004] M. Bengisu, E. Yılmaz, H. Oylum, H. Bağlama, *Euchis' 04 - 6th International Conference of the European Chitin Society, August 31 - September 3, (2004)*.
- [Yılmaz, 2004] H. Oylum, E. Yılmaz, M. Bengisu, N. Hasırcı, *Euchis' 04 - 6th International Conference of the European Chitin Society, August 31 - September 3, (2004)*.
- [Caner, 1997] H. Caner, H. Hasipoğlu, O. Yılmaz, E. Yılmaz, *Eur. Polm. J.*, 34(3/4), 493-497 (1997).
- [Focher, 1990] B. Focher, P.L. Beltrame, A. Naggi and G. Torri, *Carbohydrate Polymer*, 12, 405-418 (1990).
- [Fu, 2011] F. Fu, Q. Wang, *Journal of Environmental Management*, 92, 407-418 (2011).

- [Helfferich,1962] F. Helfferich, McGraw–Hill, New York (1962).
- [Singh, 1999] R. Singh, A.R. Khwaja, B. Gupta and S.N. Tandon, *Talanta* 48, 527-535 (1999).
- [Yilmaz, 2005] E. Yilmaz, H. Oylum, M. Bengisu, N. Hasirci, In *Adv. in Chitin Sci.*: Struszyk, H., Domard, A., Peter, M.G., Pospieszny, H., Eds. ESUS: Poznan, Poland, 8, 426-429, (2005).
- [Bengisu, 2005] M. Bengisu, E. Yilmaz, H. Oylum, H. Baglama, In *Adv. in Chitin Sci.*: Struszyk, H., Domard, A., Peter, M.G., Pospieszny H., Eds. ESUS: Poznan, Poland, 8, 329-333, (2005).
- [McDowall, 1984] D.J. McDowall, B.S. Gupta, V.T. Stannett, *Pr. Poly. Sci.*,10, 1-50, (1984).
- [Filho, 2004] J.A.R. Filho, E.E. Bach, R.R. Vargas, D.A.W. Soares, A.A.A. de Queiroz, *J. Appl. Polym. Sci.*, 92(2), 1310-1318, (2004).
- [Jayakumar, 2008] R. Jayakumar, H. Tamura, *Int. J. Biol. Macromol.*, 43(1), 32-36, (2008).



- [Tanodekaew, 2004] S. Tanodekaew, M. Prasitsilp, S. Swasdison, B. Thavornyutikarn, T. Pothsree, R. Pateepasen, *Biomaterials*, 25(7-8), 1453-1460, (2004).
- [Nunez, 1998] M.E. Nunez, E.R.E. de San Miguel, J.C. Aguilar, M.T.J. Rodriguez and J. de Gyves, *Solv. Extr. Ion Exch.* 16, 1421-1436, (1998).
- [Dujardin, 2000] M.C. Dujardin, C. Caze and I. Vroman, *React. Funct. Polym.* 43, 123–132, (2000).
- [Bıçak, 2002] N. Bıçak, H.B. Sönmez, *React. Funct. Polym.* 51, 55-60, (2002).
- [Bıçak & Gazi, 2003] N. Bıçak, M. Gazi, *Journal of Macromolecular Science, Part A: Pure and Applied Chemistry A40-6*, 585-591, (2003).
- [Zhou, 2004] D. Zhou, L. Zhang, J. Zhou, S. Guo, *Water Research*, 38(11), 2643-2650, (2004).
- [Amass, 1998] W. Amass, A. Amass, B. Tighe, *Polym. Int.* 47, 89-144, (1998).
- [Illum, 1998] L. Illum, *Pharm. Res.*, 15(9), 1326-1331, (1998).
- [Guibal, 2004] E. Guibal, *Separation Purification Technol.*, 38, 43-74, (2004).

[Varma, 2004] A.J. Varma, S.V. Deshpande, J.F. Kennedy, Carbohydrate Polymers, 55(1), 77-93, (2004).

# APPENDIX

## A-1

### A Preliminary Work Carried Out on Drug Loading and Drug Release

#### Calibration for Naproxen

$$x_i = 1.0e-004 * (0.2000 \quad 0.2667 \quad 0.3000 \quad 0.3200 \quad 0.3500)$$

$$y_i = 0.2230 \quad 0.3050 \quad 0.4090 \quad 0.5190 \quad 0.7960$$

$$y = a x + b$$

$$a = 3.5006e+004$$

$$b = -0.5554$$

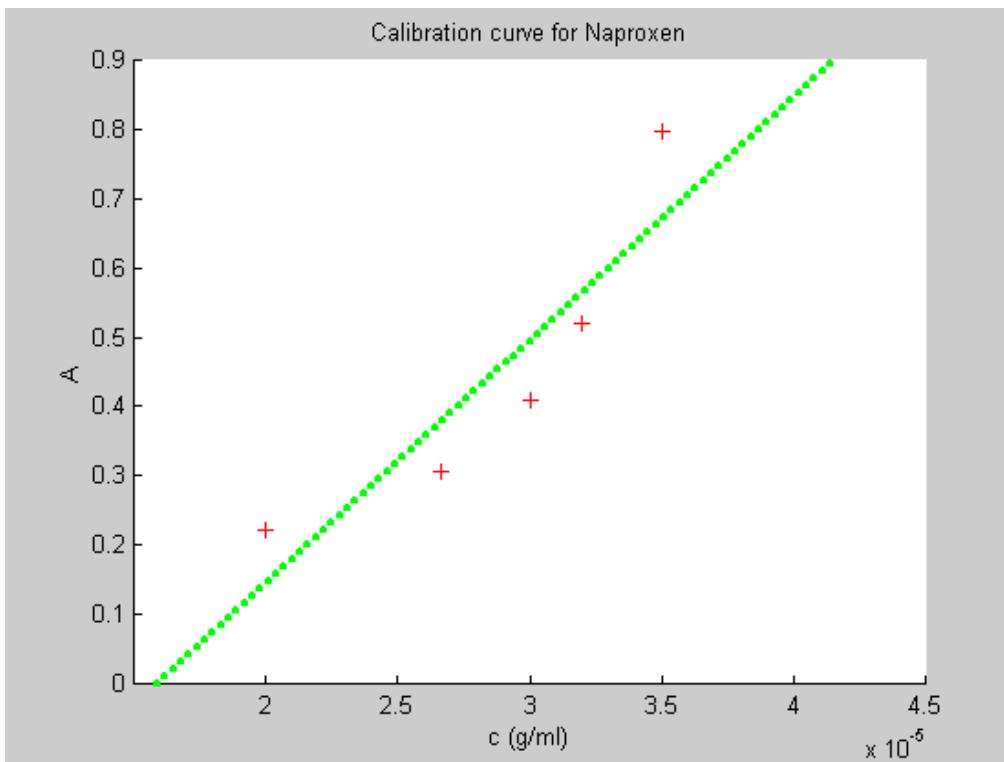


Figure A-1.1. Calibration Curve for Naproxen

## Calibration for Ibuprofen

$$x_i = 1.0e-003 * (0.0400 \ 0.1200 \ 0.2000 \ 0.4000 \ 1.0000)$$

$$y_i = 0.0170 \ 0.0980 \ 0.1310 \ 0.1810 \ 0.4420$$

$$y = a x + b$$

$$a = 414.3509$$

$$b = 0.0279$$

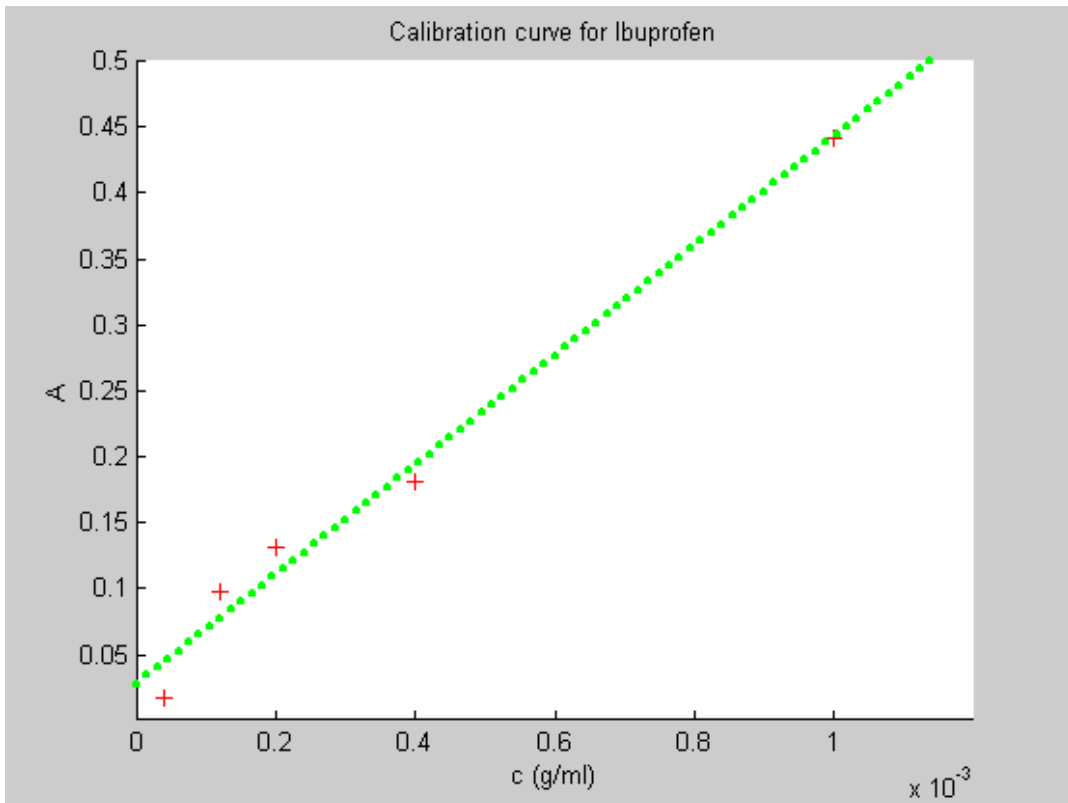


Figure A-1.2. Calibration Curve for Ibuprofen

## Calibration for Acetyl Salicylic Acid

$$x_i = 1.0e-004 * ( 0.2000 \quad 0.2667 \quad 0.3000 \quad 0.3333 )$$

$$y_i = 0.0310 \quad 0.0380 \quad 0.0620 \quad 0.0810$$

$$y = a x + b$$

$$a = 3.7371e+003$$

$$b = -0.0498$$

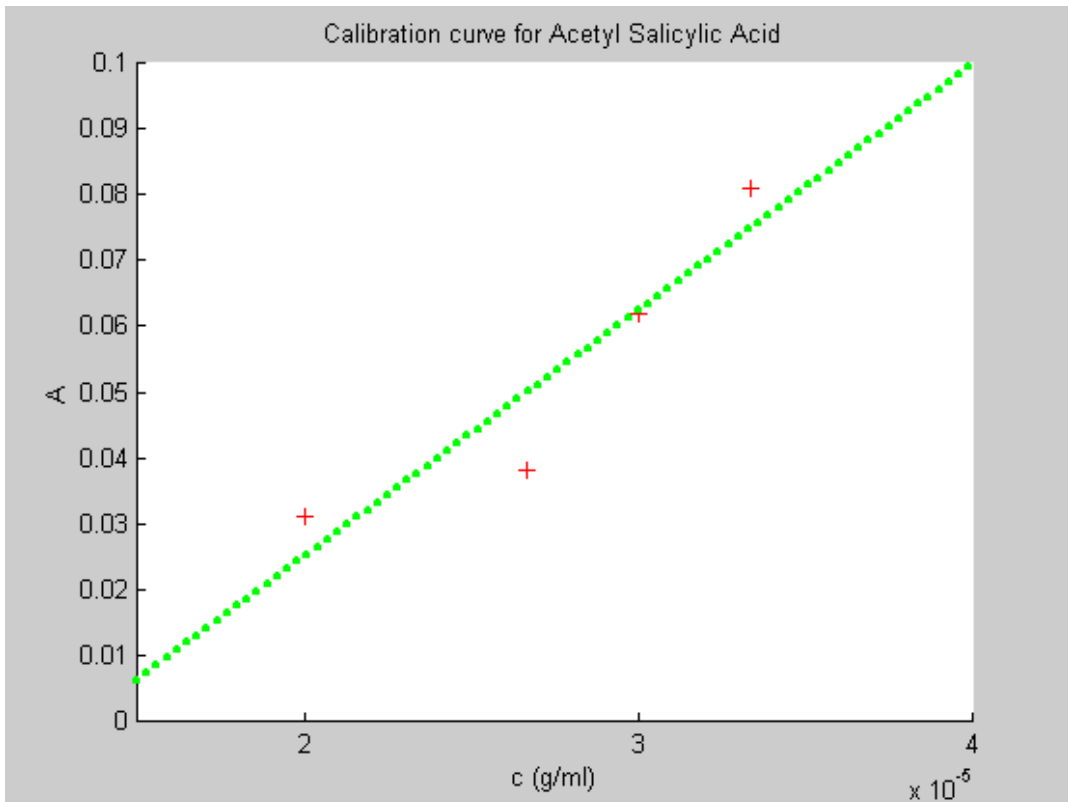


Figure A-1.3. Calibration Curve for AcetylSalicylicAcid.

## Drug Loaded Chitin Beads

Drug encapsulated chitin beads at room temperature were formed.

For this purpose anti inflammatory agents ibuprofen, naproxen and acetylsalicylicacid were used. Drug encapsulated chitin beads of anti inflammatory agents ibuprofen, naproxen and acetylsalicylicacid have been prepared and their photos show that these beads show different physical appearance from each other. Optical pictures of drug loaded chitin beads are shown in Figure A-1.1.

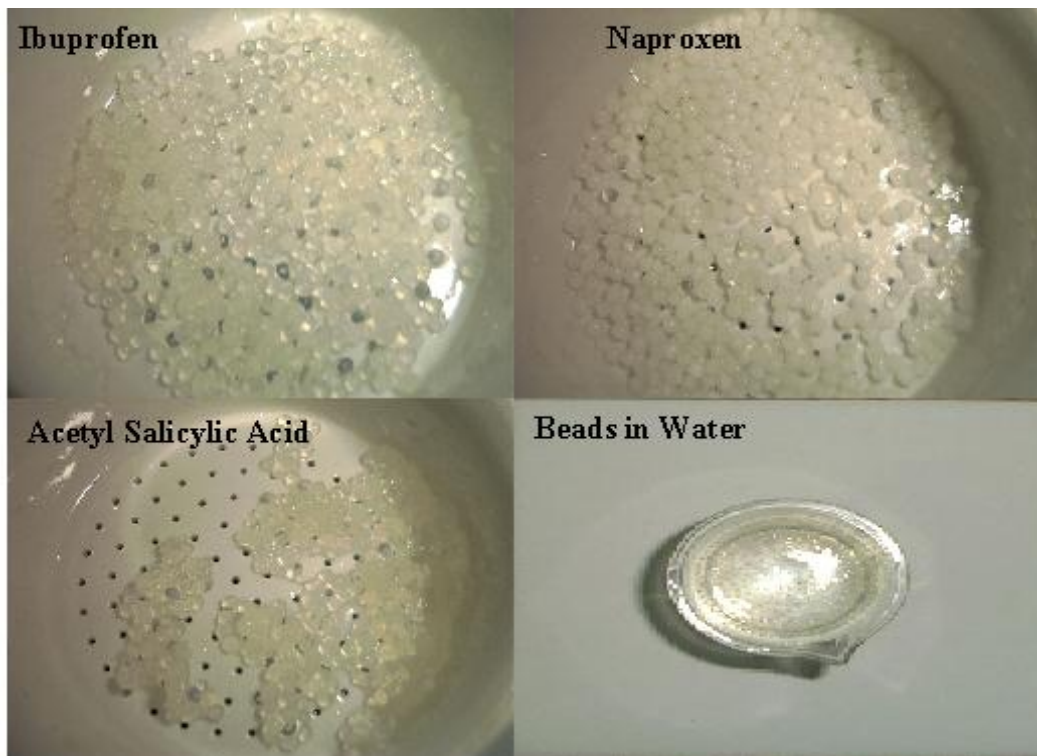


Figure A1.4. Drug Encapsulated Chitin Beads

### Gravimetric Results for % Drug Released

#### % Release for Ibuprofen

y1 = 18.5484 22.5806 29.0323 19.6237 29.3011 23.9247

x1 = 0.5000 1.5000 2.5000 3.5000 4.5000 5.5000

#### % Release for Naproxen

x1 = 0.5000 1.5000 2.5000 3.5000 4.5000 5.5000

y1 = 32.9571 42.6637 46.7269 35.2144 42.8894 37.4718

#### % Release for ASA

x1 = 0.5000 1.5000 2.5000 3.5000 4.5000 5.5000

y1 = 19.3980 25.0836 15.0502 12.0401 20.4013 11.0368

**Comparison of Chitin with Grafted Chitin in Organic solvents**

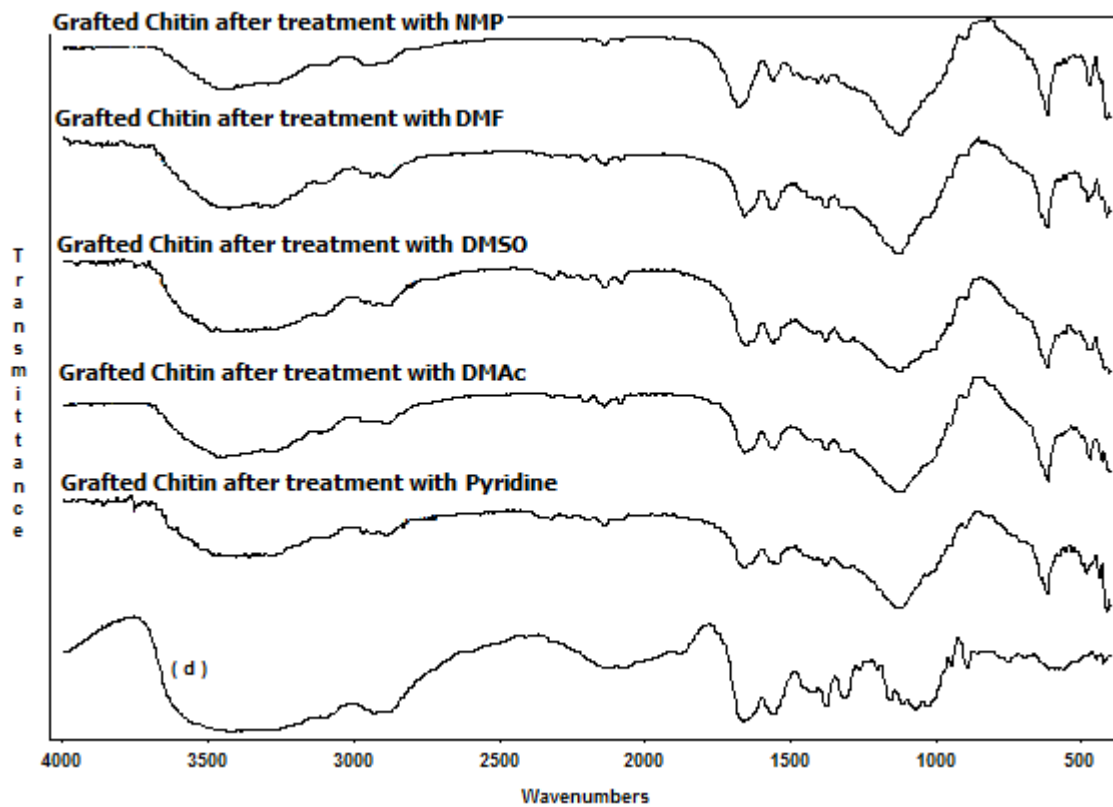


Figure A-2.1. FTIR Spectrum for Chitin (d) and P4VP Grafted Chitin in Organic Solvents.

## A-3

### **Poly (4-Vinyl Pyridine) Grafted Chitin Beads**

#### A-3.1.

#### **Additional Pictures for Poly (4-Vinyl Pyridine) Grafted Chitin Beads**

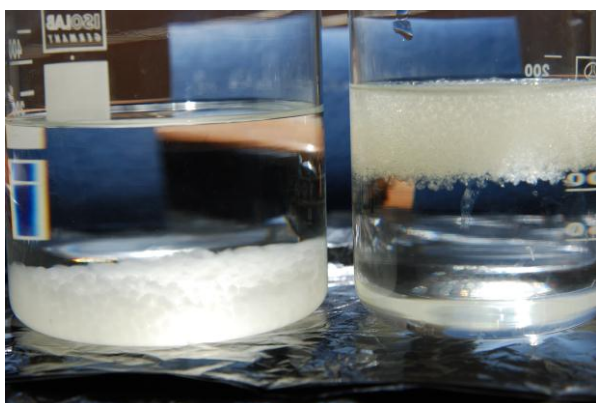


Figure A 3.1.1. Water Purified Grafted (Left Side) Chitin and Water Purified non-grafted Blank Chitin Beads (Right Side).



Figure A-3.1.2. Water Purified Filtered non-grafted Blank Chitin Beads (Wet).



Figure A-3.1.3. Chitin-g-P4VP while Drying.





Figure A-3.1.4. Chitin-g-P4VP Beads after the Soxhlet Purification in Et-OH, before Water Purified.

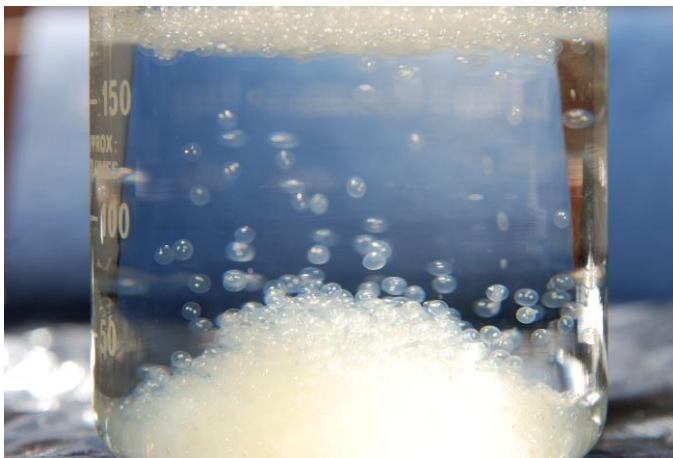


Figure A-3.1.5. Chitin-g-P4VP during the Water Purification.

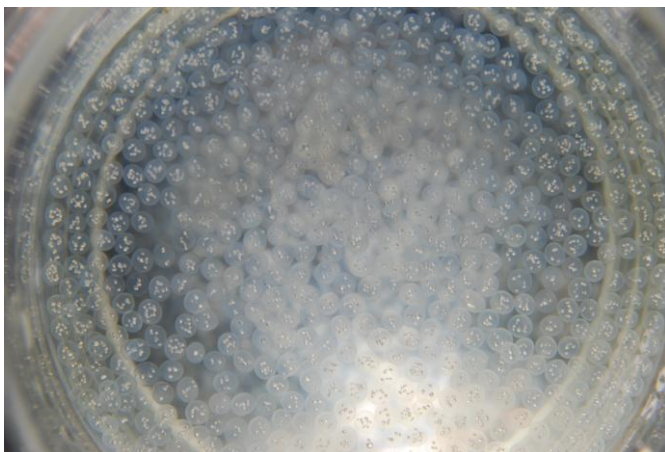


Figure A-3.1.6: Chitin-g-P4VP in Water.

### A-3.2.

#### FTIR spectroscopy of Chitin and Poly (4-Vinyl Pyridine) Grafted Chitin Beads

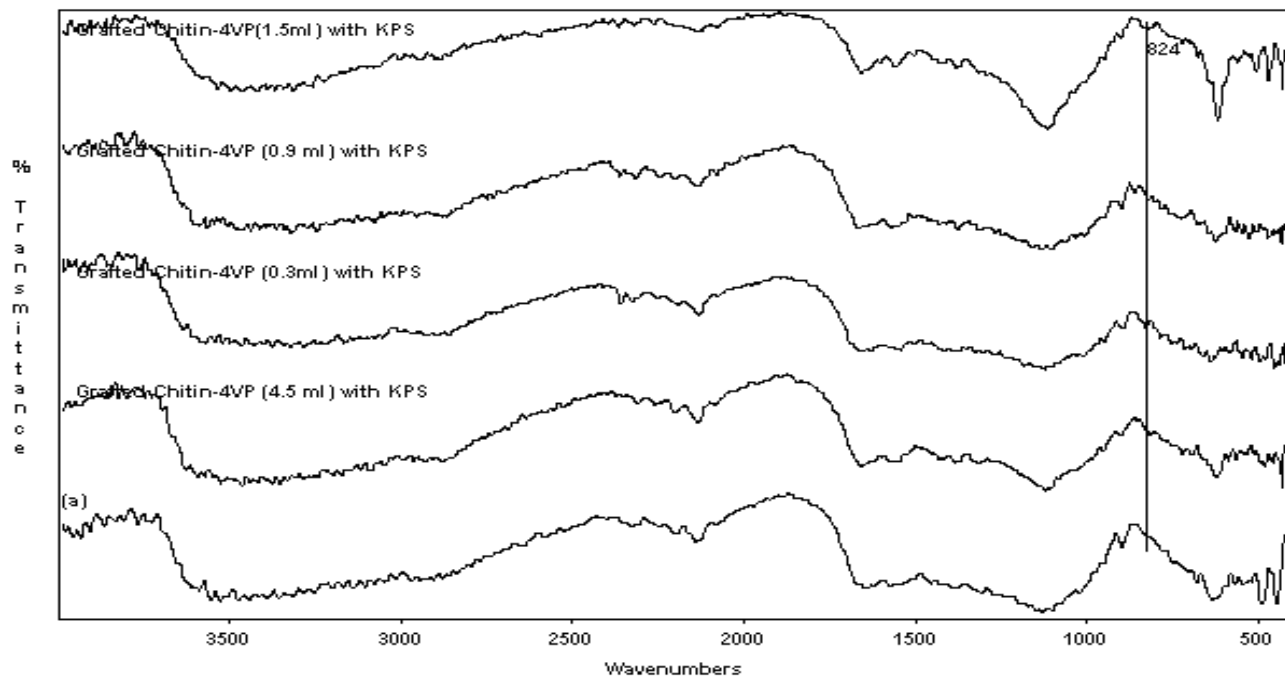


Figure A-3.2.1. FTIR spectra of poly (4-vinyl pyridine) grafted chitins compared to (a) non-grafted blank chitin (non-grafted blank: without 4VP, under the same conditions as grafted).

**A-4**

**Some Chitin and Chitosan SEM Microstructures**

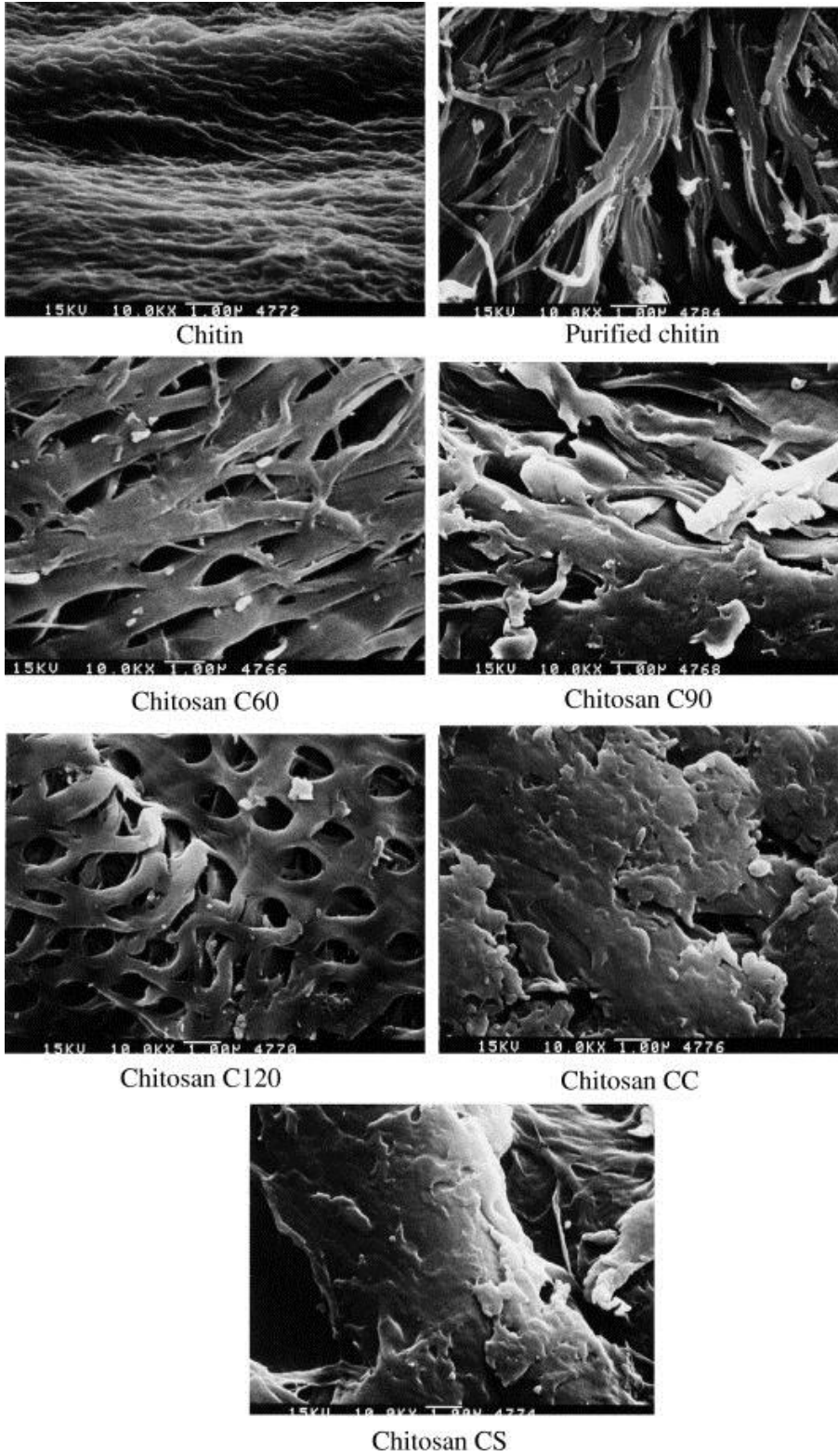


Figure A-4.1. Different Chitin and Chitosan SEM Microstructures.

## A-5

### Cholesterol Adsorptions for Poly (4-Vinyl pyridine) Grafted Chitin Beads

*Equation for the calibration curve*

$$A=51.784 C - 0.0479 \quad R \text{ squared: } 0.8874$$

For 0.5 mg/ml Cholesterol:

<i>Abs(ini)</i>	<i>c-dry (g)</i>	<i>c-wet (g)</i>	<i>blank wet (g)</i>
<b>0.1940</b>	<b>0.0341</b>	<b>0.3063</b>	<b>0.3386</b>

<i>0.5 mg/ml</i>			
<i>time, min</i>	<i>c dry</i>	<i>c wet</i>	<i>blank wet</i>
30	0.176	0.159	0.189
60	0.130	0.117	0.126
120	0.129	0.119	0.133
180	0.134	0.156	0.158
after 1 day	0.115	0.113	0.111

<i>% chol.(c-dry)</i>	<i>% chol.(c-wet)</i>	<i>% chol.(B-wet)</i>
9.9	2.1	0.3
35.0	4.7	3.7
35.6	4.6	3.4
32.8	2.3	2.0
43.3	4.9	4.6

For 1.0 mg/ml Cholesterol:

<i>Abs(ini)</i>	<i>c-dry (g)</i>	<i>c-wet (g)</i>	<i>blank dry (g)</i>	<i>blank wet (g)</i>
<b>0.263</b>	<b>0.0369</b>	<b>0.3039</b>	<b>0.0365</b>	<b>0.3028</b>

<i>time, min</i>	<i>c dry</i>	<i>c wet</i>	<i>blank dry</i>	<i>blank wet</i>
30	0.183	0.195	0.188	0.172
60	0.179	0.192	0.191	0.185
120	0.201	0.211	0.206	0.192
180	0.149	0.254	0.217	0.185

<i>% chol.(c-dry)</i>	<i>% chol.(c-wet)</i>	<i>% chol.(B-dry)</i>	<i>% chol.(B-wet)</i>
40.5	4.2	38.4	5.6
42.5	4.4	36.8	4.8
31.4	3.2	29.2	4.4
57.7	0.6	23.5	4.8

**For 5.0 mg/ml cholesterol:**

<b><i>Abs(ini)</i></b>	<b><i>c-dry (g)</i></b>	<b><i>c-wet (g)</i></b>	<b><i>blank wet (g)</i></b>
<b>0.726</b>	<b>0.0321</b>	<b>0.3024</b>	<b>0.3086</b>

<b><i>time, min</i></b>	<b><i>c dry</i></b>	<b><i>c wet</i></b>	<b><i>blank wet</i></b>
30	0.592	0.641	0.625
60	0.400	0.417	0.606
120	0.696	0.572	0.683
180	0.598	0.574	0.600

<b><i>% chol.(c-dry)</i></b>	<b><i>% chol.(c-wet)</i></b>	<b><i>% chol.(B-wet)</i></b>
77.9	5.2	6.1
189.6	19.1	7.3
17.4	9.5	2.6
74.4	9.4	7.6

## A-6

### Quaternized Chitin-g-(poly (4-vinyl pyridine)) Beads

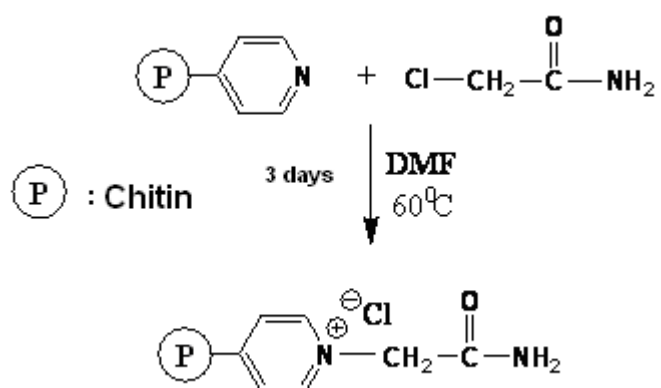


Figure A-6.1. Chitin-g-P4VP quaternized with 2-chloroacetamide in DMF.

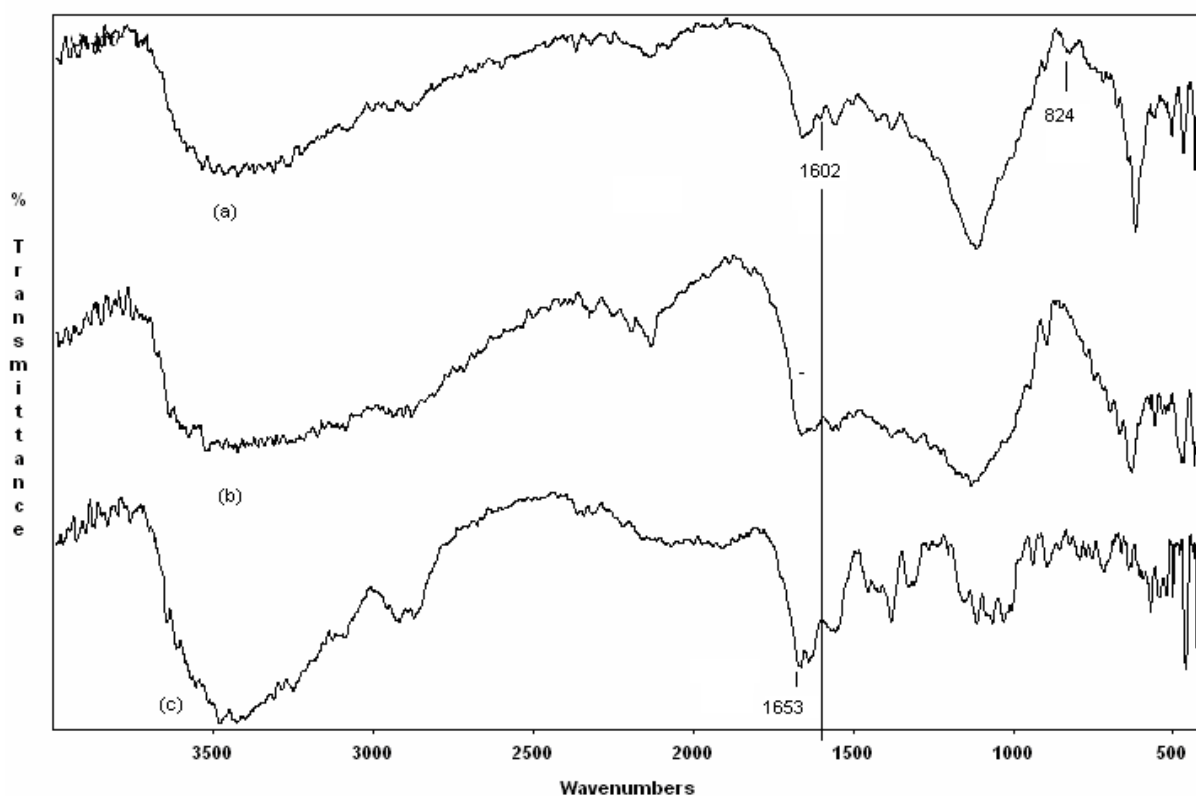


Figure A-6.2. FTIR spectrum of (a) chitin-g-P4VP, (b) quaternized chitin-g-P4VP, (c) chitin.

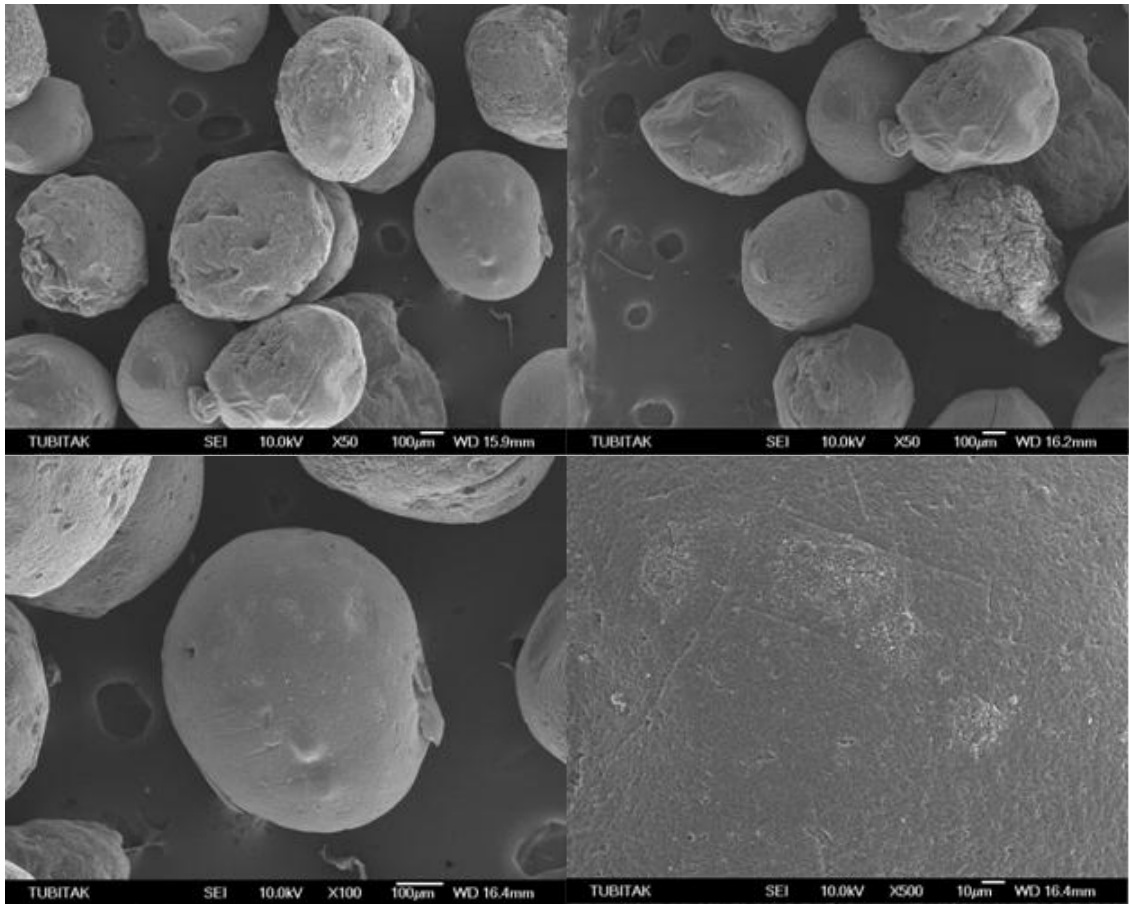


Figure A-6.3. SEM for Quaternized Chitin-g-P4VP Beads

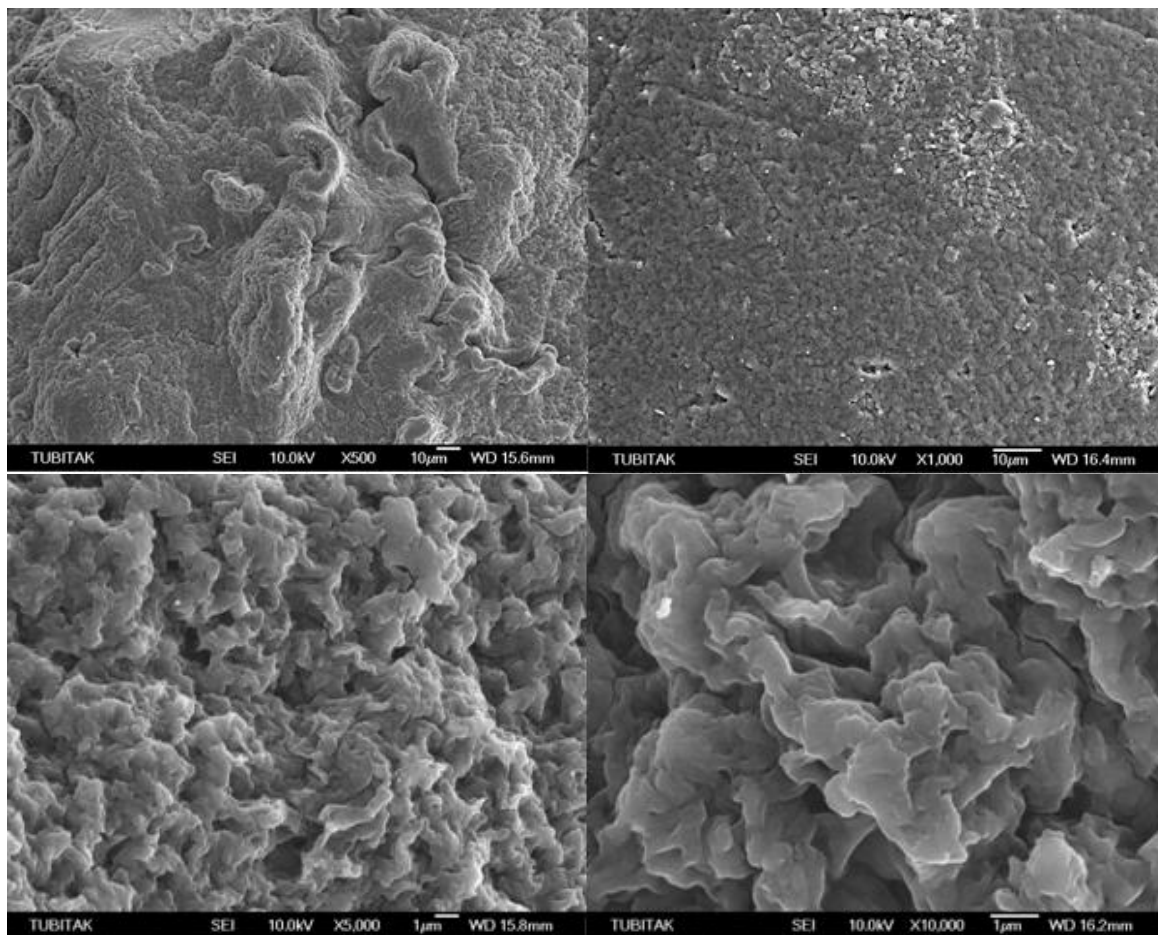


Figure A-6.4. SEM for Quaternized Chitin-g-P4VP Beads



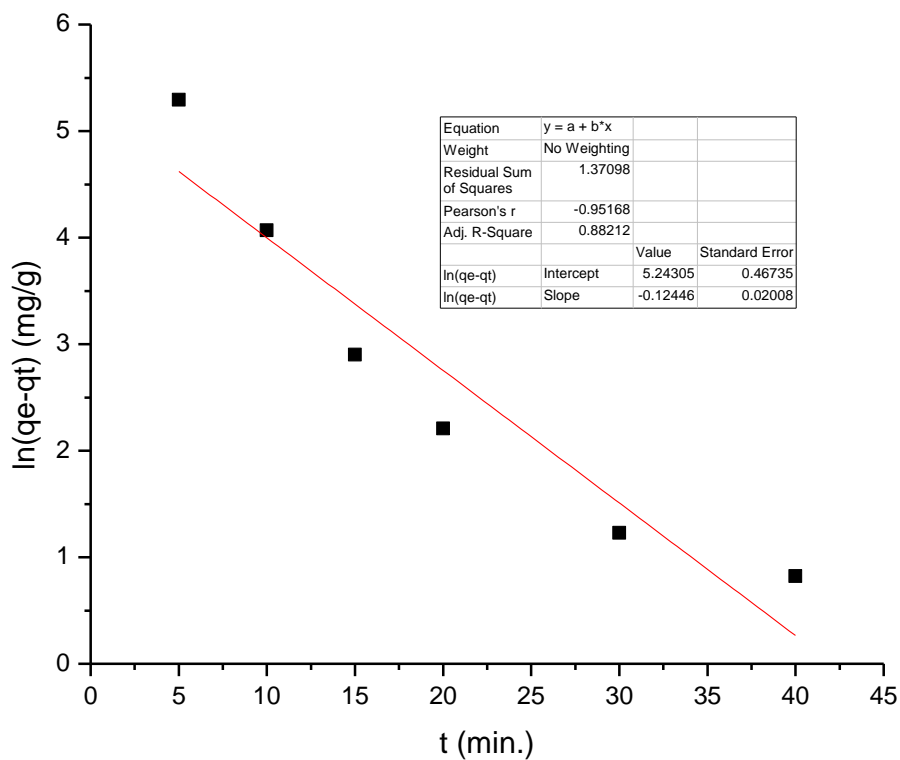


Figure A-6.5.  $Hg^{2+}$  ions adsorption on qP4VP-g-Chitin through pseudo-first order kinetic models including statistical results.

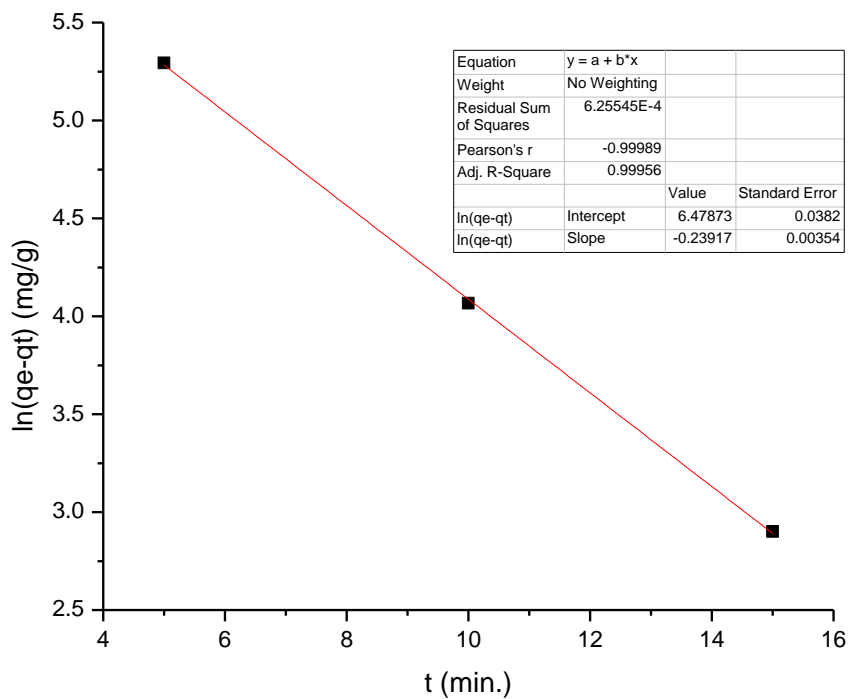


Figure A-6.6.  $Hg^{2+}$  ions adsorption on qP4VP-g-Chitin through pseudo-first order kinetic models including statistical results (first 15 minutes).

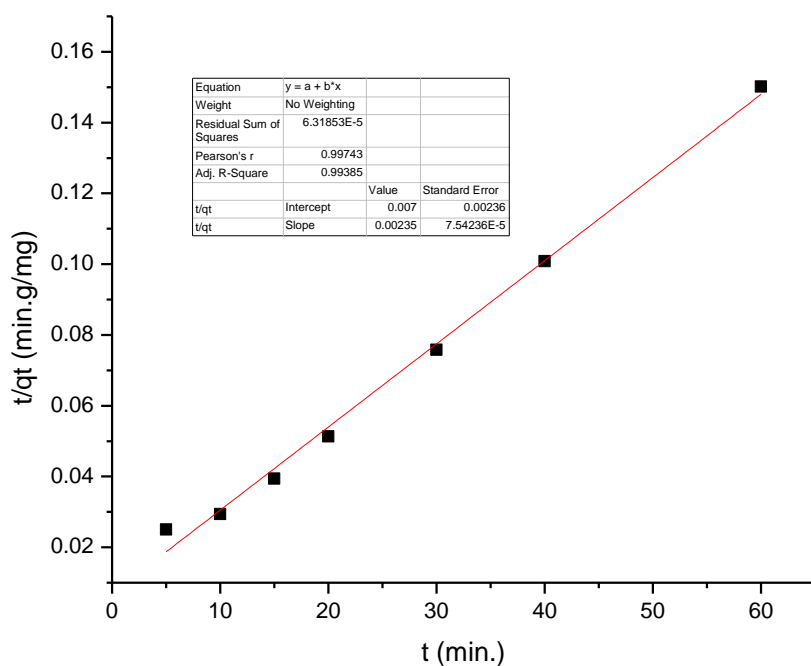


Figure-A-6.7.  $\text{Hg}^{2+}$  ions adsorption on qP4VP-g-Chitin through pseudo second-order kinetic models including statistical results.

**A-7**

**Burning Test for Chitin in DMAc and NMP with Weak Acids (MA, OA, AA)**

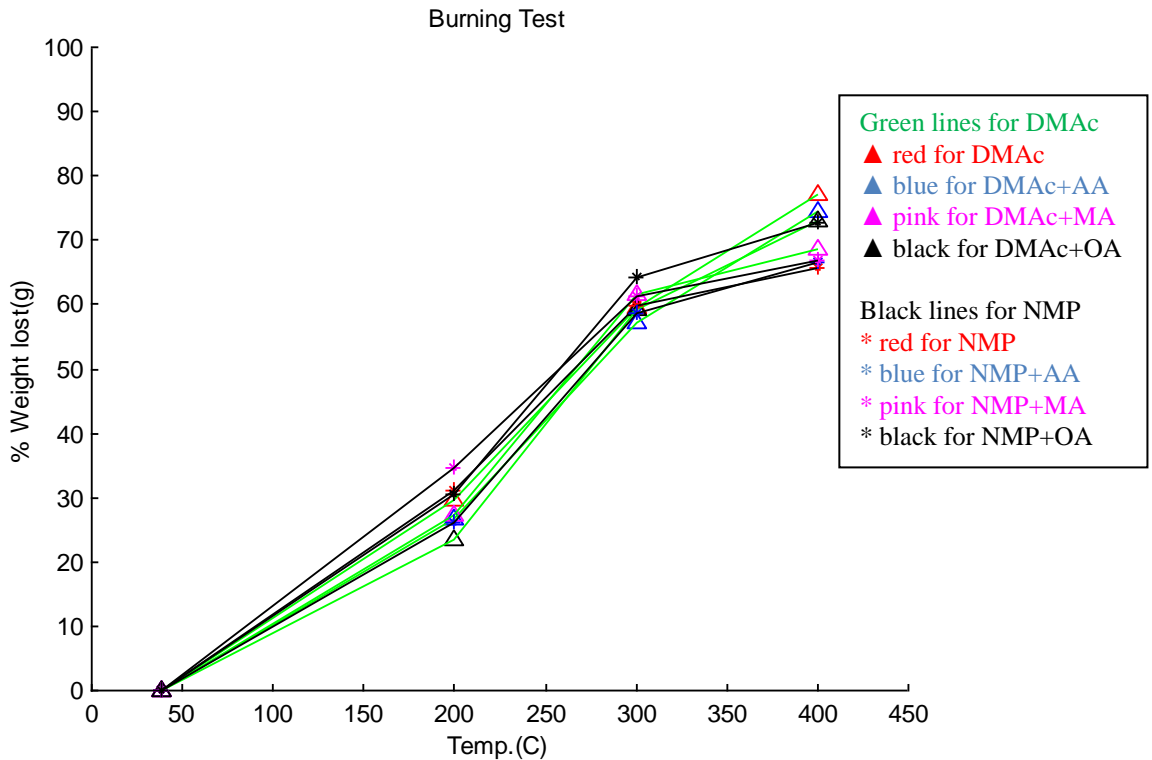


Figure A-7.1. Burning Test for Chitin in DMAc and NMP with Weak Acids (MA, OA, AA). (See the Matlab program for the detail).

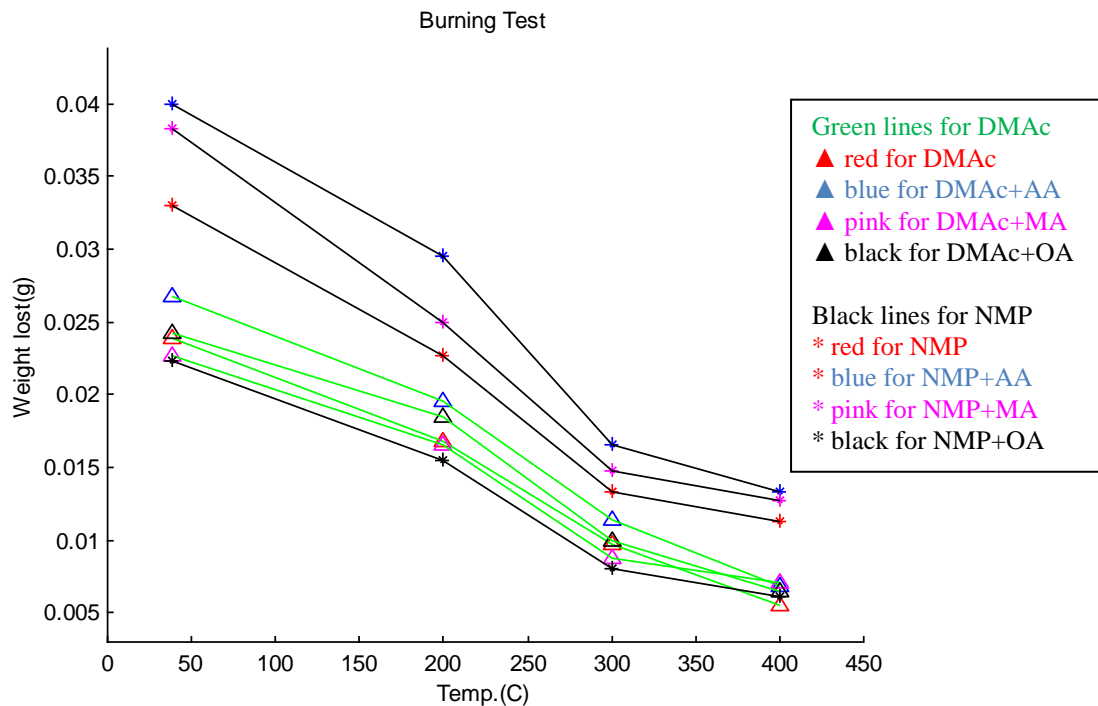


Figure A-7.2. Burning Test for Chitin in DMAc and NMP with Weak Acids (MA, OA, AA). See the Matlab program for the detail.

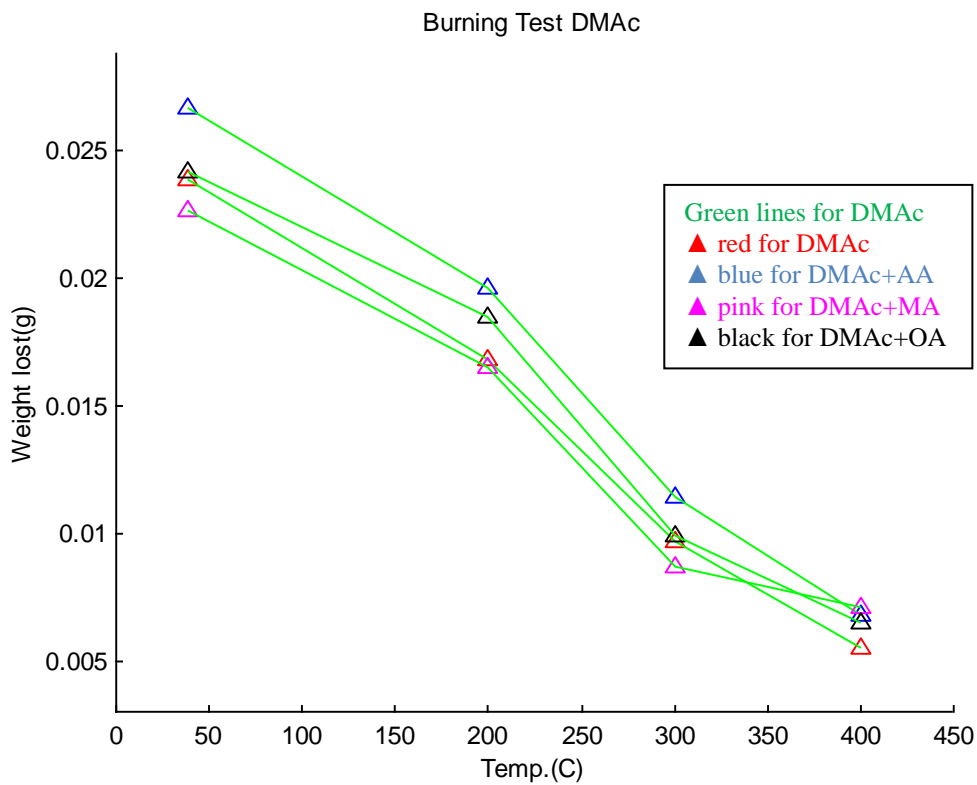


Figure A-7.3. Burning Test for Chitin in DMAC with Weak Acids (MA, OA, AA). See the Matlab program for the detail.

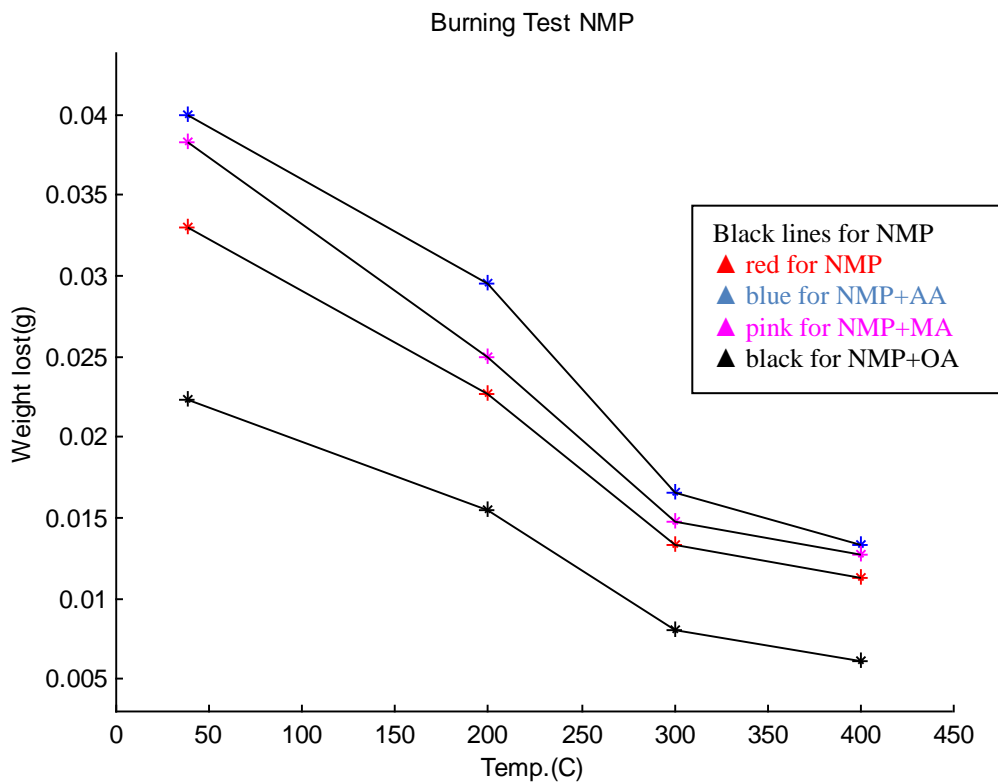


Figure A-7.4. Burning Test for Chitin in NMP with Weak Acids (MA, OA, AA). See the Matlab program for the detail.

[Temp. °C]x1 = 38 200 300 400	
[DMAc] w1 = 0.0239 0.0168 0.0097 0.0055	[%Lost] y1 = 0 29.7071 59.4142 76.9874
[DMAc+AA] w2 = 0.0267 0.0196 0.0114 0.0068	[%Lost] y2 = 0 26.5918 57.3034 74.5318
[DMAc+MA] w3 = 0.0227 0.0165 0.0087 0.0071	[%Lost] y3 = 0 27.3128 61.6740 68.7225
[DMAc+OA] w4 = 0.0242 0.0185 0.0099 0.0065	[%Lost] y4 = 0 23.5537 59.0909 73.1405
[NMP] w5 = 0.0330 0.0227 0.0133 0.0113	[%Lost] y5 = 0 31.2121 59.6970 65.7576
[NMP+AA] w6 = 0.0399 0.0295 0.0165 0.0133	[%Lost] y6 = 0 26.0652 58.6466 66.6667
[NMP+MA] w7 = 0.0383 0.0250 0.0148 0.0127	[%Lost] y7 = 0 34.7258 61.3577 66.8407
[NMP+OA] w8 = 0.0223 0.0155 0.0080 0.0061	[%Lost] y8 = 0 30.4933 64.1256 72.6457

### Matlab Program for Burning Tests for Chitin Gels

```

x1=[38 200 300 400];

d1=18.3326;
w1=[18.3565-d1 18.3494-d1 18.3423-d1 18.3381-d1];
y1=[100-(w1(1)/w1(1)*100) 100-(w1(2)/w1(1)*100) 100-(w1(3)/w1(1)*100) 100-(w1(4)/w1(1)*100)];

d2=11.9397;
w2=[11.9664-d2 11.9593-d2 11.9511-d2 11.9465-d2];
y2=[100-(w2(1)/w2(1)*100) 100-(w2(2)/w2(1)*100) 100-(w2(3)/w2(1)*100) 100-(w2(4)/w2(1)*100)];

d3=14.4121;
w3=[14.4348-d3 14.4286-d3 14.4208-d3 14.4192-d3];
y3=[100-(w3(1)/w3(1)*100) 100-(w3(2)/w3(1)*100) 100-(w3(3)/w3(1)*100) 100-(w3(4)/w3(1)*100)];

d4=17.6216;
w4=[17.6458-d4 17.6401-d4 17.6315-d4 17.6281-d4];
y4=[100-(w4(1)/w4(1)*100) 100-(w4(2)/w4(1)*100) 100-(w4(3)/w4(1)*100) 100-(w4(4)/w4(1)*100)];

d5=15.2517;
w5=[15.2847-d5 15.2744-d5 15.2650-d5 15.2630-d5];
y5=[100-(w5(1)/w5(1)*100) 100-(w5(2)/w5(1)*100) 100-(w5(3)/w5(1)*100) 100-(w5(4)/w5(1)*100)];

d6=13.0306;
w6=[13.0705-d6 13.0601-d6 13.0471-d6 13.0439-d6];
y6=[100-(w6(1)/w6(1)*100) 100-(w6(2)/w6(1)*100) 100-(w6(3)/w6(1)*100) 100-(w6(4)/w6(1)*100)];

d7=14.4916;
w7=[14.5299-d7 14.5166-d7 14.5064-d7 14.5043-d7];
y7=[100-(w7(1)/w7(1)*100) 100-(w7(2)/w7(1)*100) 100-(w7(3)/w7(1)*100) 100-(w7(4)/w7(1)*100)];

d8=13.8832;
w8=[13.9055-d8 13.8987-d8 13.8912-d8 13.8893-d8];

```

```

y8=[100-(w8(1)/w8(1)*100) 100-(w8(2)/w8(1)*100) 100-(w8(3)/w8(1)*100) 100-
(w8(4)/w8(1)*100)];

hold on
axis([0 max(x1)+50 0 100]);
xlabel('Temp. (C)');
ylabel('Weight(g)');
title('Burning Test');

plot(x1,y1,'r^');
plot(x1,y1,'g-');

plot(x1,y2,'b^');
plot(x1,y2,'g-');

plot(x1,y3,'m^');
plot(x1,y3,'g-');

plot(x1,y4,'k^');
plot(x1,y4,'g-');

plot(x1,y5,'r*');
plot(x1,y5,'k-');

plot(x1,y6,'b*');
plot(x1,y6,'k-');

plot(x1,y7,'m*');
plot(x1,y7,'k-');

plot(x1,y8,'k*');
plot(x1,y8,'k-');

hold off

```

## A-8

### Swelling Tests for Chitin in DMAc and NMP with (MA, OA, AA) for Nonsolvent Gelation and Thermoreversible Gelation

Note: Red data acid-buffer,  
Blue data Phosphate-buffer,  
Pink data Et-OH

Green lines TR Gellation  
Black lines NS Gellation

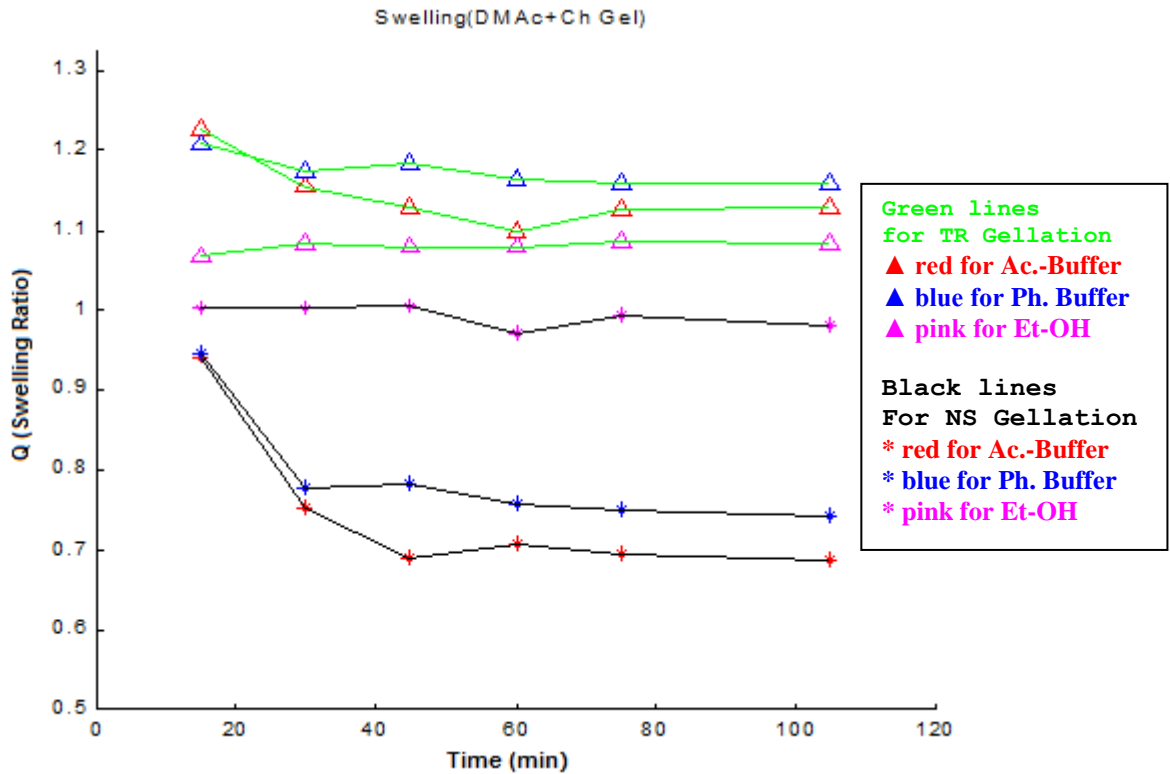


Figure A-8.1. Swelling Tests for DMAc+Chitin Gels (wet) for Nonsolvent Gelation and Thermoreversible Gelation.

#### DMAc+ Chitin Gel (Wet)

[Time]	x1 =	15	30	45	60	75	105
[TR- A.B]	y1 =	1.2268	1.1538	1.1274	1.0984	1.1264	1.1269
[TR- P.B]	y2 =	1.2068	1.1731	1.1830	1.1645	1.1585	1.1592
[TR- EtOH]	y3 =	1.0672	1.0839	1.0796	1.0805	1.0857	1.0842
[NS- A.B]	y4 =	0.9412	0.7527	0.6881	0.7066	0.6934	0.6876
[NS- P.B]	y5 =	0.9455	0.7753	0.7811	0.7569	0.7487	0.7417
[NS- Et-OH]	y6 =	1.0025	1.0015	1.0046	0.9711	0.9914	0.9813

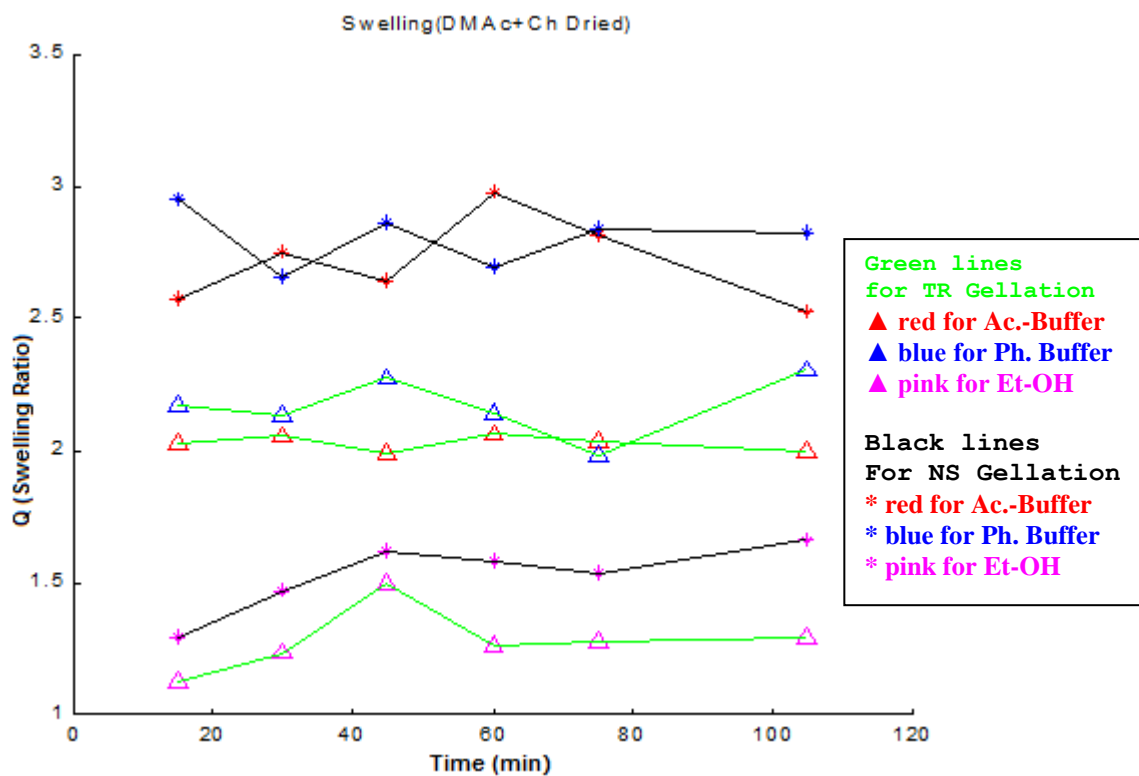


Figure A-8.2. Swelling Tests for DMAc+Chitin Gels (dried) for Nonsolvent Gellation and Thermoreversible Gellation.

### DMAc+ Chitin Dried

[Time]	x1 =	15	30	45	60	75	105
[TR- A.B]	y1 =	2.0227	2.0530	1.9924	2.0606	2.0303	2.0000
[TR- P.B]	y2 =	2.1716	2.1343	2.2761	2.1418	1.9851	2.3060
[TR- EtOH]	y3 =	1.1273	1.2364	1.5000	1.2636	1.2818	1.2909
[NS- A.B]	y4 =	2.5730	2.7528	2.6404	2.9775	2.8202	2.5281
[NS- P.B]	y5 =	2.9506	2.6543	2.8642	2.6914	2.8395	2.8272
[NS- EtOH]	y6 =	1.2903	1.4677	1.6129	1.5806	1.5323	1.6613



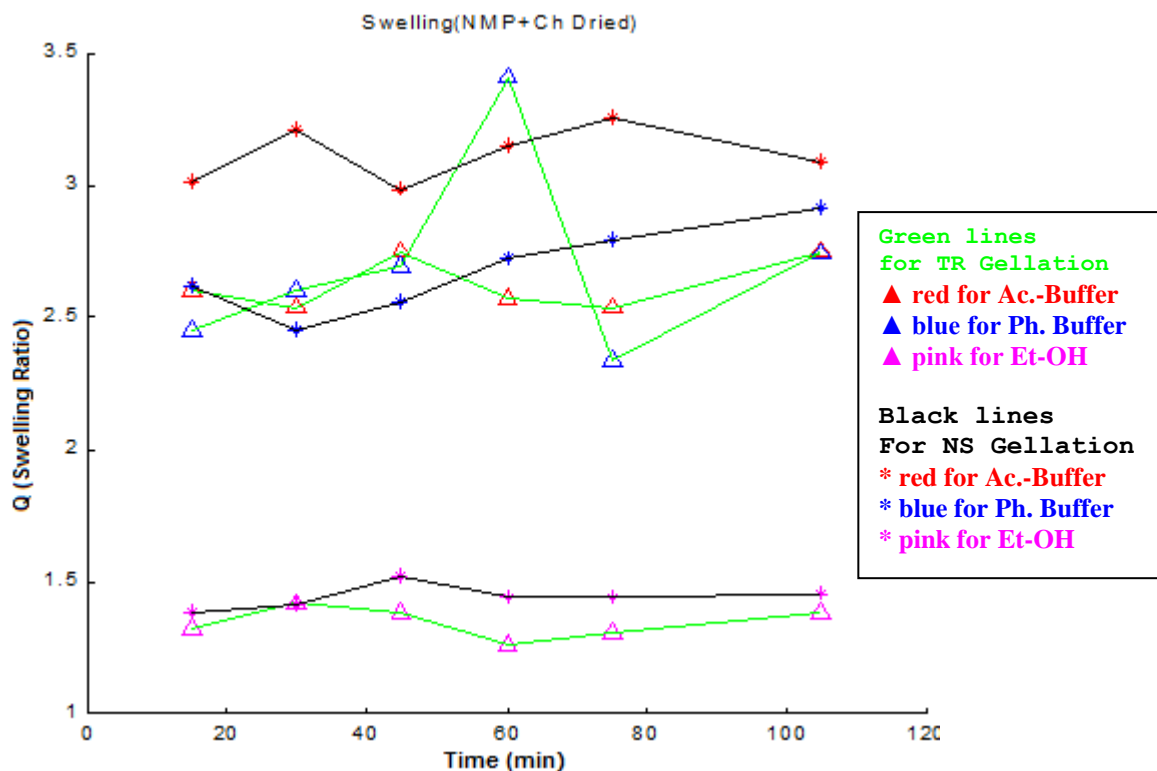


Figure A-8.3. Swelling Tests for NMP+Chitin Gels (dried) for Nonsolvent Gelation and Thermoreversible Gelation.

### NMP+ Chitin Dried

[Time]	x1 =	15	30	45	60	75	105
[TR- A.B]	y1 =	2.6087	2.5362	2.7536	2.5797	2.5362	2.7536
[TR- P.B]	y2 =	2.4507	2.6056	2.6901	3.4085	2.3380	2.7465
[TR- EtOH]	y3 =	1.3231	1.4154	1.3846	1.2615	1.3077	1.3846
[NS- A.B]	y4 =	3.0145	3.2174	2.9855	3.1449	3.2609	3.0870
[NS- P.B]	y5 =	2.6232	2.4493	2.5652	2.7246	2.7971	2.9130
[NS- A.B]	y6 =	1.3836	1.4110	1.5205	1.4384	1.4384	1.4521

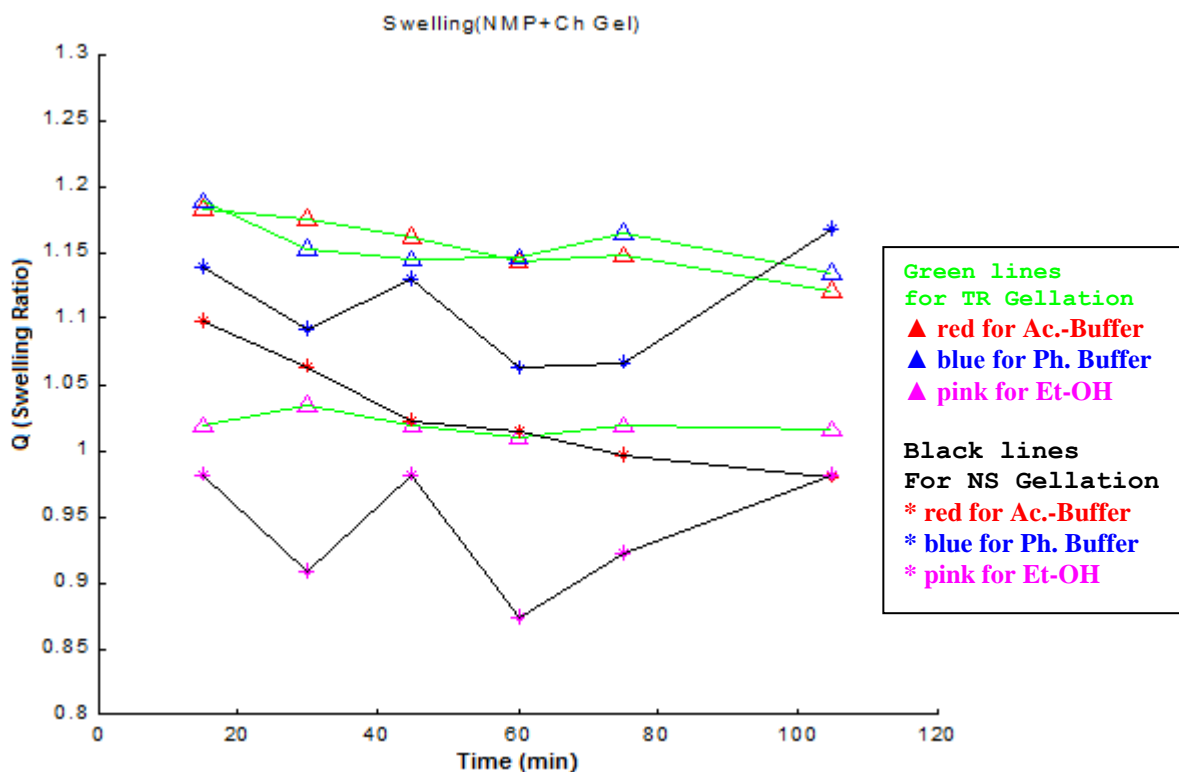


Figure A-8.4. Swelling Tests for NMP+Chitin Gels (Wet) for Nonsolvent Gelation and Thermoreversible Gelation.

### NMP+ Chitin Gel (Wet)

[Time]	x1 =	15	30	45	60	75	105
[TR- A.B]	y1 =	1.1824	1.1754	1.1621	1.1426	1.1481	1.1208
[TR- P.B]	y2 =	1.1886	1.1531	1.1440	1.1460	1.1653	1.1339
[TR- EtOH]	y3 =	1.0180	1.0339	1.0191	1.0095	1.0180	1.0159
[NS- A.B]	y4 =	1.0980	1.0634	1.0231	1.0144	0.9971	0.9798
[NS- P.B]	y5 =	1.1394	1.0913	1.1298	1.0625	1.0673	1.1683
[NS- EtOH]	y6 =	0.9825	0.9079	0.9825	0.8728	0.9211	0.9825

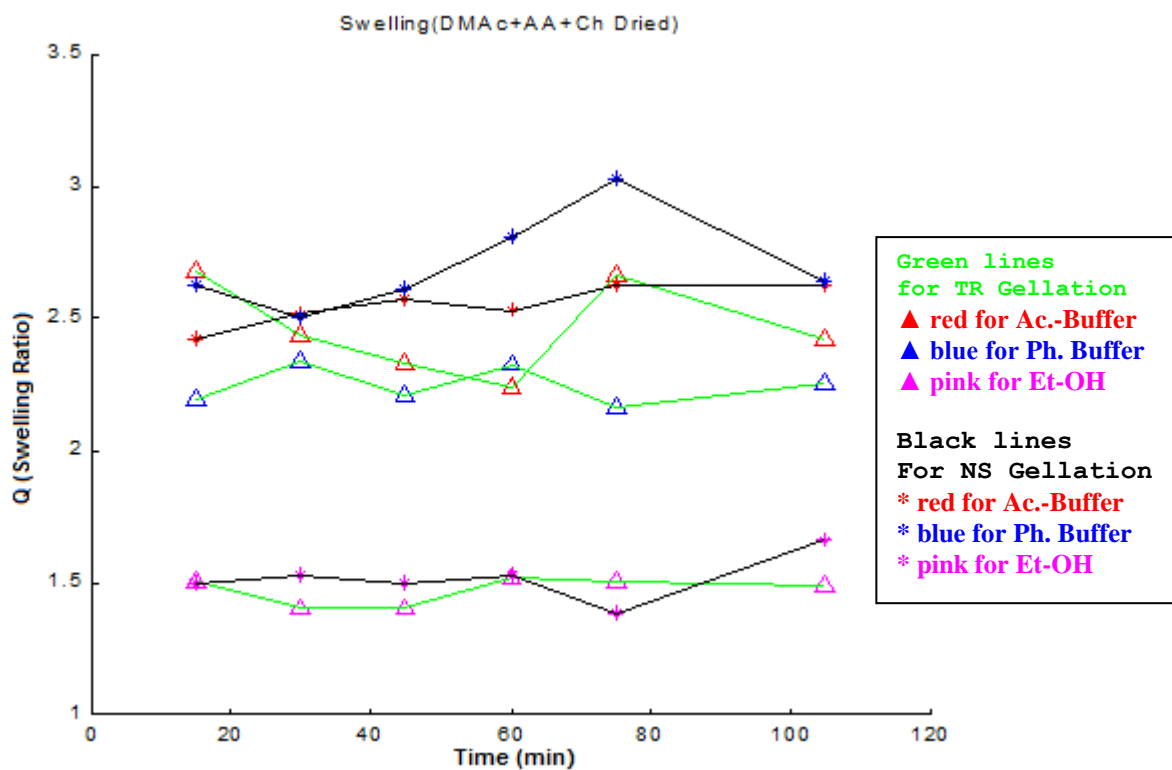


Figure A-8.5. Swelling Tests for DMAc+AA+Chitin Gels (dried) for Nonsolvent Gelation and Thermoreversible Gelation.

### DMAc+ AA+ Chitin Dried

[Time]	x1 =	15	30	45	60	75	105
[TR- A.B]	y1 =	2.6818	2.4394	2.3333	2.2424	2.6667	2.4242
[TR- P.B]	y2 =	2.1972	2.3380	2.2113	2.3239	2.1690	2.2535
[TR- EtOH]	y3 =	1.5063	1.4051	1.4051	1.5190	1.5063	1.4937
[NS- A.B]	y4 =	2.4247	2.5205	2.5753	2.5342	2.6301	2.6301
[NS- P.B]	y5 =	2.6250	2.5000	2.6094	2.8125	3.0312	2.6406
[NS - EtOH]	y6 =	1.5000	1.5294	1.5000	1.5294	1.3824	1.6618

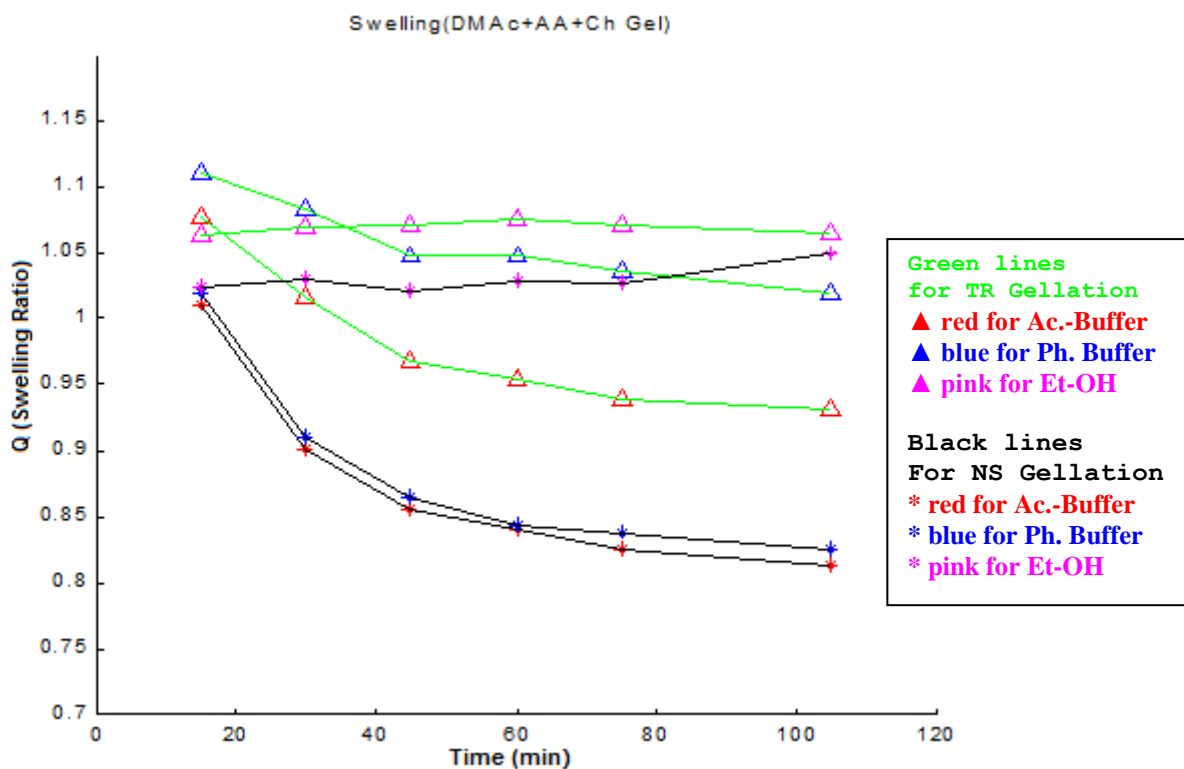


Figure A-8.6. Swelling Tests for DMAc+AA+Chitin Gels (Wet) for Nonsolvent Gelation and Thermoreversible Gelation.

### DMAc+ AA+ Chitin Gel (Wet)

[Time]	x1 =	15	30	45	60	75	105
[TR- A.B]	y1 =	1.0762	1.0161	0.9678	0.9538	0.9385	0.9311
[TR- P.B]	y2 =	1.1107	1.0821	1.0469	1.0482	1.0358	1.0202
[TR- EtOH]	y3 =	1.0631	1.0691	1.0709	1.0751	1.0715	1.0655
[NS- A.B]	y4 =	1.0102	0.9007	0.8555	0.8409	0.8248	0.8131
[NS- P.B]	y5 =	1.0204	0.9102	0.8647	0.8443	0.8383	0.8240
[NS - EtOH]	y6 =	1.0242	1.0293	1.0217	1.0280	1.0268	1.0484

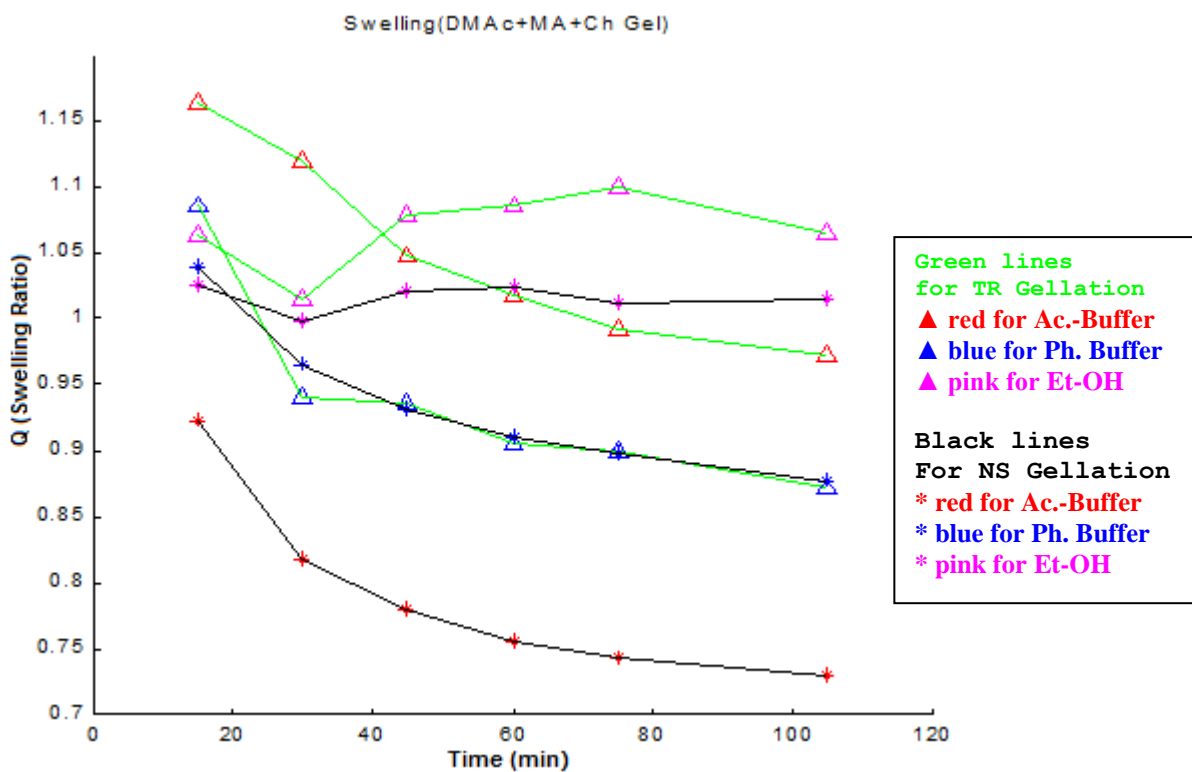


Figure A-8.7. Swelling Tests for DMAc+MA+Chitin Gels (Wet) for Nonsolvent Gelation and Thermoreversible Gelation.

### DMAc+ MA+ Chitin Gel

[Time]	x1 =	15	30	45	60	75	105
[TR- A.B]	y1 =	1.1632	1.1198	1.0482	1.0187	0.9918	0.9722
[TR- P.B]	y2 =	1.0856	0.9404	0.9365	0.9058	0.8990	0.8712
[TR- EtOH]	y3 =	1.0632	1.0149	1.0789	1.0860	1.1009	1.0658
[NS- A.B]	y4 =	0.9227	0.8167	0.7786	0.7564	0.7426	0.7288
[NS- P.B]	y5 =	1.0392	0.9652	0.9316	0.9103	0.8980	0.8778
[NS - EtOH]	y6 =	1.0260	0.9977	1.0214	1.0237	1.0124	1.0158

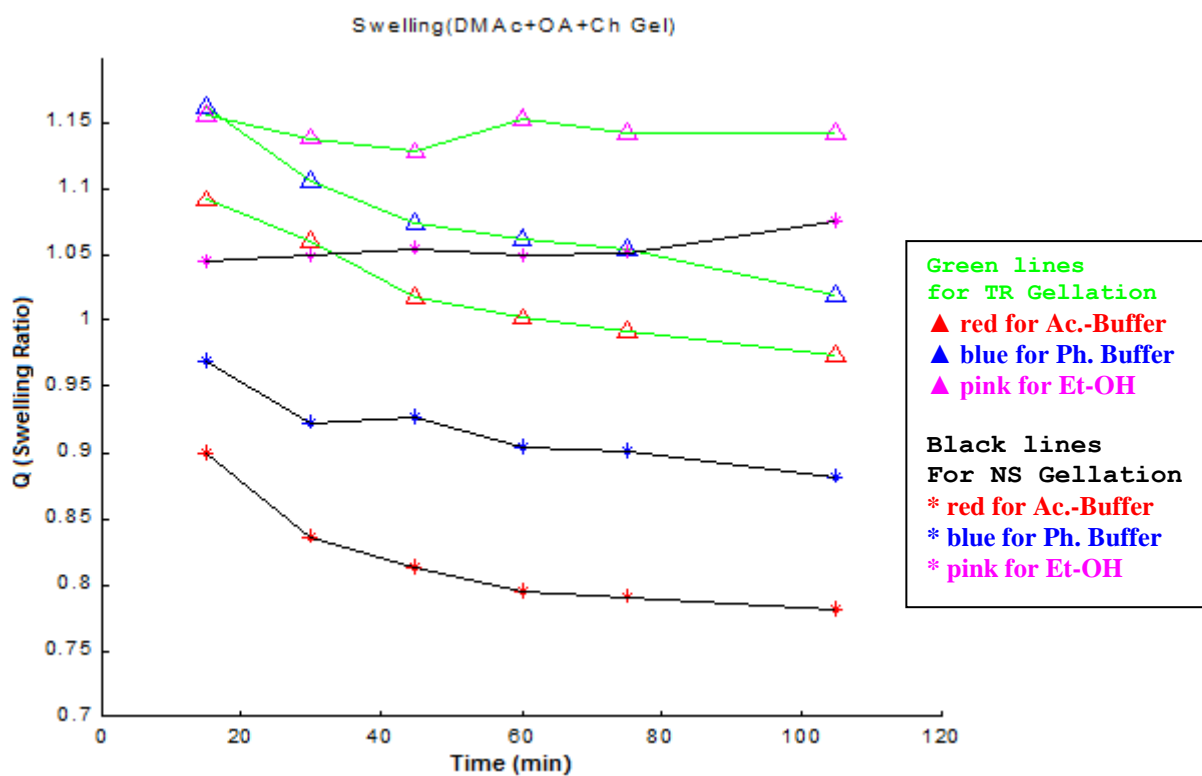


Figure A-8.8. Swelling Tests for DMAc+OA+Chitin Gels (Wet) for Nonsolvent Gelation and Thermoreversible Gelation.

### DMAc+ OA+ Chitin Gel

[Time]	x1 =	15	30	45	60	75	105
[TR- A.B]	y1 =	1.0915	1.0612	1.0181	1.0017	0.9918	0.9743
[TR- P.B]	y2 =	1.1622	1.1069	1.0732	1.0628	1.0546	1.0202
[TR- EtOH]	y3 =	1.1557	1.1384	1.1280	1.1529	1.1433	1.1433
[NS- A.B]	y4 =	0.8991	0.8365	0.8122	0.7948	0.7913	0.7809
[NS- P.B]	y5 =	0.9692	0.9231	0.9275	0.9033	0.9011	0.8813
[NS - EtOH]	y6 =	1.0444	1.0496	1.0548	1.0496	1.0522	1.0757

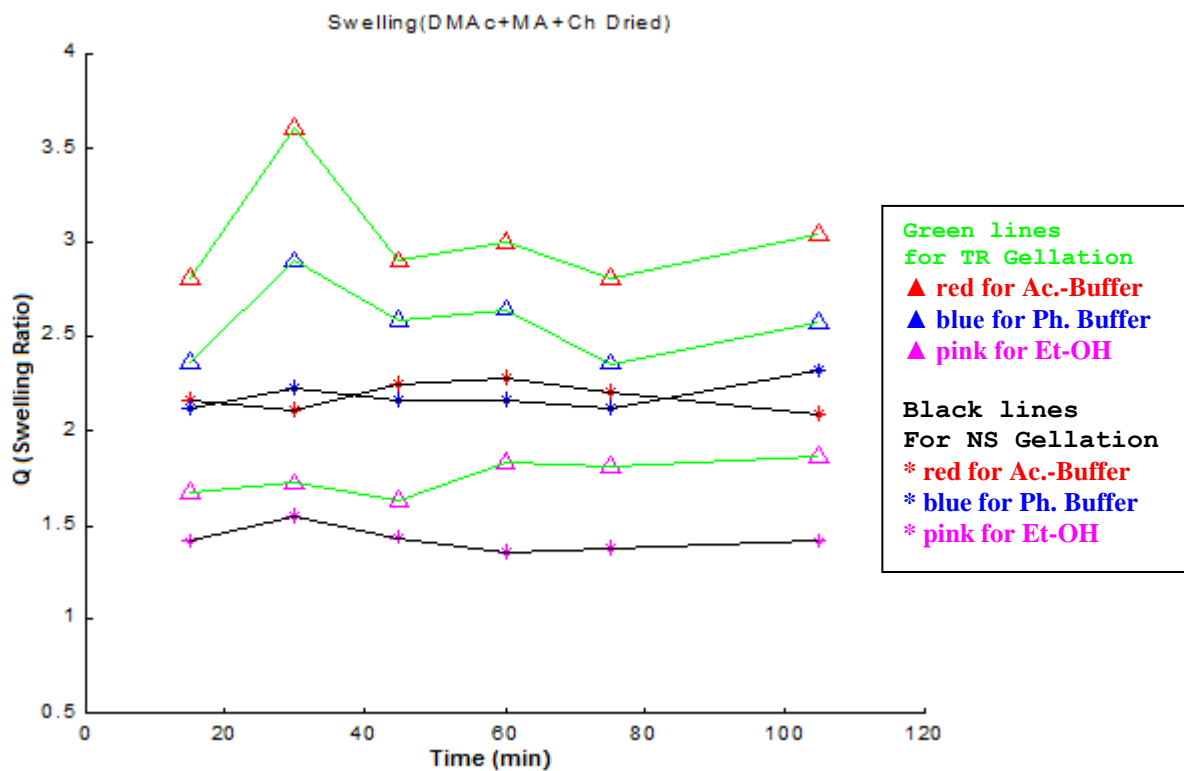


Figure A-8.9. Swelling Tests for DMAc+MA+Chitin Gels (dried) for Nonsolvent Gelation and Thermoreversible Gelation.

### DMAc+ MA+ Chitin Dried

[Time]	x1 =	15	30	45	60	75	105
[TR- A.B]	y1 =	2.8049	3.6098	2.9024	3.0000	2.8049	3.0488
[TR- P.B]	y2 =	2.3725	2.9020	2.5882	2.6471	2.3529	2.5686
[TR- EtOH]	y3 =	1.6744	1.7209	1.6279	1.8372	1.8140	1.8605
[NS- A.B]	y4 =	2.1591	2.1136	2.2500	2.2727	2.2045	2.0909
[NS- P.B]	y5 =	2.1250	2.2292	2.1667	2.1667	2.1250	2.3125
[NS - EtOH]	y6 =	1.4130	1.5435	1.4348	1.3478	1.3696	1.4130

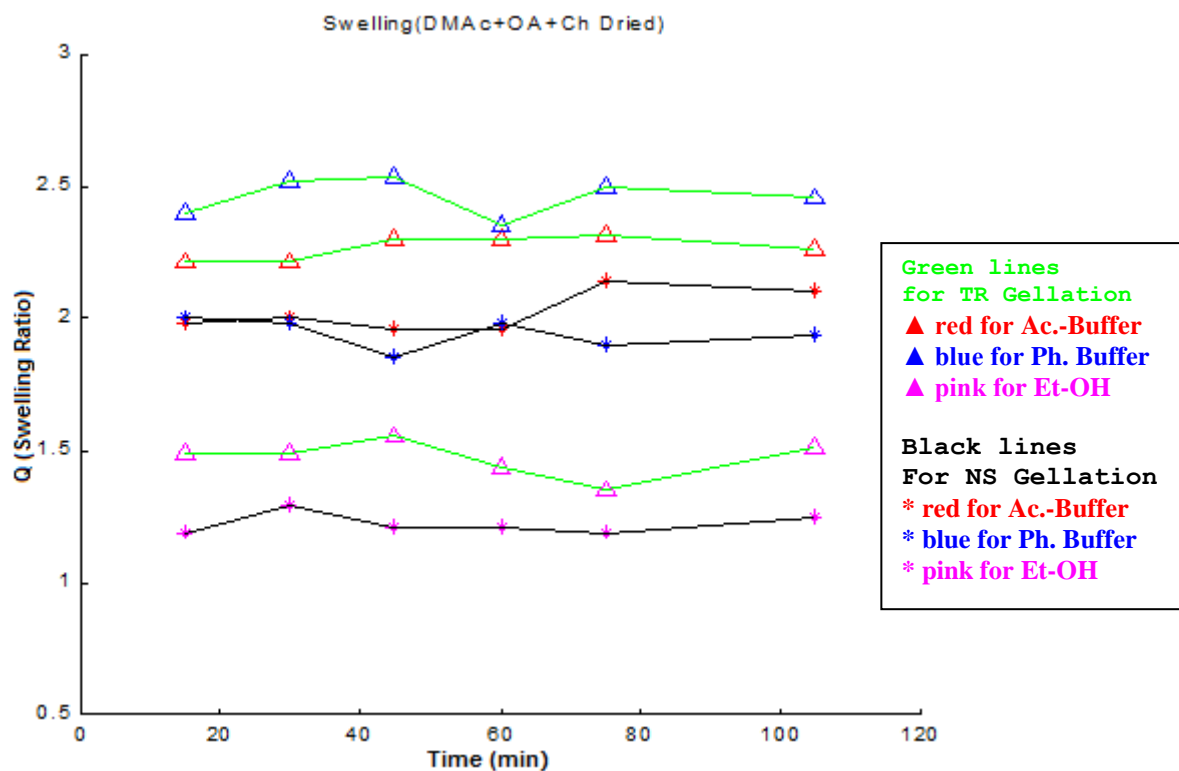


Figure A-8.10. Swelling Tests for DMAc+OA+Chitin Gels (dried) for Nonsolvent Gelation and Thermoreversible Gelation.

### DMAc+ OA+ Chitin Dried

[Time]	x1 =	15	30	45	60	75	105
[TR- A.B]	y1 =	2.2167	2.2167	2.3000	2.3000	2.3167	2.2667
[TR- P.B]	y2 =	2.3958	2.5208	2.5417	2.3542	2.5000	2.4583
[TR- EtOH]	y3 =	1.4884	1.4884	1.5581	1.4419	1.3488	1.5116
[NS- A.B]	y4 =	1.9792	2.0000	1.9583	1.9583	2.1458	2.1042
[NS- P.B]	y5 =	2.0000	1.9796	1.8571	1.9796	1.8980	1.9388
[NS- EtOH]	y6 =	1.1875	1.2917	1.2083	1.2083	1.1875	1.2500



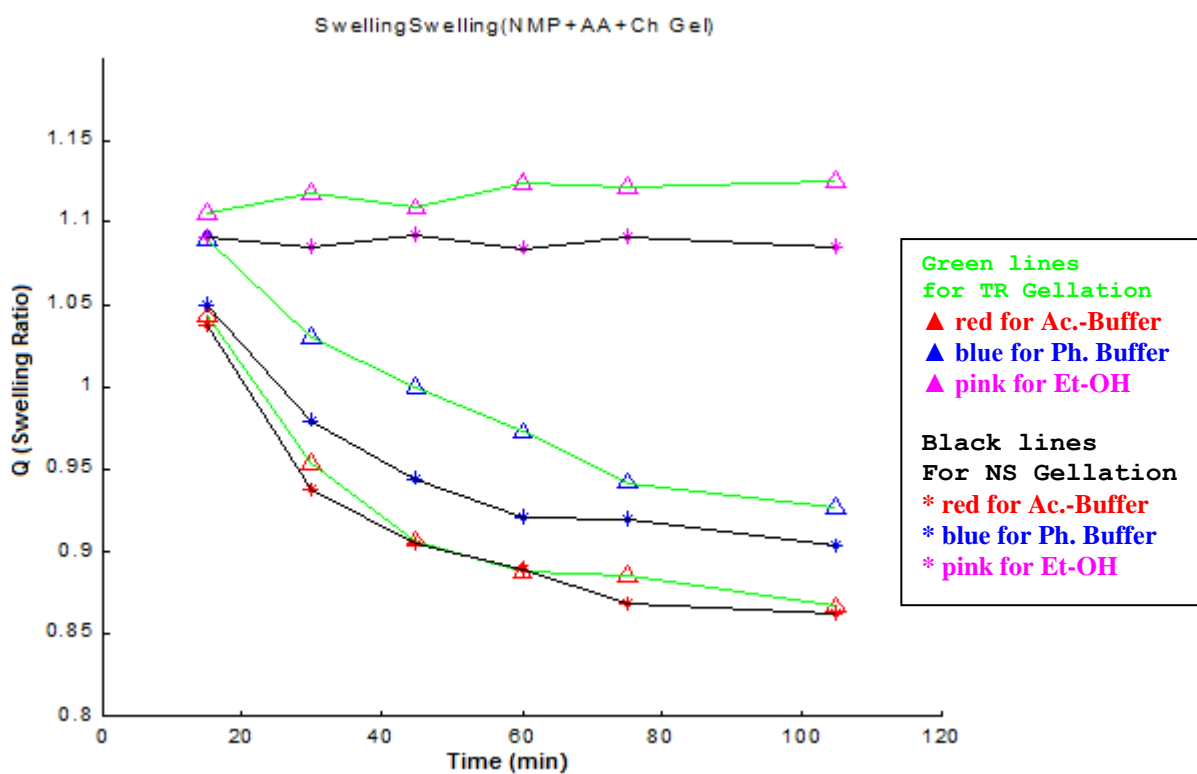


Figure A-8.11. Swelling Tests for NMP+AA+Chitin Gels (Wet) for Nonsolvent Gelation and Thermoreversible Gelation.

### NMP+ AA+ Chitin Gel

[Time]	x1 =	15	30	45	60	75	105
[TR- A.B]	y1 =	1.0425	0.9534	0.9067	0.8881	0.8860	0.8663
[TR- P.B]	y2 =	1.0895	1.0301	1.0000	0.9722	0.9414	0.9271
[TR- EtOH]	y3 =	1.1048	1.1181	1.1086	1.1238	1.1210	1.1248
[NS- A.B]	y4 =	1.0367	0.9368	0.9039	0.8887	0.8685	0.8622
[NS- P.B]	y5 =	1.0493	0.9791	0.9447	0.9208	0.9193	0.9028
[NS- EtOH]	y6 =	1.0910	1.0850	1.0926	1.0835	1.0910	1.0850

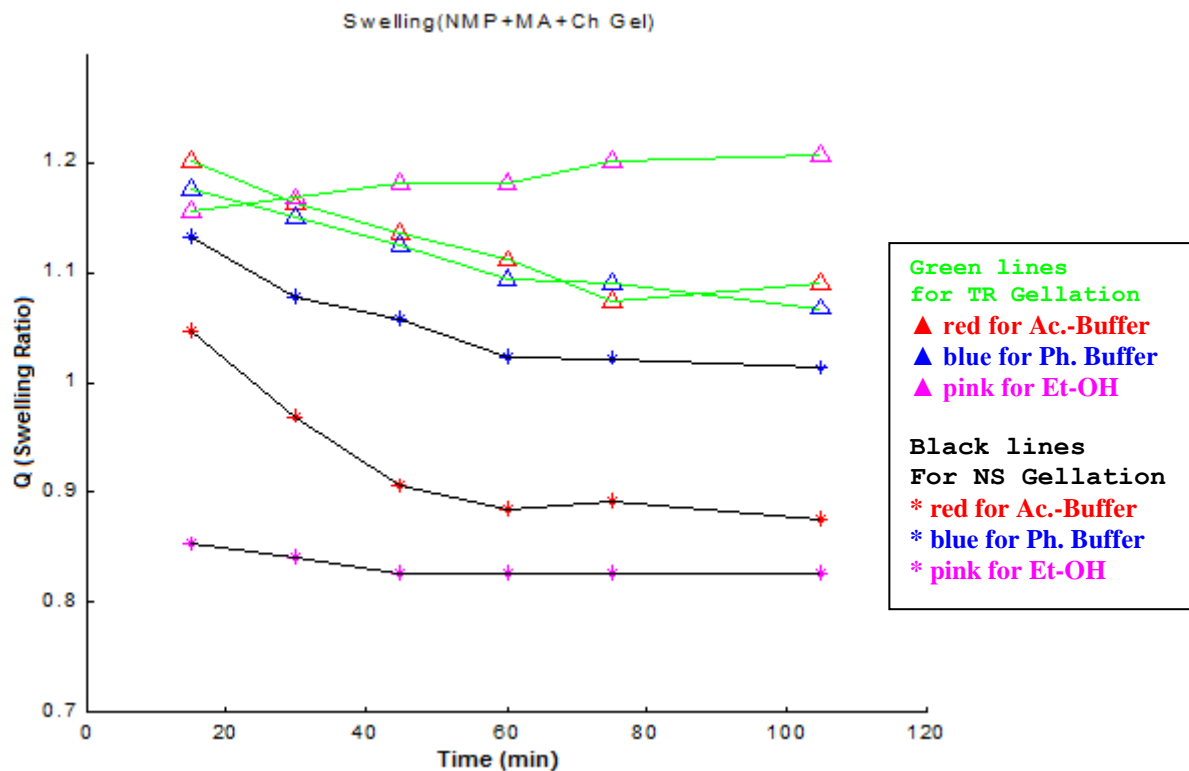


Figure A-8.12. Swelling Tests for NMP+MA+Chitin Gels (Wet) for Nonsolvent Gelation and Thermoreversible Gelation.

### NMP+ MA+ Chitin Gel

[Time]	x1 =	15	30	45	60	75	105
[TR- A.B]	y1 =	1.2023	1.1634	1.1362	1.1113	1.0755	1.0911
[TR- P.B]	y2 =	1.1767	1.1496	1.1264	1.0946	1.0899	1.0682
[TR- EtOH]	y3 =	1.1558	1.1686	1.1813	1.1813	1.2011	1.2068
[NS- A.B]	y4 =	1.0471	0.9686	0.9058	0.8841	0.8925	0.8768
[NS- P.B]	y5 =	1.1328	1.0776	1.0569	1.0241	1.0224	1.0138
[NS- EtOH]	y6 =	0.8537	0.8403	0.8275	0.8268	0.8275	0.8262

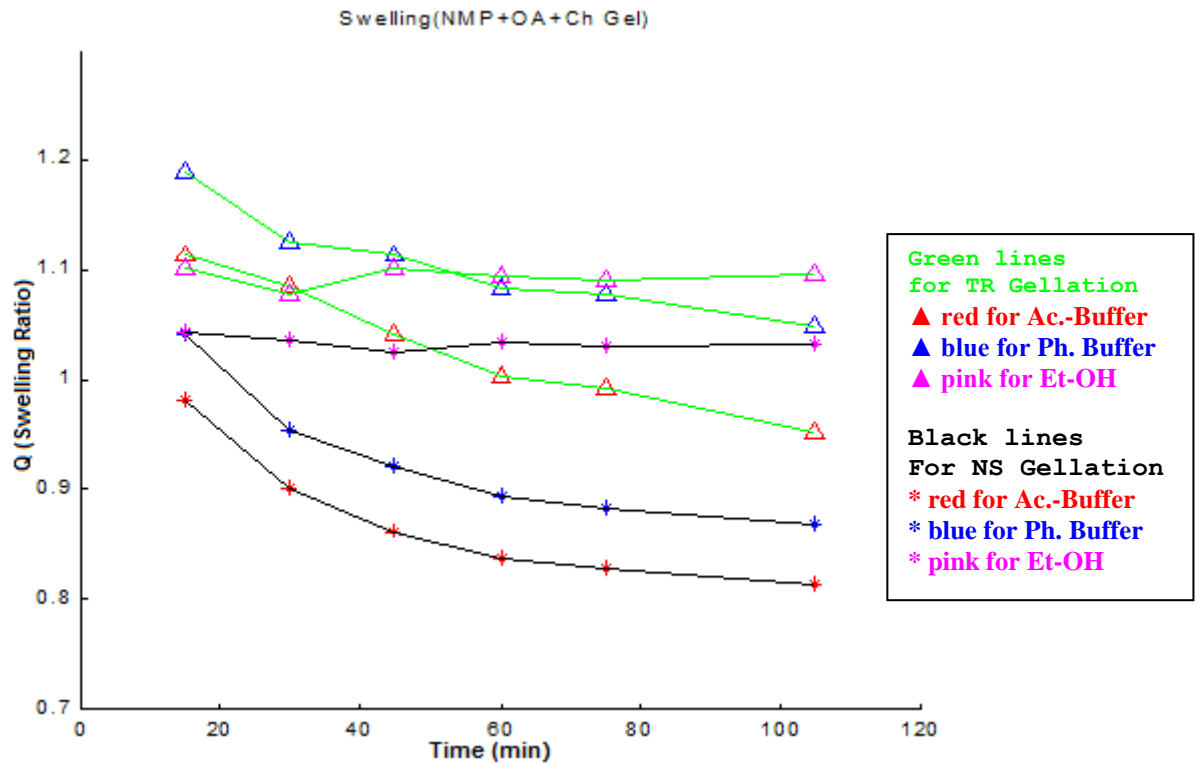


Figure A-8.13. Swelling Tests for NMP+OA+Chitin Gels (Wet) for Nonsolvent Gellation and Thermoreversible Gellation.

### NMP+ OA+ Chitin Gel

[Time]	x1 =	15	30	45	60	75	105
[TR- A.B]	y1 =	1.1134	1.0852	1.0405	1.0021	0.9918	0.9512
[TR- P.B]	y2 =	1.1895	1.1258	1.1141	1.0841	1.0783	1.0483
[TR- EtOH]	y3 =	1.1015	1.0776	1.1009	1.0937	1.0901	1.0955
[NS- A.B]	y4 =	0.9820	0.8999	0.8626	0.8370	0.8293	0.8151
[NS- P.B]	y5 =	1.0408	0.9534	0.9210	0.8943	0.8827	0.8686
[NS- EtOH]	y6 =	1.0429	1.0361	1.0260	1.0350	1.0316	1.0327

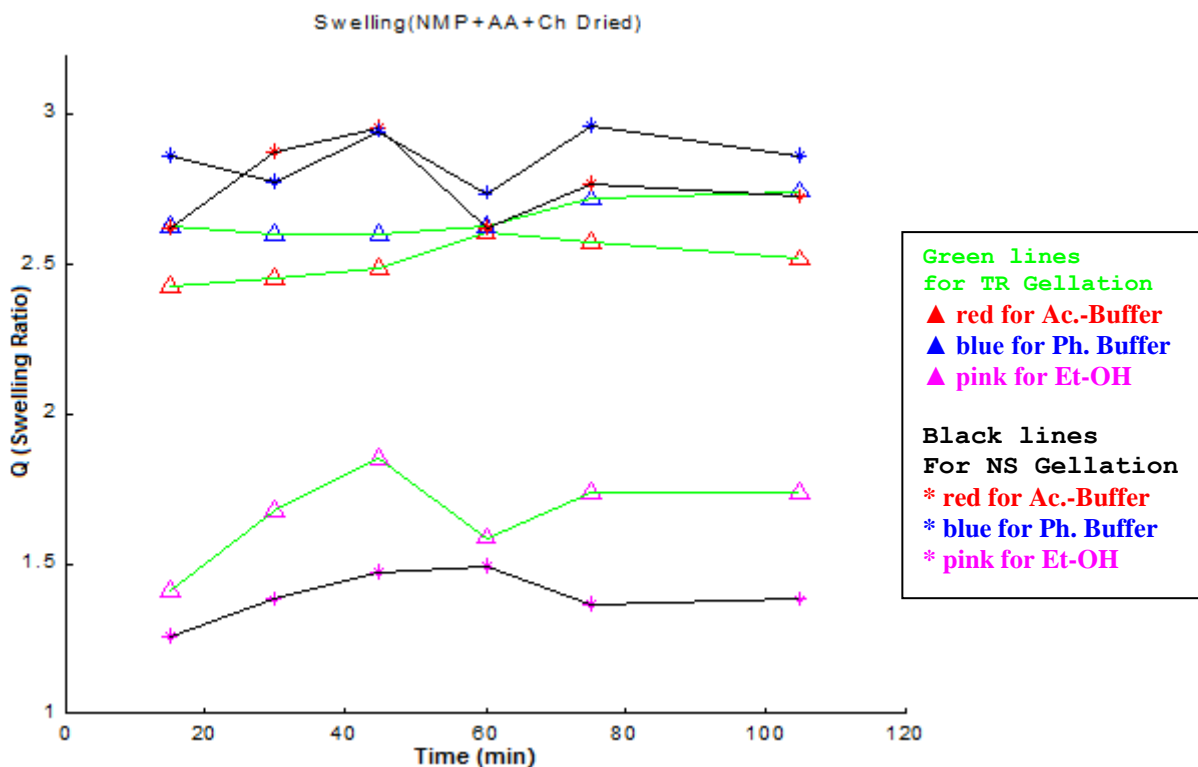


Figure A-8.14. Swelling Tests for NMP+AA+Chitin Gels (Dried) for Nonsolvent Gelation and Thermoreversible Gelation.

### NMP+ AA+ Chitin Dried

[Time]	x1 =	15	30	45	60	75	105
[TR- A.B]	y1 =	2.4242	2.4545	2.4848	2.6061	2.5758	2.5152
[TR- P.B]	y2 =	2.6286	2.6000	2.6000	2.6286	2.7143	2.7429
[TR- EtOH]	y3 =	1.4118	1.6765	1.8529	1.5882	1.7353	1.7353
[NS- A.B]	y4 =	2.6170	2.8723	2.9574	2.6170	2.7660	2.7234
[NS- P.B]	y5 =	2.8571	2.7755	2.9388	2.7347	2.9592	2.8571
[NS- EtOH]	y6 =	1.2553	1.3830	1.4681	1.4894	1.3617	1.3830

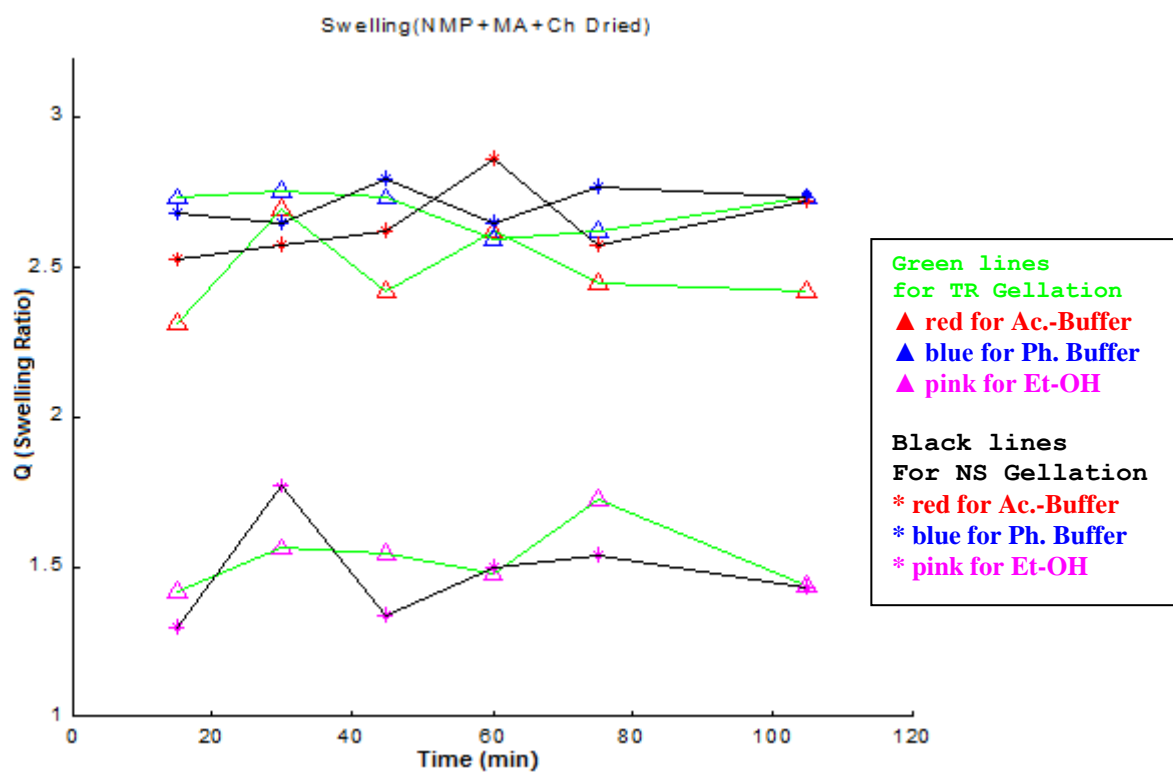


Figure A-8.15. Swelling Tests for NMP+MA+Chitin Gels (Dried) for Nonsolvent Gelation and Thermoreversible Gelation.

### NMP+ MA+ Chitin Dried

[Time]	x1 =	15	30	45	60	75	105
[TR- A.B]	y1 =	2.3111	2.6889	2.4222	2.6222	2.4444	2.4222
[TR- P.B]	y2 =	2.7297	2.7568	2.7297	2.5946	2.6216	2.7297
[TR- EtOH]	y3 =	1.4200	1.5600	1.5400	1.4800	1.7200	1.4400
[NS- A.B]	y4 =	2.5238	2.5714	2.6190	2.8571	2.5714	2.7143
[NS- P.B]	y5 =	2.6765	2.6471	2.7941	2.6471	2.7647	2.7353
[NS- EtOH]	y6 =	1.3000	1.7667	1.3333	1.5000	1.5333	1.4333

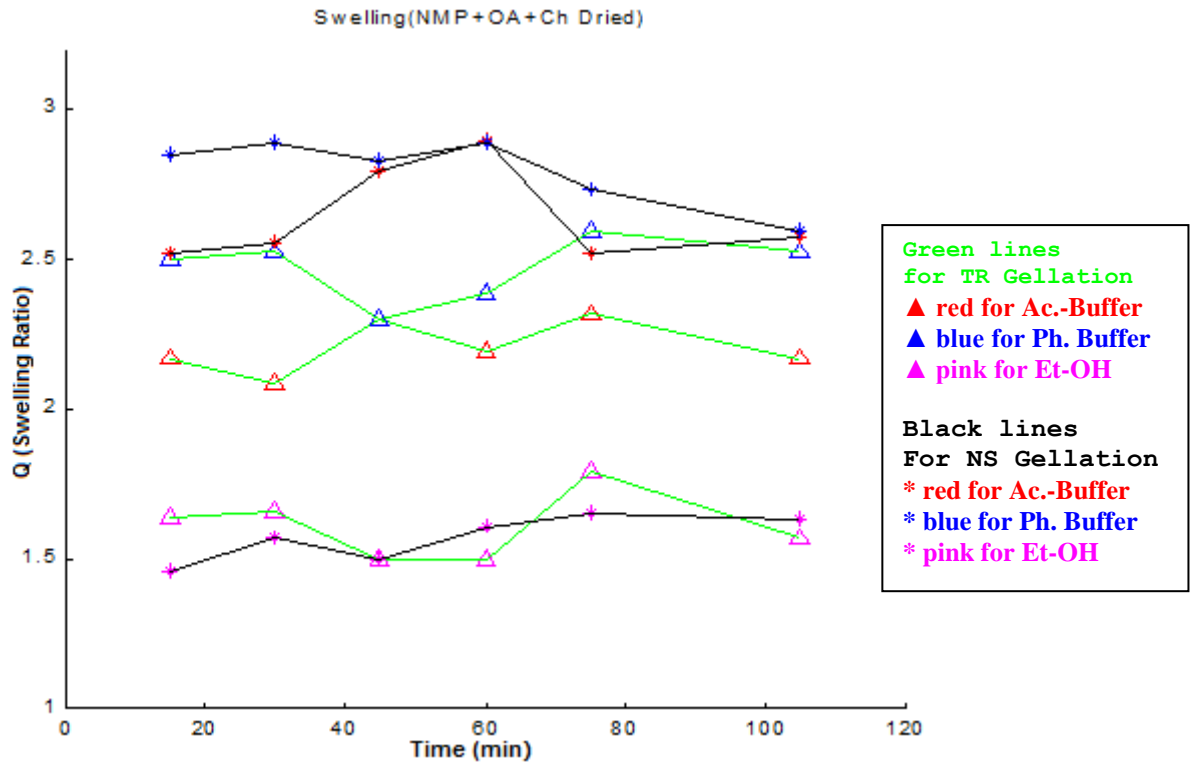


Figure A-8.16. Swelling Tests for NMP+OA+Chitin Gels (Dried) for Nonsolvent Gellation and Thermoreversible Gellation.

### NMP+ OA+ Chitin Dried

[Time]	x1 =	15	30	45	60	75	105
[TR- A.B]	y1 =	2.1702	2.0851	2.2979	2.1915	2.3191	2.1702
[TR- P.B]	y2 =	2.5000	2.5227	2.2955	2.3864	2.5909	2.5227
[TR- EtOH]	y3 =	1.6379	1.6552	1.5000	1.5000	1.7931	1.5690
[NS- A.B]	y4 =	2.5185	2.5556	2.7963	2.8889	2.5185	2.5741
[NS- P.B]	y5 =	2.8462	2.8846	2.8269	2.8846	2.7308	2.5962
[NS- EtOH]	y6 =	1.4565	1.5652	1.5000	1.6087	1.6522	1.6304

```

% Matlab Program for Swelling Test

x1=[15 30 45 60 75 105];
a=1931;
y1=[2369/a 2228/a 2177/a 2121/a 2175/a 2176/a];
a=3022;
y2=[3647/a 3545/a 3575/a 3519/a 3501/a 3503/a];

a=3242;
y3=[3460/a 3514/a 3500/a 3503/a 3520/a 3515/a];

a=2260;
y4=[2127/a 1701/a 1555/a 1597/a 1567/a 1554/a];

a=2439;
y5=[2306/a 1891/a 1905/a 1846/a 1826/a 1809/a];

a=1975;
y6=[1980/a 1978/a 1984/a 1918/a 1958/a 1938/a];

hold on
axis([0 max(x1)+15 0.5 max(y1)+.1]);
xlabel('Time(min.)');
ylabel('Q');
title('Swelling(DMAc+Ch Gel) ');
plot(x1,y1,'r^');
plot(x1,y1,'g-');
plot(x1,y2,'b^');
plot(x1,y2,'g-');
plot(x1,y3,'m^');
plot(x1,y3,'g-');
plot(x1,y4,'r*');
plot(x1,y4,'k-');
plot(x1,y5,'b*');
plot(x1,y5,'k-');
plot(x1,y6,'m*');
plot(x1,y6,'k-');
hold off

```

## A-9

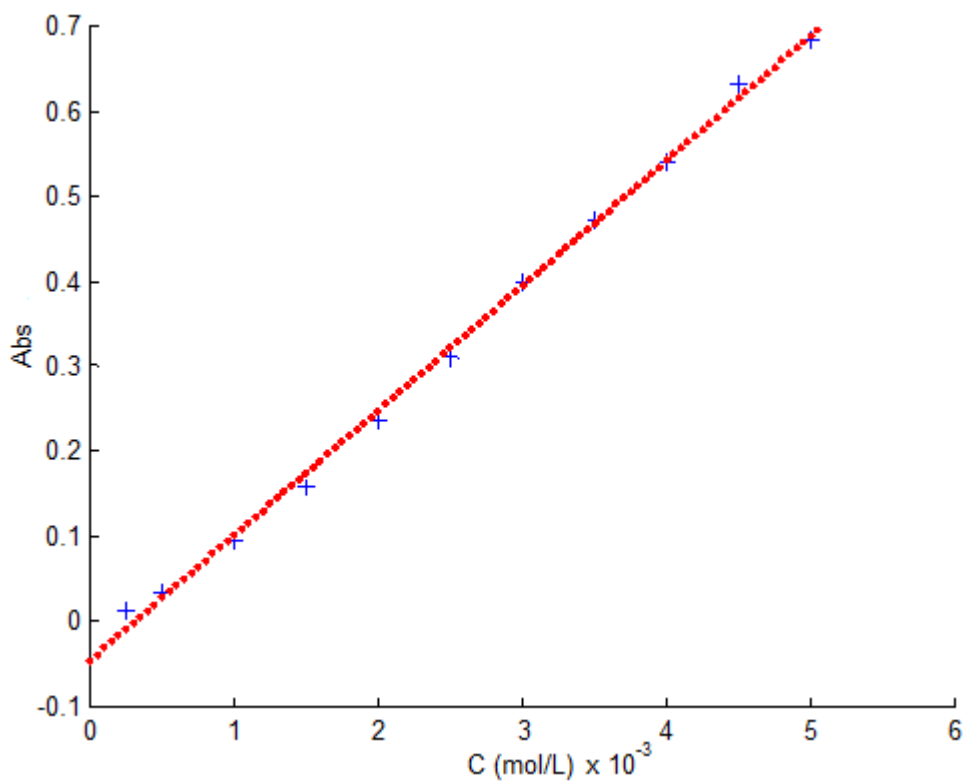


Figure A-9.1. Calibration Curve for Fe<sup>3+</sup>.

### Calibratin curve for Fe<sup>3+</sup>:

$$\text{Abs} = 146.7119 \times \text{Conc} - 0.0452$$

The original data are as follows:

<b>Conc (mol/L) x 10<sup>-3</sup></b>	<b>Abs (505 nm)</b>
0.25	0.013
0.50	0.034
1.00	0.095
1.50	0.158
2.00	0.235
2.50	0.310
3.00	0.400
3.50	0.473
4.00	0.541
4.50	0.632
5.00	0.683